Isolation, characterization and differentiation of trabecular meshwork stem cells for the study and treatment of primary open-angle glaucoma

Padmapriya, Sathiyanathan

2015

Padmapriya, S. (2015). Isolation, characterization and differentiation of trabecular meshwork stem cells for the study and treatment of primary open-angle glaucoma. Doctoral thesis, Nanyang Technological University, Singapore.

https://hdl.handle.net/10356/65622

https://doi.org/10.32657/10356/65622

NANYANG TECHNOLOGICAL UNIVERSITY

Isolation, Characterization and Differentiation of Trabecular Meshwork Stem Cells for the Study and Treatment of Primary Open-angle Glaucoma

PADMAPRIYA SATHIYANATHAN

SCHOOL OF BIOLOGICAL SCIENCES

2015

Isolation, Characterization and Differentiation of Trabecular Meshwork Stem Cells for the Study and Treatment of Primary Open-angle Glaucoma

PADMAPRIYA SATHIYANATHAN

SCHOOL OF BIOLOGICAL SCIENCES

A thesis submitted to the Nanyang Technological University in partial fulfillment of the requirement for the degree of Doctor of Philosophy

2015

Acknowledgements

The project was conceptualized by Dr Lawrence Stanton and Dr Tina Wong (Singapore National Eye Center). I would like to express my sincere gratitude to my supervisor, Dr Stanton for his patience, motivation and invaluable guidance.

I thank Dr Cheryl Tay and Ms Stephanie Chu for our joint work on the CFU-F assay, MSC phenotype assessment (immunofluorescence), *in vitro* differentiation of TM-MSC into mesenchymal lineages and GSEA analysis of TM-MSC. My sincere thanks also go to Dr Irene Aksoy, Dr Akshay Binge and Dr Tay for their fruitful discussions and help on protocols. I thank our lab manager, Ms Rani Ettikan, for procuring reagents and other products for the research.

I acknowledge my thesis advisory committee members: Dr Peter Dröge, Dr Ravi Kambadur and Dr Tara Huber for their insightful comments and keeping me on track.

The work was funded by the Singapore National Medical Research Council: NMRC/TCR/002-SERI/2008 and A*STAR.

Table of Contents

List of Figures

Introduction

Results

List of Tables

Abbreviations

Ac-LDL	Acetylated – low density lipoprotein
Ad-MSC	Adipose-derived MSC
BM-MSC	Bone marrow-derived MSC
CTM	Corneoscleral trabecular meshwork
DAPI	4',6-diamidino-2-phenylindole
DMEM	Dulbecco's Modified Eagle Medium
EB	Embryoid Body
ECM	Extracellular matrix material
FBS	Fetal bovine serum
FC	Fold change
GO	Gene ontology
GSEA	Gene set enrichment analysis
HAT	Histone acetyltransferase
HDAC	Histone deacetylase
HUGO	Human Genome Organization
iPSC	Induced Pluripotent Stem Cells
IOP	Intraocular Pressure
JCT	Juxtacanalicular connective tissue
MEF	Mouse embryonic fibroblast
MSC	Mesenchymal stem cells
NPC	Neural progenitor cells
PBS	Phosphate-buffered saline
PBST	Phosphate-buffered saline with tween-20
PCR	Polymerase chain reaction
PET	Progenitors for Endothelium and Trabeculum
PFA	Paraformaldehyde
POAG	Primary open-angle glaucoma
qRT-PCR	Quantitative reverse transcription - polymerase chain reaction
RGC	Retinal ganglionic cells
RPE	Retinal pigmented cells
RT-PCR	Reverse transcription polymerase chain reaction
SC	Schlemm's canal
SD-plaque	Sheath-derived plaque
TADLIS	TGFβ3, ascorbic acid, dexamethasone, linoleic acid, ITS and sodium pyruvate
TUNEL	Terminal deoxynucleotidyl transferase dUTP nick end labeling
TM	Trabecular meshwork
TM-MSC	Trabecular meshwork-derived mesenchymal stem cells
TSA	Trichostatin A
UTM	Uveal trabecular meshwork

Abstract

Primary open-angle glaucoma (POAG) is the most common form of glaucoma, a leading cause of irreversible blindness worldwide. Development of POAG is associated with increased resistance to aqueous humour outflow through the malfunctioning trabecular meshwork (TM). Cell-based therapy may be an effective approach to treat POAG but limited by lack of expandable pool of stem cells and mature cells of the TM. *In vivo* studies have demonstrated the existence of a stem cell niche in the insert region of the TM. Understanding of the insert cells is limited since they had not been isolated for study *in vitro*. Primary TM cells also have limited lifespan which challenges its application. The purpose of the study is to isolate the elusive TM progenitors and differentiate them into functional TM cells for clinical application.

To this end, an isolation methodology was designed to isolate TM stem cells which expressed stem cell markers (*MYC, OCT4, NANOG, KLF4, REX1* and *NES*), had proliferative potential and confirmed to be of TM origin (by expression of *AQP1, HMFG1, ANK3* and *ABCG2*). Further characterization found them to resemble mesenchymal stem cells (MSC), display MSC marker profile ($CD73^+$, $CD90^+$ $CD105^+$, $CD11b^-$, $CD19^-$, $CD34^-$, $CD45^-$ and $HLA\text{-}DR^-$) and differentiate *in vitro* into several mesenchymal lineages, thus confirming them as MSC.

Novel TM differentiation markers were identified by gene expression profiling of TM, cornea, sclera and TM-MSC. *CDH23*, *KCNAB1*, *FGF9*, *SPP1*, and *HEY1* were selected among the genes highly expressed in the TM compared to the other samples. *BDNF* was downregulated in the TM relative to TM-MSC. Their differential expression was verified by qRT-PCR and immunofluorescence. TM differentiation markers of interest were then used to screen for TM inducing conditions from a range of small molecules and plating conditions. Several small molecules (TSA, BCI, SC1, forskolin and BI-D1870) and aggregation culture were found as TM differentiation inducers. Importantly, a medium composition tested induced robust differentiation into functional TM cells.

Aging in TM was studied by genome-wide expression analysis to identify molecular changes that accompany TM aging. Several biological processes affected with age were identified which were suggestive of TM aging being connected to the deregulation of cell cycle control, cellular stress, inflammatory response and migration which are enriched in the aged TM.

Remarkably, processes associated with TM function remained unaffected by age. These observations provide evidence that cell loss arising from apoptosis and migration may play a role in TM degeneration with age, and likely contribute to age-related structural changes as well as increased susceptibility to POAG.

Several valuable findings have been made in the study. Importantly, TM stem cell isolation methodology and methods to differentiation them into functional TM cells have been established. This will provide scalable pools of TM cells, useful for various applications. Hence, the study is of significance to the TM field, and could advance regenerative efforts for POAG, in addition to fostering better understanding of TM aging.

1. Introduction

1.1 Glaucoma

Glaucoma is the second leading cause of blindness worldwide after cataracts, and the main cause of irreversible blindness. It collectively refers to a group of ocular disorders defined by a characteristic pattern of damage to the optic nerve, resulting in progressive loss of vision. Elevated intraocular pressure (IOP) of the eye often accompanies the disease due to abnormalities in the anterior portion of the eye and is an important risk factor for the disease. Elevated IOP exerts excessive pressure on the retina, damaging the retinal ganglionic cells (RGC) forming the optic nerve and compromises the corresponding visual field. It is also classified as a neurodegenerative disease as the optic nerve is affected and presents the same pathophysiological features as common forms of neurodegenerative disease.

Figure 1. Illustration of the peripheral vision loss caused by glaucoma. Patients increasingly only see objects in the center of the visual field as the disease progresses, culminating in total blindness. (Image adapted from www.sanantonio-lasik.com).

Glaucoma is aptly dubbed the ‘silent thief of sight’ as the disease typically manifests in a slow and progressive manner without pain. So, signs and symptoms often go unnoticed until late stage. Deterioration of vision typically starts at the peripheral visual field, and slowly spreads to the central field. Although a ‘normal’ perception of vision is experienced by the affected individual in the early stage, as the disease progresses he/ she can only see objects in the center of the visual field, a phenomenon termed ‘tunnel’ vision, in the advanced stage (Fig. 1). Hence, significant and permanent loss of vision has already occurred before one becomes aware of the condition. If left untreated, absolute glaucoma will result where there is total blindness, with lack of pupillary response and reflex to light. The eye also has a stony

appearance. Most forms of glaucoma are slow and painless, but there are some that present sudden decrease in vision with ocular pain, red eye and seeing halos. Other signs and symptoms may also vary depending on the type of glaucoma.

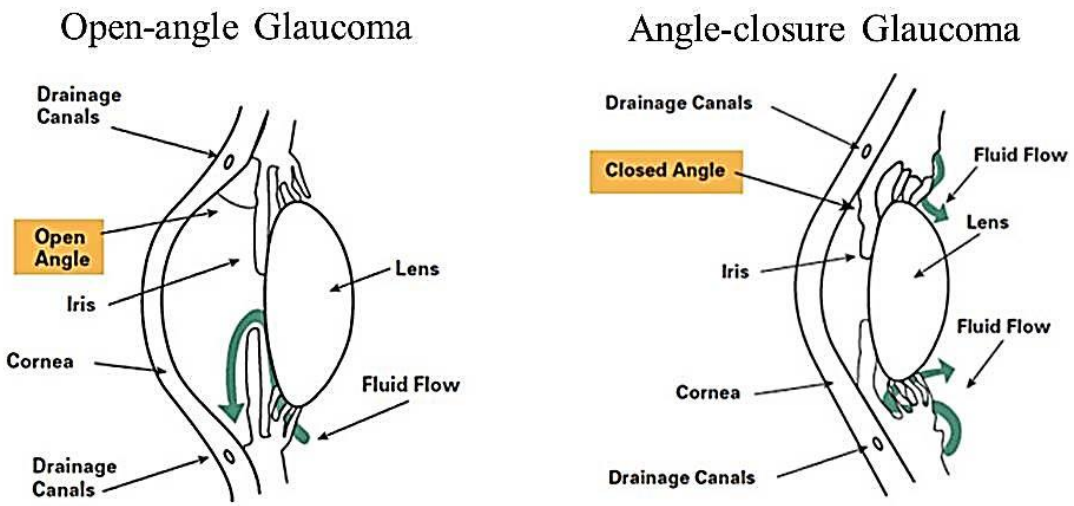

Figure 2. Categorization of glaucoma. The various forms of glaucoma can be grouped into open-angle and angle-closure glaucoma, depending on the iridocorneal angle. (Image adapted from www.glaucoma.org).

About 60 types of glaucoma are known, which are broadly divided into open-angle and closed-angle (Fig. 2). The 'angle' refers to the area between the iris and the cornea through which more than 98% of the aqueous humour flows to exit the eye through the various outflow pathways. The trabecular meshwork (TM) which is located at the base of the angle, adjacent to the cornea, is responsible for draining majority of the aqueous humour. The iridiocorneal angle is narrowed or even completely closed in closed-angle glaucoma, blocking the outflow of aqueous humour via the TM, causing a buildup and consequently rise in IOP. Developmental defects, secondary issues and trauma account for this class of glaucoma. In open-angle glaucoma, the iridocorneal angle is unaffected and the aqueous can freely pass through it to enter the outflow pathways. However, abnormalities in the outflow tissues, particularly the TM, lead to increased resistance and impede outflow. Although source of the disease may differ, both classes elevate the IOP which contributes to the optic neuropathy.

Angle-closure glaucoma can be further subdivided based on the mechanism of outflow obstruction that reduces the iridocorneal angle. In primary angle-closure glaucoma, the growing lens in the shorter than average eye may produce a pupillary block by impeding the

outflow through the pupil. This creates a pressure gradient across the iris which pushes it forward, mechanically covers the TM and impedes outflow. Secondary angle-closure glaucoma such as that caused by the adherence of the iris to the lens in uveitis (inflammation of the uvea comprising of iris, ciliary body and choroid) or by formation of blood clot due to trauma, also induces a pressure gradient across the iris, generating a 'push' mechanism and causes it to bow forward.

Developmental defects may also alter the chamber angle. Primary congenital glaucoma arises from the arrested movement of the iris and ciliary body away from the TM during development, and instead they cover the TM by remaining in close proximity to it. Various other forms of chamber angle malformation also exist such as anidridia, Reiger's syndrome and Peter's syndrome. Aberrant development of the lens and zonule can also affect the chamber angle by secondary pupillary block. Examples include microspherophakia (lens is spherical instead of being oval-shaped), homocystinuria (methionine metabolism disorder which can cause malpositioning of lens) and Marfan syndrome (a connective tissue disorder which dislocates the lens).

Although the chamber angle is normal in open-angle glaucoma, obstruction to outflow is at the level of filtering tissues, specifically the TM, and the mechanism of obstruction depends on the type of disease. Primary open-angle glaucoma is believed to result from dysfunctional TM, as is also the case for juvenile open-angle glaucoma (associated with impaired development of the TM) and corticosteroid-induced glaucoma. Toxic compounds can damage the trabecular cells and lead to secondary open-angle glaucoma like in chalcosis (copper poisoning) and siderosis (iron deposition in tissues).

TM can also be occluded by cellular debris and hinder the outflow. Inflammatory conditions may cause the meshwork to be obstructed by macrophages and induce hemolytic, melanomalytic and phacolytic glaucomas. Degenerated red blood cells clog the trabecular meshwork in ghost-cell glaucoma. Pseudoexfoliation syndrome and pigmentary glaucoma are caused by the liberation of fibrillary material from the lens capsule and pigments from the iris pigmented epithelium respectively. Such aggregates accumulate in the anterior segment structures including the TM. It is apparent that most forms of open-angle glaucoma are due to structural and/ or functional disruption of the meshwork, and underscore the importance of the TM in maintaining normal IOP and ocular health.

In a small group of open-angle glaucomas, the aqueous flow through the TM is unaffected. In these instances, the obstruction is post-trabecular. Vascular conditions can increase the episcleral venous pressure or orbital pressure and impede the outflow. Alkali burns can damage collector channels and aqueous veins which also hamper the drainage and culminate in glaucoma. There are numerous other forms of glaucoma, each caused by their own means of interference to the aqueous flow.

Despite the many types of glaucoma, screening and diagnosis remains the same. Individuals beyond 40 years and those with a family history of glaucoma and/ or hypertension are recommended to undergo regular screening. During the screening, the visual fields will be checked with frequency doubling technology perimetry and the optic nerve will be evaluated ophthalmoscopically. Patients with abnormalities in the visual field will be referred to an ophthalmologist for further evaluation. The optic disks and visual fields will be examined, and measurements of IOP and central corneal thickness will be taken. A patient will be diagnosed with glaucoma upon findings of the characteristic pattern of optic nerve damage and corresponding nerve fiber layer deficit of visual field. Gonioscopy will then determine the subtype of glaucoma by checking the anterior chamber angle using a mirrored contact lens prism. Individual tests can then be done to identify the cause of obstruction to aqueous outflow. Depending on the severity of the disease, hypotensive therapies of drugs, surgery or both may be recommended.

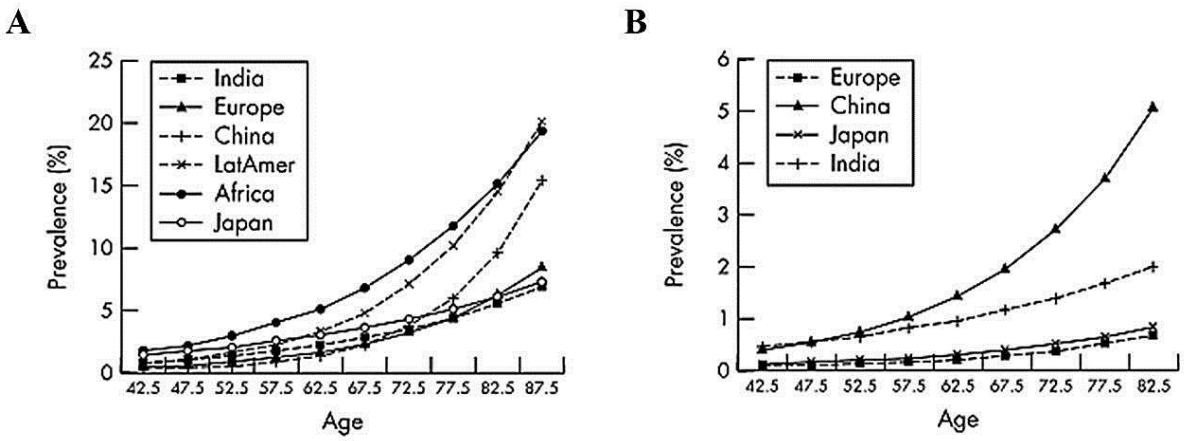

Figure 3. Prevalence data for age-related prevalence of open-angle (A) and angle-closure glaucoma (B). Highest prevalence is in the African region for open-angle glaucoma and in China for angle-closure glaucoma. (Source: Quigley and Broman, 2006).

Population based studies project 60.5 million people affected with glaucoma in 2010 worldwide, and this number is predicted to rise by 20 million over the next decade [1]. It is evident that glaucoma is a complex disease with its prevalence influenced by age, ethnicity, gender, family history and environment among other multiple contributory factors. Glaucoma can manifest at any age, but it is six times more common in people beyond their 60s. The distribution of glaucoma subgroups varies from population to population. Open-angle glaucoma has higher world prevalence at 1.96% in 2010, with it being most prevalent in the African region (Fig. 3A), while the prevalence of angle-closure glaucoma is about 0.69%, and most common in the Chinese population (Fig. 3B). Both subgroups are at lowest prevalence in Europeans and Indians. Women are more affected by glaucoma at 59.1% of the world population, due to greater prevalence of angle-closure glaucoma in women and better longevity.

Certain forms of glaucoma have higher penetrance in families with affected members, indicating genetic susceptibility. Genetic linkage studies have identified several associated genes, but their exact function in the pathophysiology of the disease remains unknown. No single environmental factor has been clearly associated with glaucoma, but various factors that influence ocular pressure like diet, exercise and smoking have been found to contribute to the disease. So far, only family history is recognized as a major risk factor for susceptibility. But as a multifactorial disease, it is important to understand risk factors better so that an improved classification of high risk group can be established and early screening can be targeted on communities with greater susceptibility. This will enable the disease to be identified early, before significant vision loss has occurred.

The World Health Organization has recognized glaucoma as a major world health concern as 8.4 million are estimated to be bilaterally blind from the disease in 2010 and the number will continue to rise to possibly 11.1 million by 2020 [1]. In addition, although not totally blind, a significant proportion of the world population already has deteriorating vision which hampers everyday life and pleasures. Many societies are aging which disproportionately increases the number of affected individuals in the older age group and places an economic burden for the country and the working class to care for them. So, glaucoma has far reaching consequences, by not only affecting the individual, but also through its social and economic impacts on the society. It is, therefore, crucial to better understand the disease to improve diagnostic and therapeutic approaches which should be made accessible worldwide.

1.2 Primary Open-Angle Glaucoma

The most common form of glaucoma is primary open-angle glaucoma (POAG, [OMIM #137760]), accounting for the major portion of the 45 million open-angle glaucoma cases in the world [1]. It was first described under the term glaucoma simplex by Haffmans in 1861 [2]. Since then its interpretation has been modified substantially. The current definition of the disease by the American Academy of Ophthalmology (AAO) states POAG as a 'progressive, chronic optic neuropathy in adults' with a 'characteristic acquired atrophy of the optic nerve' [3]. The means of obstruction cannot be visualized and it is not caused by secondary reasons like maldevelopment or clogging of outflow channels by detached material, and hence the term primary. Diagnosis of POAG is made with the findings of damage to the optic nerve and corresponding loss of visual field, in the event of an open anterior chamber angle, and exclusion of other optic neuropathies (e.g., induced by cytomegalovirus infection, ischemia or deficiency of vitamin B12) and other types of glaucoma. Elevated IOP is often present, but not necessary for diagnosis.

Early symptoms are unnoticed by affected individuals who generally only become aware of the condition after significant loss of vision in the advanced stage, like most forms of glaucoma. This is due to asymmetric deterioration of the visual fields. Patients discern the atrophy as they start missing stairs, see portions of words lost when reading and have difficulties performing day to day tasks like driving. By this stage, considerable irreversible damage has occurred to the visual field, and the only option is to slow down the disease progression with treatment.

The two major risk factors for POAG are age and IOP. The onset is mostly detected beyond the 50s. Epidemiology study of POAG patients in 8 populations found 7% were less than 55 years old, 44% were within the age group of 55-74 years and the remaining largest portion were older [4]. Other studies have also corroborated the observation based on incident and prevalent data [5], [6]. Accordingly, the prevalence of POAG increases exponentially with age.

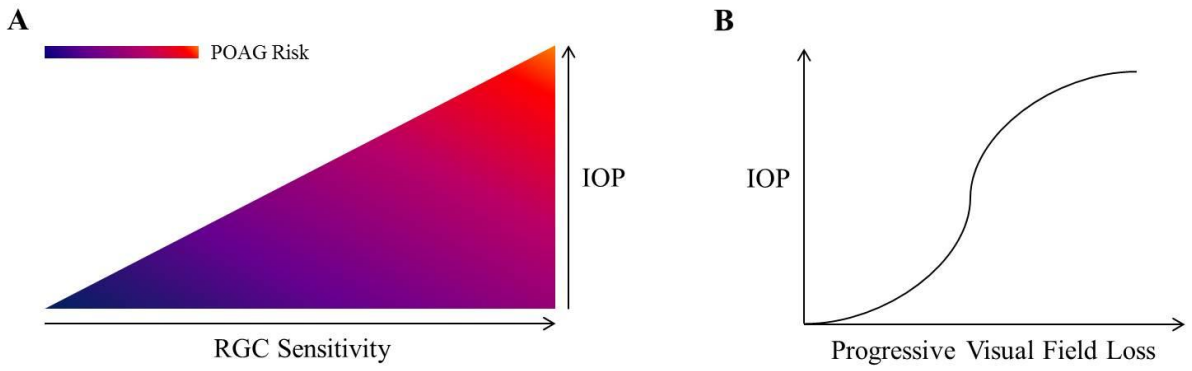

Figure 4. Association of IOP and RGC sensitivity with POAG risk. (A) IOP and sensitivity of RGC are positively correlated to the incidence of POAG. (B) IOP has dose-response effect on the loss of visual field as the disease progresses.

IOP is not always high in POAG subjects so this further classifies POAG into elevated-pressure glaucoma and low-pressure glaucoma (also known as normal-tension glaucoma). IOP is elevated (> 21 mmHg) in two thirds of the patients, while the rest have IOP that is within the average range, but often in the upper fraction. Central corneal thickness influences IOP measurement but several studies fail to take it into account, and thus may have resulted in inaccurate IOP reading.

It is also believed that factors that sensitize the RGC may play a role in their susceptibility to damage. Vasospastic diseases are common in patients with low-tension glaucoma. It is likely that vascular disorders can limit blood flow to the RGC and make them vulnerable to damage albeit the low IOP. Other determinants like genetics and lifestyle may also predispose the RGC to injury. It has been postulated that nature of the optic disc such as size and shape, and attributes of the lamina cribrosa can cause the variation in susceptibility to IOP too [7]–[9]. A combination of RGC sensitivity and IOP seems to determine the manifestation of POAG, where increase in sensitivity and IOP raise the risk of POAG (Fig. 4A). High sensitivity and elevated IOP will almost always result in the disease. Dose-response correlation exists between IOP and progressive visual field loss once the disease manifests, with extremely high IOP accelerating the loss of visual field (Fig. 4B). Hence, IOP is an important risk factor that determines both manifestation and progression of the disease.

There are other factors that contribute to the increased risk of POAG which include myopia, gender, family history and ethnicity. Epidemiologic studies in several major populations across the globe have found that people with myopia have higher prevalence of POAG than

control subjects [10]–[12]. Recently, positive correlation between axial length and incidence of POAG has been established [13]. In axial myopia where the axial length is longer than normal, the scleral support at the optic disc is weak, and consequently leads to an increased vulnerability to damage. More women than men are affected by POAG mainly due to their greater longevity. People with first degree relatives affected with POAG have higher odds of having POAG. This could be attributed to the several genetic linkages that have been established for POAG which predispose members of an affected pedigree to POAG more than others, as will be discussed later. People of African descent have the highest prevalence of POAG in the world, followed by Latinos, while it is relatively low for Europeans and Indians, indicating racial influence on the disease susceptibility.

Unlike certain forms of glaucoma known to be associated with diabetes mellitus and systemic hypertension, it is still unclear whether they contribute to POAG due to contradicting reports [14]–[17]. Atherosclerosis, migraine, C reactive protein, body mass index and smoking are some traits found to co-occur with some glaucoma types, but no association was found with POAG [14], [18]–[21]. Differences in the disease mechanism could account for this disparity.

It is widely believed that increase in resistance in the outflow pathway leads to the buildup of aqueous humour, increasing the IOP which damages the optic nerve and results in POAG. The site of resistance is generally accepted to be at the level of the TM due to abnormal findings in the meshwork of POAG specimens. Increase in extracellular matrix material and significant decline in the trabecular cells have been observed in the diseased tissue. These abnormalities in the TM are believed to interfere with its filtering and phagocytic mechanisms that are essential in aqueous drainage to maintain healthy IOP. The mechanism behind TM dysfunction is not known, but extensive studies have shown its involvement in the disease pathology which will be discussed in detail in later sections.

In fact, POAG is induced in animal models commonly using laser photocoagulation of the TM, where laser is applied circumferentially on the tissue, resulting in its scarring [22]. The clogging of intertrabecular spaces with excessive matrix then transiently elevates the IOP. Optic disc cupping, thinning of nerve fiber rim and selective loss of RGC that follow are all typical changes in the glaucomatous eye. Other perturbations to the meshwork in the form of latex microspheres [23] and autologous fixed red blood cells [24], [25] are also utilized in

open-angle glaucoma models, underscoring the importance of the meshwork integrity for IOP maintenance.

1.3 Anatomy and Development of the Eye

The eye (clinically known as the globe) is a slightly asymmetrical spherical structure that lies in the orbital cavity, held in place by extraocular muscles which rotate it so as to focus the image onto the fovea centralis in the retina to maximally focus the image. The detail is then transmitted to the brain through the optic nerve for processing and perception.

The globe consists of three different layers, namely the external fibrous tunic, the vascular tunic and the retina internally (Fig. 5A). The cornea and sclera form the outermost layer of the globe, with the cornea forming one-sixth of the coat. The cornea is the anterior, transparent part of the globe where most refraction of light occurs and together with the lens allows the image to be sharply focused onto the retina. It is an avascular tissue, comprising of five distinct layers with the multicellular epithelium anteriorly and single layer of endothelial cells posteriorly. A mostly collagenous stroma exists in the middle, bordered by the Bowman's layer and Descemet's membrane which are essentially basement membranes for the corneal epithelium and endothelium respectively.

Cornea is continuous with the sclera which appears as the 'white of the eye' on its anterior side behind the conjunctiva and this junction is called the limbus. The sclera is a fibrous tissue appended to extraocular muscles and is part of the supporting wall of the globe. It is surrounded by a thin film known as Tenon's capsule which separates the globe from the other orbital tissues and is continuous with the muscle sheaths such that the globe moves within this capsule. Sclera also blends with the dura of the central nervous system posteriorly and this is the site where the optic nerve exits through the lamina cribrosa.

Situated at the corneoscleral limbus is the TM, a spongy tissue about 1 mm wide, which is responsible for the filtration of most of the aqueous humour from the eye, together with the canal of Schlemm (also termed scleral venous sinus), a circular canal posterior to it (Fig. 5B). The Schlemm's canal is made up of a single layer of endothelial cells and connects to the aqueous veins in the sclera and allows the aqueous to drain into the bloodstream via the

scleral plexus. TM is continuous with the scleral spur which is the origin of the ciliary body. These ocular structures are present at the chamber angle and play an important role in aqueous humour drainage.

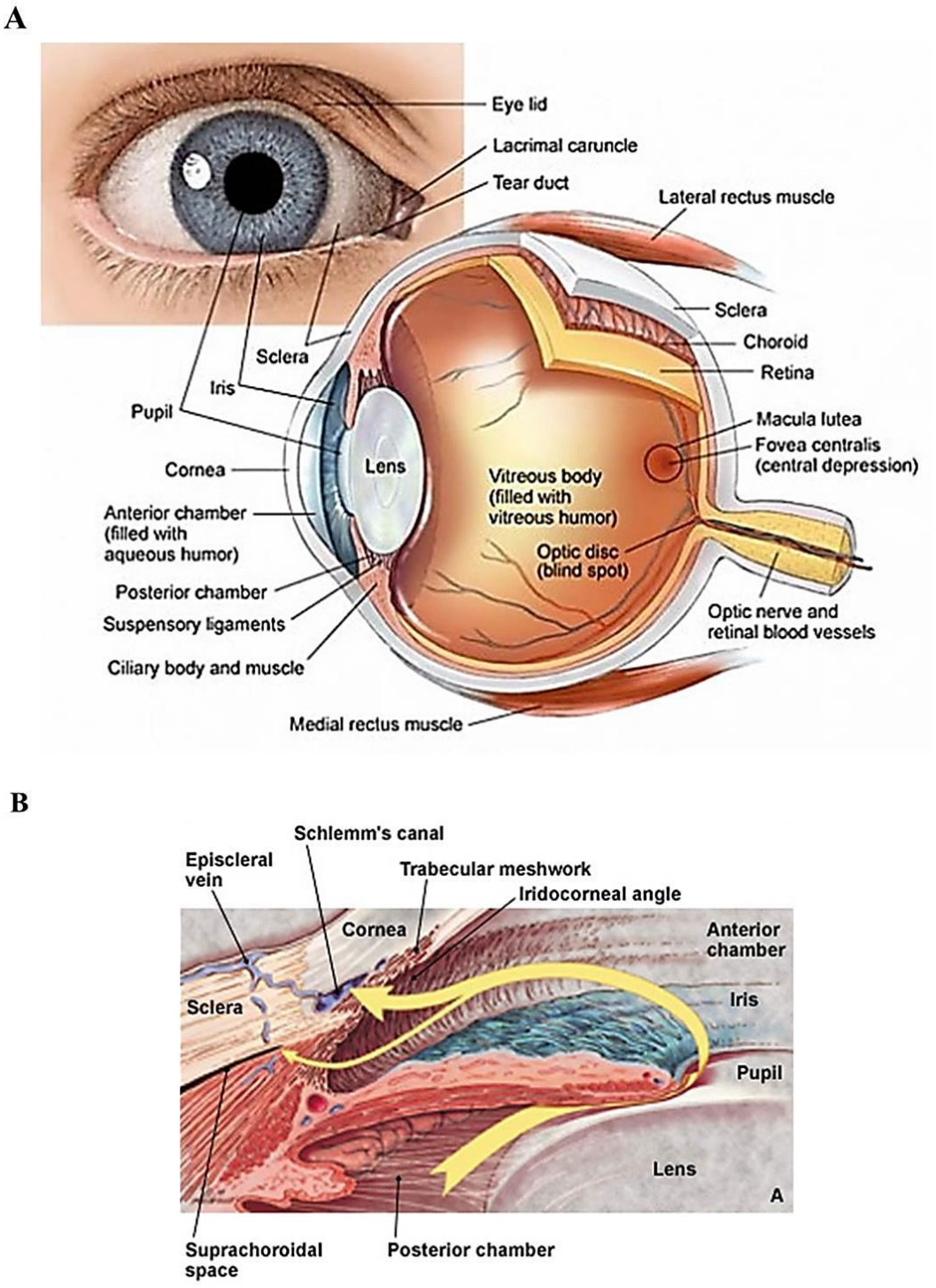

Figure 5. Anatomy of the human eye. (A) Cross section of the eyeball through its axial length as seen above. (Image source: phygrls via wikispaces). (B) Ocular structures at the iridocorneal angle. Aqueous humour exits the eye predominantly via the trabecular meshwork outflow pathway. (Image source: Andrews, 1999).

The middle tunic consists of the choroid, ciliary body and iris. Choroid is a highly vascular, pigmented coat beneath the sclera and it contributes to one of the two circulations of the eye. Its arteries are received from the ophthalmic artery and they provide oxygen and nutrients to the outer layers of the retina. Ciliary body connects the choroid with the iris and it contains ciliary muscle and ciliary processes. It is also connected to the lens via zonule fibers. Ciliary muscles take part in the accommodation process, where they contract or relax to change the shape of the lens (a biconvex, crystalline body behind the iris) according to the distance of the object to focus it. Ciliary processes are arranged in a circle, posterior to the iris and secrete aqueous humour. Iris is a pigmented circular muscle with an aperture in the middle, the pupil, which allows light to enter the eye.

The retina is the innermost layer of the globe and is divided into two main strata of external, pigmented stratum and internal, transparent nervous stratum. Retina is nourished externally by the choroid and internally by the central retinal artery derived from the optic artery. The internal stratum consists of the ganglionic cells, interneurons and photoreceptors (rods and cones), while the external stratum is formed by the pigmented epithelium. Light penetrates through the transparent nerve layers to reach the photoreceptors, which in turn transmit the signal to the interneurons. The signal is then transferred to the ganglionic cells which transmit it through their axons that extend through the retina and assemble as optic nerve at the optic disk. Stimulation from the inverted image projection on the retina is eventually converted into upright perception of the object upon higher order processing in the visual forebrain.

Retina also contains definite areas that are slightly different from the rest of the retina, specifically the macula and optic disc. Macula is distinguished as a small, yellowish area of the retina which contains the fovea centralis, a slight depression, which in turn has a small pit called the foveola. The faveola has only cones and participates in detailed colour vision. The optic disc is insensitive to light since it is free of photoreceptors and hence is the ‘blind spot’. At the center of the optic disc where the nerve and vessels enter/ leave, a depression known as ‘cupping’ is present which becomes pronounced with glaucoma.

There are three chambers of fluid in the globe, namely the anterior chamber located between the cornea and iris, the posterior chamber bordered by the iris, zonule fibers and lens, and the vitreous chamber between the lens and retina. Both the anterior and posterior chambers are filled with aqueous humour, whereas the vitreous chamber is filled with a more viscous mass,

called the vitreous body. Only the aqueous humour level affects IOP since it fluctuates, while the vitreous humour does not contribute to it as it is fairly constant throughout lifetime. The eye develops from two of the three germ layers, namely the ectoderm and mesoderm. The major period of organogenesis is between three to nine weeks of gestation and it continuous to develop postnatally as well. The anterior part of the neural tube derived from the ectoderm forms the forebrain and on each side of the primitive forebrain, an evagination called the optic vesicle develops (Fig. 6). The optic vesicle is surrounded by paraxial mesoderm. As the optic vesicle enlarges, it touches the surface ectoderm which induces the latter to proliferate forming the lens plate at the point of contact and it detaches as the lens vesicle. The optic cup continues to grow and invaginates to form a bilayered optic cup. The optic cup develops into the retina with the external layer differentiating into the external pigmented coat, while the internal layer forms the internal neural coat. The two layers eventually fuse and the intraretinal space disappears.

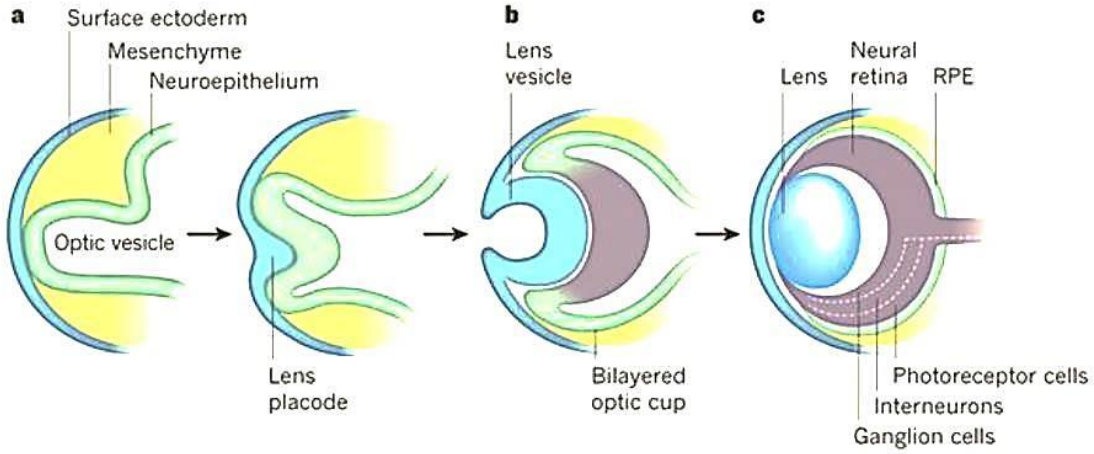

Figure 6. Development of the human eye. (a) The mesenchyme infiltrates the space between the optic vesicle and surface ectoderm. The optic vesicle enlarges and touches the surface ectoderm, where it induces the formation of lens placode. (b) The lens plate grows, invaginates and detached as lens vesicle while the optic vesicle folds inward to form the bilayered optic cup. (c) The lens lies on the tips of the optic cup which develops into the multilayered retina. TM is derived from the mesenchyme between the surface ectoderm and lens. (Image source: Ali & Sowden, 2011).

The aqueous chambers form under the influence of the lens. The anterior chamber develops as a space in the mesenchyme infiltrating the lens and surface ectoderm. The anterior mesoderm becomes the stroma and endothelium of the cornea, while the corneal epithelium is formed by the overlying surface ectoderm. TM and the Schlemm's canal are also derived from the anterior mesoderm. The posterior mesoderm gives rise to the iris stroma and the

surrounding mesenchyme develops into the choroid and sclera which will envelop most of the globe. The extraocular muscles and ciliary muscles are also derived from the mesenchyme. Cells in the developing lens which lies on the optic cup multiply and deposit lens fibers to make it functional.

The lips of the optic cup contribute to the pigmented epithelium, dilator and constrictor muscles of the iris, and epithelium of the ciliary body. Mesoderm inside the optic cup forms the primary vitreous body that gives rise to the zonule fibers between the lens and ciliary body. The primary vitreous body later degenerates and becomes the acellular vitreous humour. The globe is protected by the eyelids which are folds of ectodermal tissue with a mesenchymal interior.

In summary, the globe develops from the ectoderm and mesoderm. The surface ectoderm gives rise to the lens, corneal epithelium and epithelium of the ocular appendages including eyelids and conjunctiva. The neural ectoderm develops into multiple layers of the retina, ciliary epithelium, pigmented epithelium and muscles of the iris, while mesoderm gives rise to corneal endothelium and stroma, sclera, TM, Schlemm's canal, iris stroma, ciliary muscles, choroid, vitreous humour, extraocular muscles and bony orbit. Although most ocular structures have a single source of origin, several such as the cornea, ciliary body and iris have dual origin.

1.4 Aqueous Humour Outflow Pathways

IOP is generated from the secretion of aqueous humour by nonpigmented epithelium in the ciliary processes. The cells actively transport nutrients and ions attained from circulation into the posterior chamber. This creates an osmotic gradient that pulls water into it as well. Some of the aqueous humour is also obtained from ultrafiltration of interstitial fluid in the ciliary body.

The aqueous humour is a transparent, colourless fluid that is similar in composition to the plasma but has lower protein content. It transports oxygen, amino acids and glucose to the avascular tissues in the eye and removes waste products. It also presents a reducing environment, with its composition of glutathione, ascorbic acid and low oxygen tension,

preventing oxidative cross-linking of the lens protein. Structurally, the aqueous keeps the eye inflated and also contributes to the refractive index of the eye. The aqueous moves past the equator and anterior surface of the lens into the pupil and enters the anterior chamber (Fig. 7).

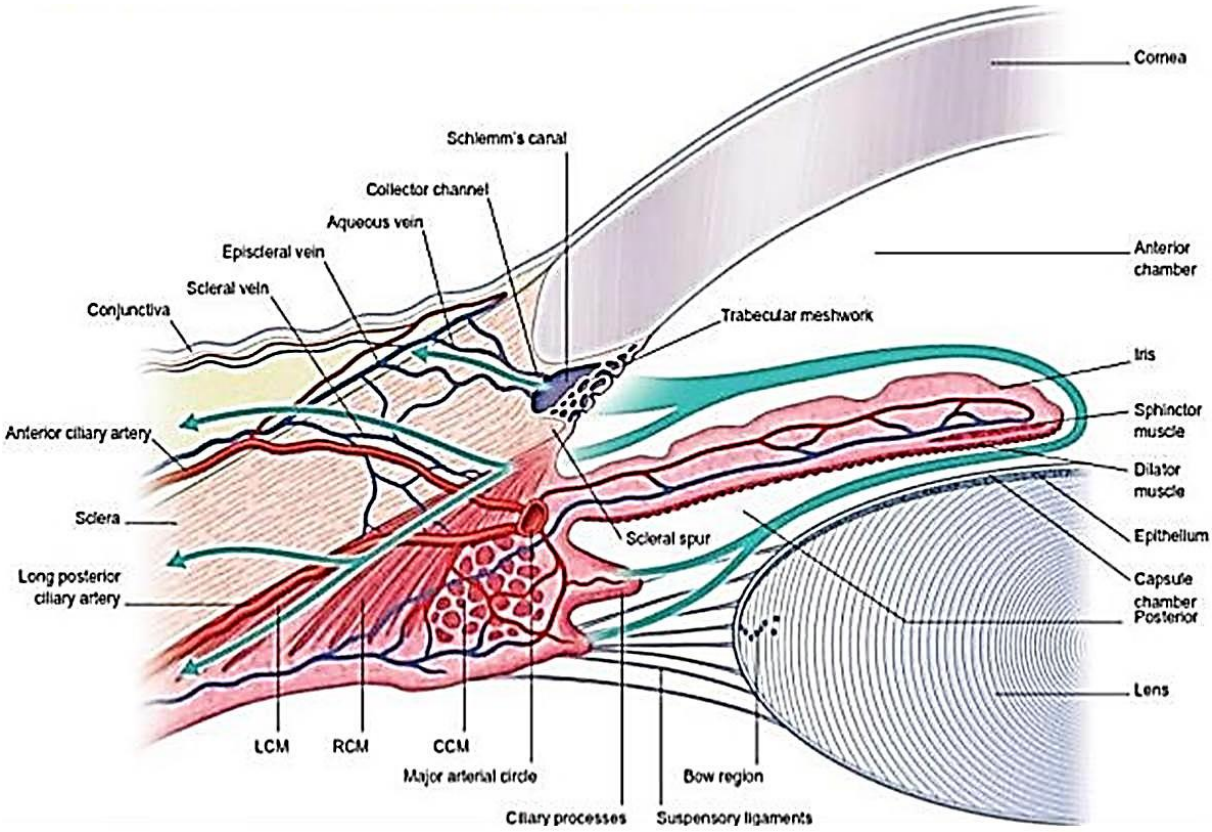

Figure 7. Secretion and outflow of the aqueous humour. The aqueous secreted by the ciliary processes into the posterior chamber flows by the lens, through the pupil and enters the anterior chamber to leave via the conventional or uveoscleral pathway.

The aqueous humour exits the anterior chamber via the uveoscleral pathway or the conventional pathway (trabecular outflow pathway) which accounts for > 90% outflow (Fig. 7). The uveoscleral pathway starts at the iris root where the aqueous enters and moves through the ciliary muscles, then suprachoroid and into the sclera to leave via the vortex veins. This outflow is pressure-independent unlike the conventional pathway where the inherent resistance posed by tissues of the outflow pathway generates a pressure gradient. The aqueous moves down the pressure gradient through the TM at the corneoscleral junction, Schlemm's canal and into collector channels connected to aqueous veins that drain into the episcleral vein which eventually empties into the optic vein. The greatest resistance to outflow is provided by the trabecular meshwork, specifically at the area overlying the Schlemm's canal.

So, the outflow pathways allow the aqueous to re-enter circulation and maintain IOP within the normal range of 10 – 21 mmHg. The trabecular outflow pathway plays a major and indispensable role in this, and thus is vital for healthy vision.

1.5 Structure and Function of the Trabecular Meshwork

The TM is essentially a spongy wedge-shaped tissue at the corneoscleral limbus and an important component of the conventional outflow pathway (Fig. 8A). It surrounds the circumference of the cornea and is discontinuous at random places. TM originates from the periocular mesenchyme consisting of cells derived from the neural crest and cranial paraxial mesoderm [26]. The cells differentiate and move apart as fenestrations form which become deposited with extracellular fibers to establish a network of beams and sheets. TM morphogenesis is accomplished by birth, but it undergoes modifications with age as will be discussed later.

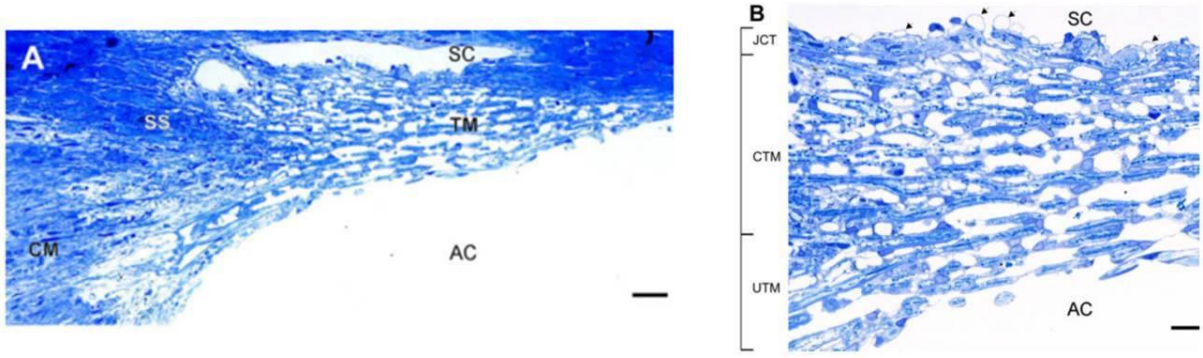

Figure 8. Light micrograph of a section through the anterior segment. (A) TM is located at the chamber angle of the anterior chamber (AC) specifically at the corneoscleral limbus and anterior to the Schlemm's canal (SC). It is continuous with the scleral spur (SS) and ciliary muscles (CM) posteriorly. (B) TM can be divided into three anatomical regions of uveal trabecular meshwork (UTM), corneoscleral trabecular meshwork (CTM) and juxtacanalicular tissue (JCT). (Scale bars: 20 µm (A), 5 µm (B); Image source: Tamm, 2009).

In primates, TM is divided into three compartments of uveal meshwork, corneoscleral meshwork and juxtacanalicular connective tissue (JCT), with the uveal layer closest to the chamber angle (Fig. 8B). The uveal meshwork consists of about 3 layers of trabecular beams and connective tissue extension from the ciliary body and iris. The corneoscleral meshwork, adjacent to it, is comprised of 8 - 15 layers of perforated laminar sheets or lamellae. The

trabecular beams and lamellae are connected between layers, forming a porous structure through which the aqueous flows to enter the JCT. The JCT is the thinnest part of the TM which measures only about 2 - 20 µm, but majority of the resistance in the TM to outflow is localized here. The JCT cells are more stellate and dispersed as 3 - 5 layers in the loose connective tissue. This region is disorganized compared to the regular arrangement of the previous two compartments, thus giving rise to its alternative term, cribriform tissue. The JCT cells reside on a disordered basement membrane and are attached to each other and the inner wall of the Schlemm's canal by their cell processes. The aqueous is transferred via gaint vacuoles and intracellular pores in the endothelial cells of the Schlemm's canal into its cavity to enter collecting channels and subsequently drains into the episcleral vein.

The intertrabecular space decreases through the meshwork on the whole and the greatest resistance to outflow is at the JCT, with limited contribution from the other strata. The inner wall of the Schlemm's canal is also believed to contribute to the resistance with its tight junctions. While most of the TM participates in the bulk flow of aqueous, there is a small anterior portion that inserts under the cornea, the TM insert region, which does not filter the aqueous. Though the insert region does not have direct functional contribution, it is essential in maintaining a healthy tissue since it is postulated as the niche for TM stem cells.

A diverse array of structural proteins composes the extracellular matrix material (ECM) of the TM. The trabecular beams and lamellae both have a core of elastic fibers surrounded by sheath material which is further engulfed by collagenous fibers (mostly type I and III) on which the basal lamina rests, covered by a continuous layer of flat trabecular cells [27]. Aggregates of long-spacing collagen are also present between the elastic fibers and basal lamina. The basal lamina is considered the true basement membrane of the TM and its components differ from that of the JCT basement membrane. The basal lamina contains collagen IV, laminin as well as other ECM constituents [28], [29] while collagen type VI and fibronectin make up the JCT basement membrane which tether to the Schlemm's canal endothelial cells and ECM of the JCT [30]–[32]. The intertrabecular spaces also contain proteoglycans, hyaluronan, and other secreted proteins such as thrombospondin 1, secreted protein, acidic, cysteine-rich (SPARC) and myocilin [33]–[37]. The aqueous is filtered by these ground compounds which are partly responsible for the resistance posed by the TM, particularly at the JCT. Modulation of the ECM is a function performed by the TM cells to maintain IOP within the normal range.

The TM cells perform two essential functions of phagocytosis of cell debris in the aqueous humour and modulation of the ECM environment [38], [39]. Animal studies have shown TM cells to uptake a variety of small particles from bioparticles to synthetic compounds *in vivo*, by cultured TM cells and perfused organ cultures [40]–[42]. The phagocytic rate seems to depend on the type and size of the particle. In a study using later microspheres, erythrocytes and zymosan particles (which are in increasing order of size), the latex microspheres were engulfed more often than the others by the TM in a perfusion organ system [42]. The ingested latex microspheres and erythrocytes were seen in all three strata of the meshwork, but uptake of zymosan was largely in the upper two regions, indicating size exclusion by the transverse increasingly small pores. So, the TM acts as a pre-filter that restrains the passage of large particles and in addition phagocytose them together with other cell debris in the aqueous fluid.

The TM is capable of homeostatic response to IOP fluctuations by modulating the ECM accordingly to reestablish it within the narrow healthy level [39], [43]. IOP is not a constant measure, rather is altered by a number of factors such as fluid intake, exercise, heart rate, body orientation, consumption of alcohol and medication. The TM cells sense the pressure change as mechanical stretch/ distortion, and mounts on a highly coordinated sequence of response to adjust the ECM resistance. Integrins and other cell adhesion proteins are believed to detect the stretch and initiate ECM turnover under the control of autocrine and paracrine growth factors such as transforming growth factor beta 2 (TGFβ2), connective tissue growth factor (CTGF), and bone morphogenetic proteins (BMPs) [44].

ECM turnover involves ECM degradation, deposition of modified ECM and subsequently adjustment to resistance. Mechanical stretch increases the expression of matrix metallopeptidases, MMP2 and MMP14, that breakdown ECM [45]–[47]. Vittal and colleagues also found increased expression of the ECM proteins, fibronectin, tenascin C, SPARC, some collagens, matrix gla protein (MGP) and cell-surface receptors including TGFβ receptor complexes, CD44 and vascular cell adhesion molecule 1 after stretching. At the same time, syndecan 1, versican and thrombospondin 2 were among other downregulated genes, indicating ECM remodelling [48]. Mechanical stretch also promotes alternative splicing of some mRNAs, including fibronectin, tenascin C and *CD44* [48], [49]. The newly modified ECM now offers less resistance, allowing more aqueous humour to flow through and alleviates IOP.

In addition to ECM remodelling, TM cells can also alter their shape to modulate resistance. Evidence of contractile filaments and alpha-isoactin filaments, a set of smooth muscle-specific components, in the TM cells postulated a contractile role to the TM [50]. Electrophysiological methods have demonstrated the contractility of both TM strips and cultured TM cells, although the maximal force is much less than that of the ciliary muscle [51]. TM cells were also not absolutely dependent on extracellular Ca^{2+} unlike ciliary muscle, as they utilize a Ca^{2+}-independent pathway as well for contraction. Though small, its contractility seems significant enough to influence the outflow as demonstrated by the bovine anterior segment with smooth muscle-specific drugs [52]. Cytoskeletal drugs targeting microtubules and microfilaments also affect the resistance by inducing contraction or relaxation of TM cells, which in turn alter the dimensions of the intertrabecular spaces [53]. Although the exact contractility mechanism is unknown, mounting evidence support the notion that TM cells alter their shape and geometry by contracting or relaxing to modulate the outflow resistance as necessary. Increased contractility will limit the outflow, while relaxation will enhance it.

Another indirect yet indispensable function performed by the TM is that it acts as a pre-filter, dissipating the pressure of the aqueous humour which the Schlemm's canal could otherwise not withstand. The flow resistance in the TM allows the aqueous pressure to decrease sufficiently by 7 - 9 mmHg to attain a level suitable for entry into the Schlemm's canal. As can be seen, the TM carries out several vital functions of clearing cell debris in the aqueous humour, maintaining IOP within the normal range by altering its outflow resistance and being a support structure to the Schlemm's canal. Therefore, proper functioning of the TM is essential for healthy vision, or else it will have detrimental effects that culminate in vision loss.

1.6 Pathophysiology of POAG

TM dysfunction and pathologic changes that result from it leads to the manifestation of POAG. Grant and colleagues discovered increased flow resistance in the TM with POAG, thus identifying it as the root cause of the disease [54]. Since then much progress has been made in elucidating the changes accompanying TM malfunction through histological,

expression and functional studies which all report significant differences between the glaucomatous and healthy tissues.

Significant decline in TM cell number is observed in the diseased tissues compared to age-matched controls [55]. Glaucomatous tissues obtained at trabeculectomy or autopsy had reduced cellularity (cells per unit area) than control tissues, with age-related decline being similar between both groups. The cell loss was apparent in all three regions of the TM, but increased loss was seen in the deeper layers than outer ones. Remnant cells in the meshwork seem to be under stress, with the increased expression of stress proteins, crystallin alpha B and inducible nitric oxide synthase. This may contribute to the higher number of apoptotic cells detected by terminal deoxynucleotidyl transferase-mediated dUTP nick end labeling (TUNEL) assay in the diseased tissues [56]–[58]. Mitochondrial defects have also been reported which may perturb Ca^{2+} regulation [59].

Genome-wide expression study by Liton and group found altered expression of certain genes with the pathology [60]. Genes involved in inflammation and acute-phase response, G-protein signalling, lipid metabolism and ionic transport were upregulated while antioxidants ceruloplasmin and paraoxonase 3, members of vacuolar protein sortin 10 domain receptor family and solute carrier family were downregulated. This indicates intrinsic factors are differentially expressed in the pathology and may compromise TM function, leading to reduced aqueous outflow. The combination of cell loss and compromised function of the damaged remnant cells in the TM is likely resulting in disease development, although exact details of this process is unclear.

Besides the pathologic changes in TM cells, the trabecular and ECM networks are also affected in POAG individuals. Thickening and fusion of the trabecular beams and lamellae with increase in long-spacing collagen and greater amount of modified ECM are seen in the glaucomatous TM [61]. Accumulation of ECM components, fibronectin, elastin and fibrillar material change the ECM composition [62], [63]. Glycosaminoglycan profiling also found an increase in chondroitin sulfate and decline in hyaluronan in the JCT of diseased tissues compared to normal controls [64], [65].

Deposition of sheath-derived (SD) plaques, which are essentially aggregates of ECM, fibrillar components and glycoproteins, increased as well especially within the JCT [61], [66]. The

amount of plaque material correlated with the severity of optic disc damage quantified as axonal loss, indicating elevated resistance caused by SD-plaque formation. Mathematical modeling suggests an increase in TM stiffness with the rise in ECM and structural components [67]. Hence, trabecular thickening together with the increase and modification of ECM components minimize the fenestrations in the meshwork and reduce the outflow facility, as well as increase the rigidity of the tissue.

Moreover, calcification markers *MGP* and *BMP2* are upregulated in the diseased tissue, suggesting calcification of the TM, which is a process known to increase stiffness [68]. Moreover, the formation of more cross-linked actin networks (CLANs) in glaucoma lines may compromise their contractility [69], which is essential in adjusting the cell shape in order to modulate the resistance. These evidences indicate that cytoskeletal changes in the TM cells affect the distention of the tissue and in turn impair aqueous outflow.

The extensive pathological changes in the cells and ECM of the meshwork described could account for the marked resistance detected in the glaucomatous TM. The exact molecular mechanism leading to these changes remains unknown.

Increased resistance posed by the dysfunctional TM hinders the passage of fluid through it and cause buildup in the anterior chamber. Consequently, the IOP increases and exerts additional pressure on the posterior structures, particularly the optic disc, where RGC axons assemble into the optic nerve (Fig. 9A). In the center of the optic disc is a slight depression, the optic cup, surrounded by neurosensory rim where the axons converge. The lamina cribrosa forms a supporting scaffold for the optic disc. The excessive pressure increases the cup-to-disc ratio, together with the deepening of the cup and the lamina cribrosa bows backward (Fig. 9B). The disc rim also thins with reduction in the number of axons, and blood vessels at the optic disc have sharp angulations, often presenting nerve fiber layer hemorrhage.

The resultant visual field loss corresponds to the lesion pattern in the optic nerve. Gradual constriction (i.e. tunnel vision) is the most common type of visual field defect. There are several other types such as nasal step defect, arcuate scotoma nasally from the blind spot, temporal wedge defect and paracentral scotoma.

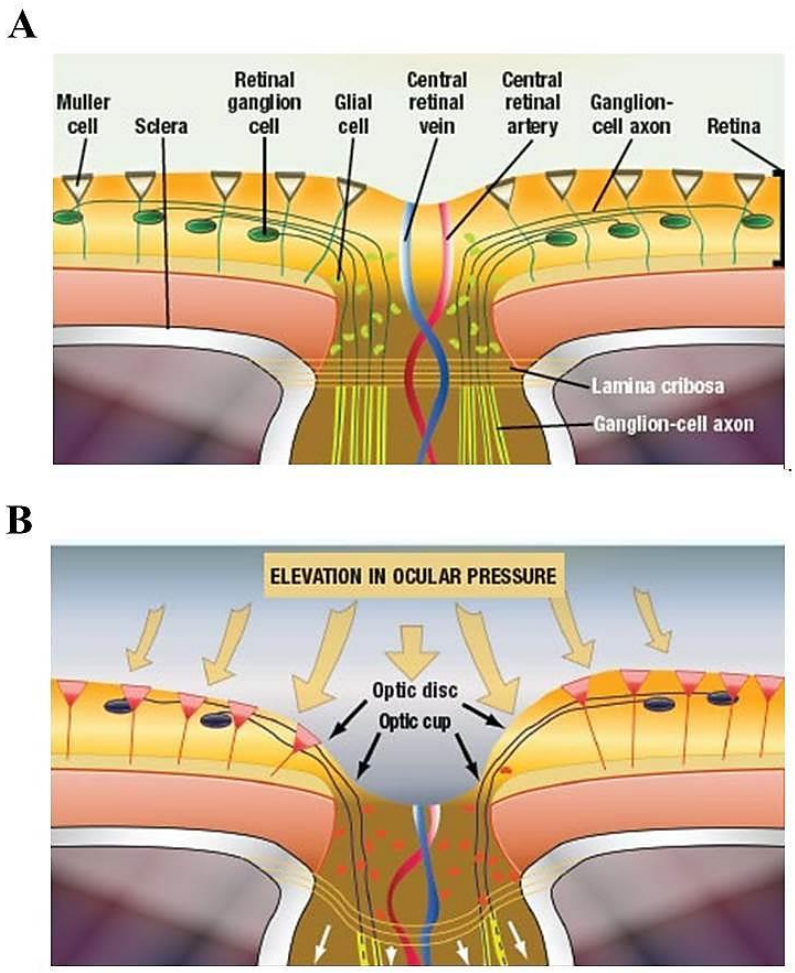

Figure 9. Schematic representation of the optic nerve damage caused by elevated IOP. (A) Normal optic disc. (B) In glaucomatous eyes, the excessive pressure widens and deepens the optic cup, thins the disc rim by reducing axon number, causes posterior bowing of the lamina cribrosa and sharp angulations of the blood vessels. Axonal damage leads to the atrophy of RGC cell bodies. (Image source: www.uspharmacist.com).

Axonal damage at the optic disc leads to RGC atrophy which could be explained by two theories of damage. Quigley and Addicks hypothesized that bowing of the lamina cribrosa posteriorly may displace holes in the lamina sheet through which the axons pass, constricting them and block axoplasmic transport [70]. This mechanical theory of damage to axons was rejected by Radius and Anderson who found the accumulation of membranous micro-organelles throughout the axon bundle, and not particularly at the lamina in a primate model [71]. Most POAG globe specimens were found to have an enlarged gap in the blood-ocular barrier in the retinal pigmented epithelium at the optic nerve head [72]. This could allow vasoactive compounds such as angiotensin and norepinephrine from the bloodstream to reach axons and interfere with axoplasmic transport as demonstrated by Sossi and Anderson in a cat

model [73]. These vasoactive compounds can also promote vasoconstriction of blood vessels at the optic nerve head and affect blood supply to the axons, which in turn could also block axoplasmic flow [73]. Obstruction of axoplasmic transport in other nerves in animal models has been shown to prevent retrograde flow of trophic factors to the cell body and causes its atrophy. The vascular theory of axonal damage seems likely but still remains to be demonstrated in a glaucomatous model.

In summary, glaucomatous changes in the TM generate an elevated resistance that impairs the outflow facility and causes aqueous humour accumulation. Consequently, the increment in IOP exerts additional strain on the optic disc, damages the optic nerve and deteriorates the visual field.

1.7 Genetics of POAG

The odds of POAG manifestation are higher at 7–10 times if an individual has a first-degree relative with the disease. Therefore, family history of POAG is a considerable risk factor for the disease. Moreover, higher prevalence in people of African origin compared to other ethnic groups and variable susceptibility to optic nerve damage, all indicate genetic association of the disease. Hence, POAG has been accepted as an inherited disorder. Based on incomplete penetrance and variability in age of onset observed in pedigrees, POAG is taken to be inherited as a complex trait where multiple genes influence its susceptibility. Environmental factors are also believed to influence susceptibility like other complex diseases by modulating the expression of these contributory genes.

Human genome organization (HUGO) lists fourteen chromosomal loci for POAG, GLC1A-N, found by family-based linkage analysis. Three genes corresponding to three of the loci have been identified as myocilin (GLC1A), optineurin (GLC1E) and WD40 repeat domain 36 (GLC1G). Their specific biochemical and cellular role in TM dysfunction is unclear, but speculations of their pathological role have been made based on their study.

Myocilin (*MYOC*), previously known as trabecular meshwork inducible-glucocorticoid response protein (*TIGR*) was the first susceptibility gene to be identified [74], [75]. Mutation of this gene is present in about 4% of POAG cases, and is inherited as an autosomal dominant

trait, with penetrance estimated at 90% [76]. Myocilin gene is on chromosome 1 (1q24.3) and encodes for a protein that is both secreted and intracellularly localized to mitochondria [77], microtubules [78], actin stress fibers [79], and exosome-like vesicles among others [80]. The secreted form associates with structural components such as long spacing collagen, elastins and SD-plaques, as well as ECM constituents including fibronectin, laminin and several collagens [81], [82]. Overexpression of the protein was found to compromise cell attachment, so it is believed to have a de-adhesive role [83]. Its effect on the outflow facility is controversial as Fautsch et al. found it to increase outflow resistance, while Caballero and colleagues reported the converse where it improved outflow, both in the perfused anterior segment system [84], [85]. In mouse models, expression level of the protein did not interfere with IOP, suggesting mutation of the protein could be contributing to the pathology instead of expression level [86], [87].

In fact, mutant forms were found not secreted and their intracellular level rose which also hindered wildtype myocilin by dimerizing with it [88], [89]. This coincided with IOP increase and RGC loss in mouse model [90], [91]. POAG specific-mutant protein is also not present in the aqueous humour of affected individuals further corroborating the loss of function attributed to the mutation. It is postulated that the mutant form interferes with its protein trafficking and the misfolded protein accumulates intracellularly. Thus, the meshwork may progressively become stiffer in the absence of the secreted protein which has de-adhesive property and the outflow resistance increases.

Optineurin (*OPTN*) is present on chromosome 10 (10q14) and susceptibility conferred by it is also inherited as an autosomal dominant phenotype. Mutation in this gene is common in normal tension glaucoma, underscoring its influence on susceptibility. It inhibits tumor necrosis factor signalling through TANK-binding kinase 1, raising the apoptotic threshold [92], [93]. Optineurin translocates from the Golgi to the nucleus upon apoptotic stimuli in a Rab8-dependent manner and blocks cytochrome c release from the mitochondria, preventing apoptosis [94]. The mutant form, however, is unable to translocate into the nucleus and fails to block apoptosis. Hence, optineurin is said to play a neuro-protective role by diminishing the RGC vulnerability to apoptosis.

WD repeat domain 36 (*WDR36*) is on chromosome 5 (5q22) and encodes for a T-cell activation protein. It is involved in ribosomal RNA processing and p53 signalling pathway as

well [95]. It is associated with higher severity of the disease [96]. Due to limited information of its variants, its exact role in TM function, let alone malfunction, is unknown. Other gene variants associated with POAG including but not limited to are optic atrophy 1 (*OPA1*), *p53*, *TNF*, apolipoprotein E (*APOE*), interleukin 1 (*IL1*), cytochrome P450 1B1 (*CYP1B1*) [97]–[101]. In these instances as well linkage with the disease has been implicated, but their pathological role is yet to be deciphered.

More than 90% of the causative genes have not been discovered. Identification of these causative genes and better understanding of the functional role of known susceptibility genes, especially in the context of the TM, will help to uncover the POAG disease process. It could also enable early diagnosis through disease marker screening even before any actual vision loss, and could potentially lead to gene therapy to correct the disorder in the future. The prospect of gene therapy, however, will be difficult due to the disease being a complex trait, where multiple factors both genetically and environmentally exert varying degree of influence. Cell therapy is far more attractive as it allows the lost and dysfunctional TM cells to be replaced with healthy ones that could restore function to the meshwork. This strategy may prove to be more effective than the therapeutic approaches of today which mostly do not target the meshwork although it is the fundamental problem behind the disease.

1.8 Therapeutic Approaches for POAG

Vision loss from glaucoma is irreversible and currently there is no known means of restoring it. So, therapeutic approaches aim to control POAG by preventing further damage to the optic nerve and therefore protect the extant visual field. This will be achieved by sufficiently decreasing the IOP 20 to 40% below pretreatment reading. Elevation in IOP can arise from accelerated rate of aqueous humour production and decrease in outflow. In reality, only the latter is true as aqueous humour secretion is unaffected. Therapeutic procedures enhance the outflow facility to decrease IOP. Three treatment options are available which are drugs, laser surgery and incisional surgery. Administering drugs is the initial preferred treatment, but invasive approaches may be necessary in the beginning itself if IOP is extremely high or extensive visual deterioration is present. Individuals with IOP > 30 mmHg are also advised to undergo treatment even if visual field is full and optic disk is healthy as risk of POAG is high at this IOP level.

Drugs available for IOP management decrease aqueous production and/ or increase outflow. Carbonic anhydrases, β-adrenergic antagonists and adrenergic agonists target aqueous production by the ciliary epithelium through their own specific mechanism of action, with the latter also able to increase outflow through a secondary mechanism. Drugs that improve drainage include cholinergic agonists, cholinesterase inhibitors and prostaglandin agonists which mainly promote outflow through the uveoscleral pathway. Only cholinergic agonists and several prostaglandin analogs can enhance both trabecular and uveoscleral outflow, but adverse side effects limit their use. These drugs are mainly applied topically and administered lifelong to keep IOP under control. Patient compliance is therefore difficult due to their prolonged usage, which is exacerbated by side effects common to such medication. For example, carbonic anhydrases can cause fatigue, anorexia, depression, altered taste, electrolyte abnormalities and blood dyscrasias, thus affecting the quality of life as well.

Severe glaucoma cases and patients who do not respond to or are sensitive to drugs are advised to undergo laser trabeculopasty. In this procedure, laser is applied on the TM to create fissures for outflow, improving the drainage facility. It is only effective for a short duration as IOP becomes elevated again within 2 to 5 years in most patients and requires repeated procedures or drug treatment. More invasive surgical intervention such as guarded filtration procedure and partial thickness procedures (i.e. canaloplasty, sclerectomy and viscocanalostomy) increase drainage into the subconjunctival space through formation of filtration bleb or newly created drainage pathway respectively. They are effective but adverse complications such as pressure dipping too low, excessive fluid in the choroid, risk of infection and cataracts are associated with them and require frequent follow-ups.

As can be seen, no one method is easy, complication-free and sustainably effective all at the same time to control IOP. Regenerative medicine could meet these criteria and current research is focused on it. Cell-based therapy is applicable in two scenarios here: 1) replace the lost RGC in the hope of recovering vision; 2) restore function to the TM by replacing the lost and damaged TM cells. The first aim is being explored by extensive research. Intravitreal transplantation of several stem cell types including embryonic stem cells (ESC), neural stem cells, mesenchymal stem cells (MSC), and müller cells have been studied in animal models to assess their capability to integrate into the retina to form new RGC [102]–[105]. But the retina does not present a permissive environment, and integration only becomes possible

upon injury to the retina, albeit at very low efficiency [106], [107]. Modification of the retinal environment with chemical compounds also improved the integration of müller cells slightly, but the integrated cells failed to express glial fibrillary acidic protein (GFAP), a mature marker of RGC, indicating they have not differentiated into neurons [108]. So, the effort for RGC regeneration is still at its infantile stage because no group has been able to produce RGC *in vivo,* let alone reestablish the axonal connections to the brain.

RGC research still holds promise as the transplanted stem cells survive in the vitreous cavity as floating bodies and were found to have neuro-protective property by secreting neurotropic factors. Eyes that received stem cells had less axonal damage and improved RGC survival. Studies utilizing neurotropic factors directly by intravitreal delivery in glaucoma models or overexpressing them in RGC *in vivo* also corroborate the decline in RGC loss [109]–[112]. The transplanted stem cells are viable at the maximum time point of 5 weeks studied, and are expected to survive much longer, providing a long-term neuro-protective effect. The protective mechanism of neurotropic factors may be translated clinically to slow down disease progression in the near future.

Another approach to halt disease advancement is by restoring function to the malfunctioning TM with cell-based therapy. This was not tested at the time when we started the project, and seemed like an attractive alternative to promote RGC survival. By replacing the lost and damaged cells in the diseased TM with mature TM cells, the newly replenished TM may be able to perform its homeostatic function of IOP regulation optimally. The remaining RGC will survive, with IOP now under control, thus preserving the rest of the visual field.

This method may also be more feasible than RGC regeneration which is challenged by the minimal integration of transplanted cells due to the limiting inner membrane of the retina. Not much limitation is expected at the TM level since it easily allows the entry of small compounds in the aqueous humour with the outflow. It may prove more effective and long-lasting than conventional treatments with less or even no complications. Finding the right stem cell type capable of differentiating into TM cells is important for this endeavor. Fortunately, studies have shown the existence of stem cells in the TM and they could have the potential to repair the diseased TM when utilized as the source of cells for the cell-based therapy.

1.9 Stem Cells in the Trabecular Meshwork

Stem/ progenitor cells are found in many adult tissues such as bone marrow, skeletal muscle, brain and skin. Although the adult stem cells are not pluripotent like ESC, they still share the characteristics of small size, high nucleus to cytoplasmic ratio, high proliferative rate and plasticity. They reside in specialized microenvironment referred to as niche. Studies have shown the presence of stem cells in the TM, specifically in the insert region of the TM, where it inserts into the cornea underneath the Schwalbe's line (Fig. 10) [113].

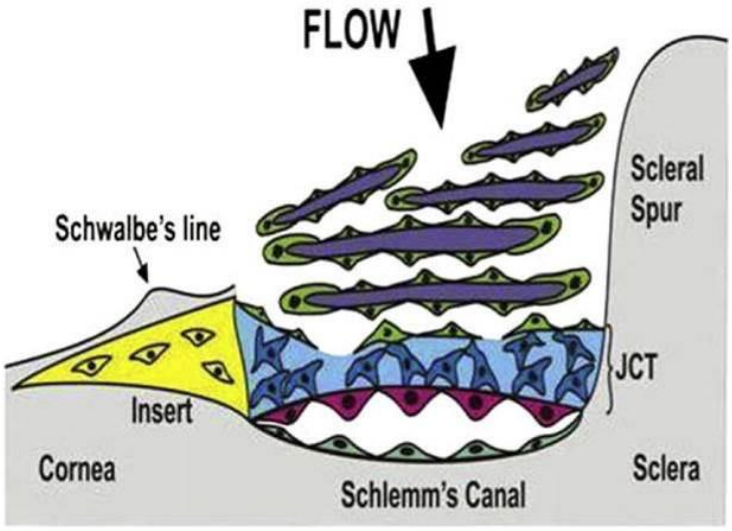

Figure 10. Anatomical division of TM into filtering and non-filtering (insert) portions. TM stem cells are postulated to be present in the insert region. (Image source: Kelley et al., 2009).

The insert region was found to express the stem cell markers nestin, alkaline phosphatase and telomerase by immunofluorescence on corneoscleral samples [114]. Expression of various stem cell markers is a phenotype of stem cells which is commonly used to identify stem cell populations. Upon wounding, the expression of these markers was retained, with the expression of additional ones such as POU class 5 homeobox 1 (OCT4) and wingless-type MMTV integration site family, member 1 (WNT1). Differentiation markers, paired box 6 (PAX6) and SRY (sex determining region Y)-box 2 (SOX2), were also detected after injury. This confirms the insert area to harbour stem cells displaying typical stem cell markers which differentiate upon injury and most likely migrate to other areas of the meshwork.

Moreover, argon laser trabeculoplasty on corneoscleral specimens followed by pulse-chase experiment with 3H-thymidine by Acott and group found cell division to increase by four

times, with close to 60% of the division confined to the insert region [115]. Normal unstimulated cell division was also detected in this area in untreated controls. No difference in cell division was detected in other regions of the meshwork as untreated controls. By 14 days, only 26% of the radiolabelled cells remained in the insert region, while 60% were present at the burn sites. Together, the study demonstrates the insert region as the niche for TM stem cells which self-renew, migrate and repopulate the site of injury to maintain the integrity of the tissue.

In addition, suspension culture of primary human TM culture in serum-free medium and on non-adherent plates formed free-floating spheres, a characteristic associated with stem cells [116]. Reporter gene activity found them to expressed genes known to be highly expressed in the TM, chitinase-3-like protein 1 (*CHI3L1*) and matrix gla protein (*MGP*), indicating their TM origin. The proliferative potential and dynamic structure of the sphere suggests that it is a population of stem cells and supports the existence of stem cells in the TM.

To our knowledge, regeneration of the TM tissue by transplantation of cells had not been explored at the time when the project was initiated in 2010. Only known means that triggered cell renewal in the TM was upon infliction of injury such as laser trabeculoplasty and phagocytic challenge [40], [115]. Other types of stem cells may be capable of replenishing the diseased TM when transplanted, but TM stem cells would be the most suited for the purpose, as it will likely be 'primed' to differentiate into mature TM cells. TM stem cells are hence essential in investigating the potential for regenerative medicine to restore function to the glaucomatous TM. These cells may be transplanted directly or differentiated *in vitro* then introduced into the anterior chamber to study their integration and function in disease models.

Although reports confirm the existence of TM stem cells, no group has been able to isolate them *in vitro* as a pure population. Even the recent suspension culture method generated spheres with differentiated inner core. So, an optimal method has to be designed to purify and propagate them in culture for study. Understanding their molecular characteristics and what renders them different from the mature TM cells is crucial for identifying signalling pathways involved in the differentiation process. This will also contribute to the development of a TM differentiation protocol, applicable for cell-based therapy and other mechanistic studies including drug-screening.

1.10 Markers of the Trabecular Meshwork

No single definitive marker is available to identify the TM cells. Expression analysis found high expression of aquaporin 1 (AQP1) in the primary human TM cells and they were capable of uptaking labelled low density proteins, showing the presence of low density lipoprotein receptor (*LDLR*) [117], [118]. Gene expression profiling of TM cells and subsequent reporter construct activity demonstrated the specificity of *CHI3L1* and *MGP* to the TM in perfused anterior segments [119], [120]. *MYOC* was also reported to be highly expressed in the TM and its expression is regulated by various factors like glucocorticoids, mechanical stretch and oxidative stress [121]. In fact, this gene was first discovered and characterized in the TM as trabecular meshwork-inducible glucocorticoid response (*TIGR*) gene [122], [123]. *MMP1* and Ankyrin 3 (*ANK3*) are also among the genes that have high expression in primary TM cells compared to cultures of Schlemm's canal endothelial cells and scleral fibroblasts as deduced by gene expression profiling [124]. These markers are collectively used to distinguish the TM. In most instances, markers' specificity to the TM in the context of the anterior segment have not been demonstrated and it is likely that they are also highly expressed in the surrounding cell types, and hence may not be suitable for identifying TM origin.

Moreover, genes differentially expressed between the TM stem cells and mature TM cells have not been identified. It remains to be known whether the aforementioned genes known to be highly expressed in the TM are differentially expressed between the two cell types. This complicates the study since TM differentiation cannot be tracked without appropriate differentiation markers. Hence, it is critical to find TM differentiation markers in order to design a TM differentiation methodology by assessing differentiation efficiency using marker expression. Again, this effort can only be initiated upon isolating the TM stem cells *in vitro* which will provide an expandable population for the study.

Other than phenotypic characterization of TM cells via marker expression, TM cells have been known to uptake acetylated and acetoactylated-LDL which differentiate them from other ocular cell types [118]. Cultured TM cells from different sources were able to uptake the modified LDL, while human corneal endothelial cells, corneal stromal cells and scleral cells could not. Moreover, phagocytosis, an indispensable function performed by the TM, has

been found to be preserved *in vitro* [38]. Therefore, marker expression together with functional assessment should be taken as essential criteria to characterize mature TM cells.

1.11 Age-correlated Changes in the Trabecular Meshwork

The prevalence of elevated IOP and POAG are significantly higher in the older populations [125]. This could be attributed to the effect of aging on the TM which creates major alterations to its structure and function. Overall, the TM increases in thickness with age due to trabecular thickening in the uveal and corneoscleral areas. The structural components, long-spacing collagen and elastic fibers, of the trabecular beams and lamellae increase with age leading to trabecular thickening [126]. Trabecular fusion is observed in older specimens, and it is believed to arise from the adhesion of denuded trabeculae that have partially lost their cell cover. Modified ECM is also added with age, particularly in the JCT. These structural changes in the meshwork could contribute to the increase in outflow resistance detected with age [127]. But most people are able to maintain normal IOP since aqueous humour production decreases with age [127].

TM cellularity significantly decreases with age. Alvarado and coworkers found the decline in trabecular cellularity was most pronounced between the late prenatal stage to the initial few years after birth [128]. The decrease in cellularity then progresses slowly in an almost linear manner. By the age of 81 years, 58% of the approximately 7.5 x 10^5 TM cells at birth are estimated to be lost at the rate of 6000 cells/year [129], [130]. Scanning electron microscope also detected enlarged cells near denuded parts of the trabeculae. The spreading of cells may be a compensatory mechanism to make up for the loss of cells. Though the cell loss was apparent in all three regions, the inner region was more affected than the outer one. The cells in the insert region did not show any significant decline in number with age, indicating only the filtrating and functional component of the meshwork was affected [129].

The decrease in TM cellularity is similar to other tissues affected by age such as skeletal muscles and neurons which have limited cell division [131]–[133]. TM cells are locked in G0/ G1-phase and are contact inhibited [134], accounting for the limited ability to undergo cell division *in vivo.* Thus, they are unable to replenish the lost cells. The mechanism for cell loss remains elusive. A number of contributory factors acting together or alone may result in

the loss of TM cells. Several theories have been postulated for the loss. The mechanical stress imposed by aqueous outflow and the movement of ciliary muscle may damage the cells and cause cell death in the more susceptible cells. Migration or death of cells that have phagocytosed debris in the aqueous may also lead to cell loss. In fact, apoptosis in TM cells that cannot breakdown the engulfed material has been shown in glaucoma, but not yet in the aging process [135]. Some groups believe the meshwork has a detoxification function, and they undergo cell death when they are unable to detoxify the toxic compounds. The aqueous itself may become deficient in factors essential for TM cell survival with age and result in cell loss too. These theories of TM cell loss are plausible considering the TM environment and function, but are yet to be demonstrated and proven.

1.12 Objectives

1. Develop a method to isolate and propagate TM stem cells as a pure population from the human TM.
2. Characterization of TM stem cells for stemness and TM origin.
3. Identification of TM differentiation markers applicable for assessing TM differentiation.
4. Design a protocol to differentiate the TM stem cells *in vitro* into mature, functional TM cells.
5. Age-correlated expression analysis to find biological processes differentially regulated with age in the TM.

Previous studies have drawn a consensus that malfunction of the TM may lead to POAG. Most conventional drug therapy for POAG either target aqueous humour secretion or increase uveoscleral outflow, instead of the TM itself. As a preventive strategy the drugs must be administered lifelong upon diagnosis, but patient compliance is difficult due to expense and associated side effects. Surgical intervention can target the TM but often its efficacy is short-lived. An effective and permanent treatment that restores function to the diseased TM like regenerative medicine is yet to be discovered. It could replace lost/ damaged cells in the glaucomatous TM, ameliorate its function enough to control IOP. To explore the feasibility of the approach, an expandable source of TM cells is indispensable.

We hypothesized that functional TM cells derived from the insert cells can be adopted as a source of cells for cell therapy to treat POAG. TM insert cells are postulated as progenitors of the TM according to studies *in vivo*. In fact, our hypothesis was very recently confirmed by Du and colleagues as they showed the integration and differentiation of human TM stem cells into mouse TM *in vivo* [136]. The principal aim of the project was to set up a scalable means of generating functional TM cells *in vitro* for translational research. There were several research gaps in the field which challenged this endeavor when the project was initiated: 1) no technique had been established to isolate the TM stem cells; 2) there were no known TM differentiation markers; 3) TM differentiation protocol had not been developed. So, the objectives were to first isolate and propagate human TM stem cells followed by characterizing them for stemness and TM origin.

Upon establishment of optimal culture conditions for TM stem cell maintenance, TM differentiation markers were to be identified by genome-wide expression profiling of *ex vivo* TM tissue and cultured TM stem cells. The profiling would reveal genes differentially expressed between the mature cells and progenitors of the TM which can be used as markers of TM lineage. Differentiation of TM stem cells into mature TM cells would then be investigated to deduce differentiation factors and matrices with TM induction potential to design an effective TM differentiation protocol. Functionality of differentiated cells would be tested through the uptake of modified LDL to determine the efficacy of differentiation. Incorporation of modified LDL is a property exhibited by mature TM cells but absent in their progenitors. These objectives should help us meet our main aim of establishing an expandable pool of differentiated TM cells.

Age-related changes in the TM could explain the correlation of POAG incidence with age. Structural modifications in the TM including cell loss found with age are phenotypic manifestations of gene expression changes in the TM. It is essential to elucidate such gene expression changes, and importantly, differentially regulated biological processes for a deeper understanding of aging in the TM. Microarray analysis of donor tissues belonging to various age groups would be performed for this study to identify differences at the genomic level and explore them further in the context of POAG.

Retrospectively, our objectives have been achieved, allowing us to establish expandable pools of TM stem cells as well as differentiated cells that are much needed to investigate the

prospect of regenerative medicine to replenish the diseased TM in POAG. After testing various adult stem cell propagation techniques, an isolation methodology for TM stem cells has been developed that selectively enriches them. Further characterization of the isolated cells demonstrated them as multipotent mesenchymal stem cells. TM differentiation markers have also been identified which are highly expressed in the TM *ex vivo* and consistently indicate the differentiated state under certain conditions. A cocktail of factors is promising among others in differentiating the cells into functionally mature TM cells. Gene expression study of aging in the TM revealed a moderate set of genes with age-related expression, and most notably, several biological processes that are affected with age that may contribute to phenotypic changes in the aging TM.

This study addresses a number of unknown aspects of the field. The construction of methodologies for TM stem cell isolation and their differentiation into TM lineage will augment the chance of cell replacement treatment becoming a reality to treat POAG. Cell based-therapy could provide long-term relief compared to conventional treatment options. Moreover, the availability of a scalable pool of TM stem cells and differentiated cells will benefit basic TM research. Gene expression analysis to study the effect of aging on the TM is essential in unravelling genomic differences in the TM with age which could contribute to structural changes that render the older population more susceptible to POAG. It will also foster a better understanding of TM mechanistic variations with age.

2.1 Materials

2.1.1 Human Ocular Tissues

Ocular tissues were derived from the corneosclera specimens procured from the Lions Eye Institute (Tampa, USA), with accordance to institutional ethics guidelines.

2.1.2 Surgical Instruments

Surgical instruments used for tissue extraction such as forceps, scalpel and crescent knife were purchased from World Precision Instruments (Sarasota, FL, USA).

2.1.3 Cell Culture Reagents

All reagents used for cell culture work were of tissue culture grade and were purchased from the following companies:

Phosphate-buffered saline	Gibco (Life Technologies, Carlsbad, CA, USA)
0.4% Trypan blue	Sigma (St. Louis, MO, USA)
Collagenase Type I	Worthington Biochemical Corporation (Lakewood, NJ, USA)
0.05% trypsin-EDTA	Gibco (Life Technologies, Carlsbad, CA, USA)
DMEM (Low glucose, pyruvate)	Gibco (Life Technologies, Carlsbad, CA, USA)
HyClone fetal bovine serum	Thermo Scientific (Waltham, MA, USA)
MEM non-essential amino acids	Gibco (Life Technologies, Carlsbad, CA, USA)
Penicillin-streptomycin	Gibco (Life Technologies, Carlsbad, CA, USA)
Versene	Lonza (Basel, Switzerland)
MesenCult basal medium	Stemcell Technologies (Vancouver, BC, Canada)
MesenCult adipogenic stimulatory supplements	Stemcell Technologies (Vancouver, BC, Canada)
MesenCult osteogenic stimulatory supplements	Stemcell Technologies, (Vancouver, BC, Canada)

2.1.4 Chemicals and Substrates

All chemicals used in this study were of at least analytical grade and were purchased from the following companies:

TRIzol® reagent	Ambion (Life Technologies, Carlsbad, CA, USA)
Giemsa stain	Sigma (St. Louis, MO, USA)
Methanol	Merck Millipore (Darmstadt, Germany)
Formalin	Sigma (St. Louis, MO, USA)
Isopropanol	Merck Millipore (Darmstadt, Germany)
Oil Red O solution	Sigma (St. Louis, MO, USA)
Dexamethasone	Sigma (St. Louis, MO, USA)
Ascorbic acid	Stemcell Technologies, (Vancouver, BC, Canada)
β-glycerophosphate	Stemcell Technologies, (Vancouver, BC, Canada)
Alizarin red S solution	Sigma (St. Louis, MO, USA)
Ethanol	Merck Millipore (Darmstadt, Germany)
Insulin-transferrin-selenium	Invitrogen (Life Technologies, Carlsbad, CA, USA)
Bovine serum albumin	PAA Laboratories (GE Healthcare, Cleveland, Ohio, USA)
Linoleic acid	Sigma (St. Louis, MO, USA)
Sodium pyruvate	Invitrogen (Life Technologies, Carlsbad, CA, USA)
TGF-β3	Peprotech (Rocky Hill, NJ, USA)
Paraformaldehyde	Sigma (St. Louis, MO, USA)
Citrate buffer, pH 6.0	Sigma (St. Louis, MO, USA)
Hydrogen peroxide	Sigma (St. Louis, MO, USA)
Diamino benzidine	(Sigma, St. Louis, MO, USA)
O.C.T compound	Tissue-Tek (VWR, Radnor, PA, USA)
Triton X-100	Sigma (St. Louis, MO, USA)
Glycine	Sigma (St. Louis, MO, USA)
4',6-diamidino-2-phenylindole	Invitrogen (Life Technologies, CA, USA)
Fluorescent mounting medium	Dako (Copenhagen, Denmark)

2.1.5 Small Molecules

Small molecules targeting signalling molecules and epigenetic modifiers were either purchased from Miltenyi Biotec (Cologne, Germany) or Sigma (St. Louis, MO, USA).

2.1.6 Antibodies

Antibodies used in this study were either procured from Abcam (Cambridge, UK), R&D Systems (Minneapolis, MN, USA), Santa Cruz Biotech (Dallas, Texas, USA) or Thermo Scientific (Wilmington, DE, USA). Details of antibodies used are presented in the supplementary table 1 (Appendix). Normal goat serum was also purchased from Abcam.

2.1.7 Kits

RNeasy mini kit	Qiagen (Venlo, Limburg, Netherlands)
High capacity cDNA reverse transcription kit	Applied Biosystems (Life Technologies, Carlsbad, CA, USA)
Go Taq® flexi DNA polymerase	Promega (Madison, WI, USA)
SYBR® Green master mix	Applied Biosystems (Life Technologies, Carlsbad, CA, USA)
TotalPrep RNA amplification kit	Ambion (Life Technologies, Carlsbad, CA, USA).

2.1.8 Instruments

CO_2 incubator	DKSH (Zurich, Switzerland)
xCELLigence system	Roche Applied Science, USA
NanoDrop ND-1000 spectrophotometer	Thermo Scientific (Wilmington, DE, USA)
Tetrad2 PCR machine	Bio-Rad (Hercules, CA, USA)
HumanHT-12 beadchip and	Illumina Inc. (San Diego, CA, USA)

BeadArray Reader	
Gel documentation system	Bio-Rad (Hercules, CA, USA)
7900HT Fast Real-Time PCR system	Applied Biosystems (Life Technologies, Carlsbad, CA, USA)
Cryostat	Leica (Solms, Germany)
Brightfield and Fluorescent microscopes	Zeiss (Oberkochen, Germany)
Guava easyCyte flow cytometer	Millipore (Merck Millipore, Darmstadt, Germany)
FACSCalibur flow cytometer	BD Biosciences (San Jose, CA, USA)

2.1.9 Softwares

Primer3Plus	www.primer3plus.com
Primerbank	www.pga.mgh.harvard.edu/primerbank
PerlPrimer	www.perlprimer.sourceforge.net
GenomeStudio	Illumina Inc. (San Diego, CA, USA)
GeneSpring	Agilent Technologies (Santa Clara, CA, USA)
DAVID	www.david.abcc.ncifcrf.gov
PANTHER	www.pantherdb.org

2.2 Methods

2.2.1 TM Extraction and Culture

2.2.1.1 Donor Eyes

Eyes attained at autopsy from consenting donors were processed for corneosclera specimens at the Lions Eye Institute (Tampa, USA). Donors had no known history of chronic illnesses. Serological tests were performed at the facility to ensure that the samples are free of transmissible diseases by testing for pathological agents such as human immunodeficiency virus (HIV), hepatitis C virus (HCV) and human L-lymphotropic virus (HTLV), *Treponema pallidum* and hepatitis B virus (HBV). Those that passed the evaluation for research use were purchased following institutional ethics guidelines.

2.2.1.2 Extraction of the TM Tissue

The corneosclera specimen that were within 14 days of donor death were used for the study. The specimen was rinsed several times with phosphate-buffered saline (PBS, Gibco; Life Technologies, USA) and stained with 0.1% trypan blue (Sigma, USA) for 1 min. We have found the trypan blue to stain the porous TM. The excess stain was washed with PBS and TM was extracted using a modified technique from Tripathi and Tripathi [137]. Briefly, under a stereomicroscope, the corneal endothelium and the scleral spur were peeled off and the stained TM tissue was gently dissected from the underlying tissue with a crescent knife. The extracted TM tissue was further processed for the isolation of TM progenitors or homogenized in TRIzol® reagent (Ambion; Life Technologies, USA) for RNA studies.

2.2.1.3 Isolation and Propagation of TM Progenitors

The whole TM tissue extracted from the corneoscleral specimen was digested with 2 mg/ml collagenase Type I (Worthington Biochemical Corporation, USA) in Dulbecco's Modified Eagle Medium (DMEM) containing HyClone defined fetal bovine serum (FBS) (Thermo Scientific, USA), on low attachment 12-well, overnight (stationary) at 37^0C in the cell culture

incubator. The resultant cell clumps were transferred to a conical tube and dissociated in 0.05% trypsin-EDTA (Gibco; Life Technologies, USA) for 10 min in the 37^0C water bath. Trypsin was then neutralized with growth medium, harvested and the resuspension was filtered through a 40 µm cell strainer (BD Biosciences, USA). Viable cell count was later determined by trypan blue exclusion test. Approximately 95% of the isolated cells were viable with an expected yield of about 3 x 10^4 cells on average from a specimen. The single cell suspension was then plated onto a tissue culture grade 12-well (for one sample) or 6-well (for a pair of sample) in hMSC medium (low glucose DMEM containing L-glutamine and sodium pyruvate, 10% FBS, 10 mM non-essential amino acids, 100 units/ml Pencillin and 100 µg/ml Streptomycin (Gibco; Life Technologies, USA)) and maintained at 37°C in 5% CO_2 with humidity in the cell culture incubator (DKSH, Switzerland). Medium was changed every 2 – 3 days.

The TM-derived cells formed colonies which were selected for expansion when they reached a cell density of 100 – 200 cells, by picking them with a micropipettor after 5 min incubation in 0.02% Versene (EDTA) (Lonza, Switzerland) at room temperature. The cell suspension was neutralized in growth medium and harvested for seeding. The cells were subsequently passaged at 80 – 90% confluence at a ratio of 1:4 with 0.05% trypsin-EDTA. The ideal seeding density was determined as 3000 cells/cm^2.

2.2.2 Clonogenic Potential and Growth Assessments

2.2.2.1 Colony Forming Unit-Fibroblast (CFU-F) Assay

CFU-F assay was performed according to Friedenstein et al., [138]. Briefly, cells isolated from the TM at passage 0 were plated at 3000 cells/well density in a 24-well format, and left undisturbed for 2 weeks in the CO_2 incubator. The cells were then fixed in methanol (Merck Millipore, Germany) for 5 min, stained with Giemsa (Sigma, USA) for 5 min and washed with PBS. The colonies were counted under the brightfield microscope and CFU-F was calculated as following: [number of colonies / 3000] x 100%.

2.2.2.2 xCELLigence System Run

For the proliferation assessment on the xCELLigence system (Roche Applied Science, USA), blank measurement was first made with 100 µl hMSC medium placed in the 96-well E-plate and cells were then seeded at a density of 3000 cells/well in 100 µl medium. Cell growth rate was measured for 5 days on the real-time cell analyzer (RTCA) single plate station in the cell culture incubator. The electrical impedance of adherent cells was recorded as cell index on the RTCA control unit.

2.2.3 Differentiation Assessments

Early passage TM progenitors at p4 to p6 were used for the various differentiations when they reached a confluence of about 90%. Adipogenic and osteogenic inductions were performed on plated cells, while cell aggregates were used for chondrogenesis. After induction, the cells were harvested for RNA work and also histologically tested to assess differentiation.

2.2.3.1 Adipogenic Differentiation and Testing

The plated cells were cultured in MesenCult basal medium with MesenCult adipogenic stimulatory supplements (Stemcell Technologies, Canada) for 4 weeks, with medium change thrice a week.

Following the differentiation treatment, the cells were subjected to adipogenesis detection. The cells were washed with PBS and fixed with 10% neutral-buffered formalin (Sigma, USA) for 30 min at room temperature. They were then rinsed in sterile water twice and incubated in 60% isopropanol (Merck Millipore, Germany) for 5 min, followed by Oil Red O (Merck Millipore, Germany) at a concentration of 0.45 mg/ml in water for 30 min. The excess stain was washed off with water and cells were checked under phase contrast for the presence of red lipid vesicles.

2.2.3.2 Osteogenic Differentiation and Testing

The culture medium of the cells to be differentiated was replaced with MesenCult basal medium containing MesenCult osteogenic stimulatory supplements (Stemcell Technologies, Canada), 10 nM dexamethasone (Sigma, USA) and 50 µg/ml ascorbic acid (Stemcell Technologies, Canada). 3.5 mM β-glycerophosphate (Stemcell Technologies, Canada) was added to the medium when multilayering was seen.

After 4 weeks of differentiation, the cells were tested for osteogenic differentiation. The cells were washed with PBS and fixed with ethanol for 30 min at room temperature. The wells were then washed twice with water, stained with Alizarin Red S (Sigma, USA) for 30 min, and rinsed off. The stained cells were observed under the brightfield microscope.

2.2.2.4 Chondrogenic Differentiation and Testing

The cells were aggregated as pellets containing 2 x 10^5 cells according to established protocols [139], [140] and maintained in MesenCult basal medium with 1 mM insulin-transferrin-selenium (Invitrogen; Life Technologies, USA), 1.25 µg/ml bovine serum albumin (PAA Laboratories; GE Healthcare, USA), 5.35 µg/ml linoleic acid (Sigma, USA), 1 mM sodium pyruvate (Invitrogen; Life Technologies, USA), 100 nM dexamethasone, 50 µg/ml ascorbic acid and 10 ng/ml TGF-β3 (Peprotech, USA) for 5 weeks, with thrice weekly medium change.

For histological analysis, the pellets were fixed with 4% paraformaldehyde (Sigma, USA) for 10 min, embedded in wax and sectioned into 5 µm sections. Slides were deparaffinised, rehydrated and epitope retrieval was performed using citrate buffer pH 6.0 (Sigma, USA) for 40 min at 100^{o}C. 3% hydrogen peroxide (Sigma, USA) treatment for 15 min at room temperature blocked endogenous peroxidase. Samples were blocked with 10% serum for 30 min prior to incubation in anti-collagen II primary antibody diluted at 1:500 (Abcam) for 45 min at room temperature. After three washes, horseradish peroxidase conjugated secondary antibody was added for 10 min and followed by diamino benzidine (Sigma, USA) for 3 min. Images were taken under a light microscope (Leica, Germany).

2.2.4 RNA Work

2.2.4.1 RNA Extraction

RNA was isolated from Trizol cell lysate using Qiagen's RNeasy Mini Kit (Venlo, Netherlands) and quantified on a NanoDrop ND-1000 spectrophotometer (Thermo Scientific, USA). In general, a ratio of absorbance at 260 nm and 280 nm of 1.8 – 2.0 is satisfactory for RNA purity. 1 µg RNA was reverse transcribed into complementary DNA (cDNA) with high-capacity cDNA reverse transcription kit (Applied Biosystems; Life Technologies, USA), according to manufacturer's instruction.

2.2.4.2 Polymerase Chain Reactions (PCR)

Primers were derived from PrimerBank [141], PerlPrimer software [142] or Primer3 [143], [144] with an annealing temperature of 55^0C. Primers used for the study are listed in Supplementary Table 2 (Appendix).

For reverse transcription PCR (RT-PCR), 1 µl cDNA template amplified through reverse transcription was mixed in PCR Buffer, 4 mM $MgCl_2$, 400 µM dNTPs, 200 nM forward and reverse primers, 0.2 µl Go Taq® Flexi DNA Polymerase (Promega, USA) and topped with ddH_20 to a 25 µl reaction volume. PCR condition was set as 95^0C 2 min followed by 95^0C 30s/ 55^0C 30s/ 72^0C 1 min for 30 cycles, then 72^0C 5 min and 4^0C forever on a Tetrad2 PCR machine (Bio-Rad, USA). 1 µl reaction sample mixed with loading dye containing gel red was separated on 1.5% agarose gel at 100 V for 1 h and imaged on the gel documentation system (Bio-Rad, USA).

For quantitative RT-PCR (qRT-PCR), the template was diluted 10x from which 4.5 µl was mixed with 5 µl SYBR® Green master mix (Applied Biosystems; Life Technologies, USA), and 0.25 µl of 10 µM forward and reverse primers each for a 10 µl reaction. Duplicates were set up for each reaction in a 384 well-plate and ran on the 7900HT Fast Real-Time PCR system (Applied Biosystems; Life Technologies, USA) for 40 cycles. For normalization of RNA content, amplification of *ACTB* was performed for each cDNA sample. The delta-delta

Ct method of comparative quantification was used to calculate the relative mRNA abundance of specific genes.

2.2.4.3 Microarray and Gene Ontology

Three biological samples representing each group were analyzed. RNA was extracted from the tissue/ cultured cell (at p4 to p6) samples using the RNeasy miniprep kit with an additional step of in-column DNase I treatment prior to elution. The RNA was then amplified for microarray with the TotalPrep RNA amplification kit according to the manufacturer's instructions (Ambion Inc.; Life Technologies, USA). The resulting purified biotin-labeled complementary RNA (cRNA) was normalized and hybridized onto HumanHT-12 beadchip (versions 2 – 4, Illumina Inc., USA) using its direct hybridization assay. The chip was later washed, blocked and Cy3-streptavidin bound to hybridized cRNA. The Illumina BeadArray Reader utilizing the Illumina BeadScan software was used to image the chip.

The image data was converted into expression profile by GenomeStudio (Illumina Inc., USA). Background was subtracted and the data was submitted to GeneSpring (Agilent, USA). Differentially expressed genes were selected by averaging the replicates and pairwise analysis was done with one-way ANOVA, Benjamini-Hochberg false discovery rate test and K-means clustering. Statistical significance according to t-test paired/ unpaired was set as $p \leq 0.05$ and data were filtered using certain fold change cut-offs. Gene ontology was performed with DAVID web-based software [145], [146]. The gene lists generated were uploaded using Entrez gene ID onto DAVID [146] for functional annotation clustering by GOTERM_BP_FAT with medium classification stringency. Only biological processes with $p \leq 0.05$ were considered. In some cases, PANTHER classification of the gene list was done by uploading the respective Entrez gene IDs [147].

2.2.5 Staining Protocols

2.2.5.1 Tissue Preparation for Immunofluorescence

The corneoscleral specimen was washed several times in PBS to remove detached cells. The excess conjunctiva was removed with an angular iris dissecting scissors and the specimen was cut in half. The cornea and sclera were trimmed and the sample comprising the corneoscleral limbus was embedded in optimal cutting temperature (OCT) compound (Tissue-Tek; VWR, USA) in a cryomold and frozen at -80°C. The frozen tissue sample was cut into 8 µm sections at the cryostat (Leica, Germany), mounted onto superfrost plus microscope slides (Thermo Scientific, USA) and air dried for 15 min at room temperature. Sections stored at -80°C were thawed at room temperature for 10 min and rehydrated with water for 5 min before proceeding to fixation and permeabilization.

2.2.5.2 Immunofluorescence

The samples were washed in PBS and fixed in 4% paraformaldehyde (PFA) (Sigma, USA) pH 7.4 for 10 min at room temperature. The cells were washed twice in PBS for 5 min and permeabilized in 0.25% Triton X-100 (Sigma, USA) in PBS for 10 min, followed by washing three times for 5 min each. To block nonspecific binding of antibodies, the samples were incubated with 10% serum and 0.3M Glycine (Sigma, USA) in PBST for 30 min. The samples were then incubated in primary antibody diluted at an optimized concentration in 1% serum in PBST overnight at 4^0C and washed thrice for 5 min each. Fluorescent protein conjugated-secondary antibody in 1% serum was added and incubated for 1 hr in dark at room temperature and washed three times. Nuclei were stained with 1 µg/ml 4',6-diamidino-2-phenylindole (DAPI) (Invitrogen; Life Technologies, USA) for 1 min and washed thrice with PBS. If samples were on glass slides, they were mounted with coverslip in a drop of fluorescence mounting medium (Dako, Denmark) and sealed with nail polish. Images were captured under the camera mode of the fluorescent microscope (Zeiss, Germany). Details of the antibodies used for the study are listed in Supplementary Table 1 (Appendix).

2.2.5.3 Flow Cytometry

Cells harvested by trypsin treatment were pelleted at the density of 10^6 cells/ml and washed in PBS, prior to blocking in 10% serum for 30 min at room temperature. For direct staining, 100 µl of the suspension was incubated with the recommended dilution of fluorescent protein-conjugated antibody for 45 min in the dark, washed and resuspended in 500 µl PBS which was subjected to flow cytometry. Indirect staining was performed similar to the immunofluorescence protocol with some modifications. The antibody concentration was doubled and 30 min incubation periods were used with one wash between the treatments. Isotype IgG was used as a negative control. The cells were either analyzed by Guava easyCyte (Millipore; Merck Millipore, Germany) or FACSCalibur flow cytometer (BD Biosciences, USA).

2.2.5.4 Ac-LDL Labelling

Cells were incubated with DiI-Ac-LDL (Invitrogen; Life Technologies, USA) at a dilution of 10 µg/ml in the culture medium for 6 hours at 37ºC in the cell culture incubator. They were then washed twice with PBS and imaged on the fluorescent microscope. Following imaging, the cells were harvested by trypsinization and resuspended in 400 µl PBS. The cell suspension was analyzed by the FACSCalibur flow cytometer to quantify the percentage of labelled cells.

2.2.6 Statistical Analysis

Data was represented as mean ± standard error of the mean for three biological replicates. Significance was tested using two-tailed t-test and p-value < 0.05.

3. Results

3.1 Isolation of Stem Cells from the Trabecular Meshwork

To study the potential of TM stem cells as cell therapy for POAG, TM stem cell first have to be isolated. When the project was initiated, no culture method had been established for TM stem cells. This chapter discusses the various stem cell culture techniques tested to isolate and propagate the cells. Monolayer culture of cells harvested from the human TM with selection procedure was found to optimally propagate them as verified by marker expression. The possibility of contamination from neighbouring tissues was also excluded using this method. So, we present a novel technique to isolate and culture the TM stem cells.

3.1.1 Optimization of Trabecular Meshwork Extraction Technique

To isolate stem cells from human TM tissue, several approaches were undertaken, which all start with harvesting the TM tissue. Corneoscleral samples attained, from human cadaveric eyes at the Lions Eye Institute (Tampa), following institutional ethics guidelines were used for TM extraction by a method adapted from Tripathi and Tripathi [137] (Fig. 11). The samples were within the maximum time limit of 14 days post-mortem which ensures viability of the cells. In fact, viability of the cells harvested from the TM was always above 90% as determined with trypan blue exclusion test (data not shown).

The corneoscleral samples were first washed with PBS several times to remove floating debris. Visualization of the TM was difficult as TM is very thin with a cross-sectional length of approximately 1 mm and developmentally starts as a colourless tissue. This was especially challenging in the younger samples as they are largely non-pigmented, but as they age pigmentation, caused by the engulfment of pigmented particles shed by the iris, renders it brown in colour and hence discernable to some extent.

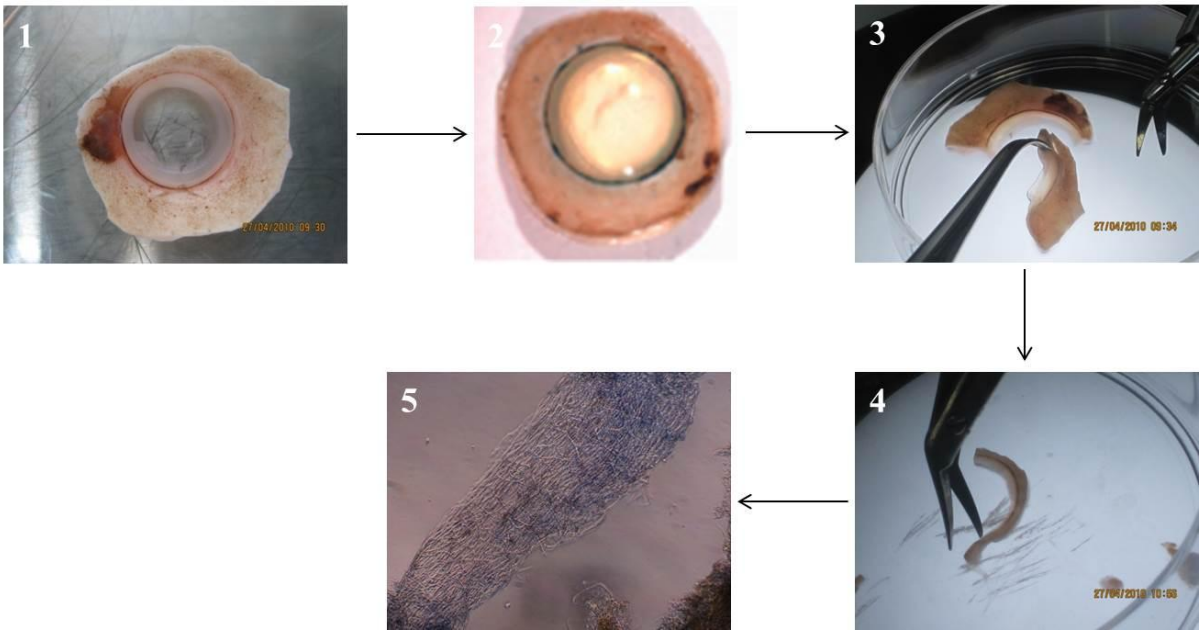

Figure 11. Optimized TM extraction methodology. (1) Anterior segment of the eye was stained with trypan blue which (2) specifically stains the TM. (3) Cornea was then dissected out, followed by (4) removal of the corneal endothelium and scleral spur, and (5) TM tissue was extracted. (TM imaged on brightfield at 100x magnification).

Trypan blue was found to stain the TM by being incorporated into the porous tissue which enhances visualization and eases extraction of the TM (Fig. 11). After rinsing off the excess stain, cornea was dissected out, followed by corneal endothelium and sclera spur removal. TM was then gently detached and used to test the various stem cell propagation techniques to identify a method to isolate the TM stem cells. Detailed description of the TM extraction procedure is available in section 2.2.1.2 of the materials and methods.

3.1.2 Stem Cell Propagation Techniques Tested

Cells enzymatically isolated from the TM and size selected were cultured under various conditions used for propagating adult stem cells. Suspension culture, originally used for neural stem cells [148], [149], has been modified to culture other adult stem cells such as mouse corneal stromal stem cells [150] and stem cells from the human hair follicles [151]. Gonzalez and colleagues found human TM cells to be capable of forming free-floating neurospheres in StemSpan™ medium using this technique [116].

An average yield of 3 x 10^4 cells can be harvested from one corneoscleral rim. The single cells were suspended in either mTeSR™ 1, human embryonic stem cell (ESC) medium or StemSpan™, which are all common stem cell maintenance media and tested for sphere formation (Fig. 12A). Spheres were generated in all three media tested and they were of similar size. They expanded with time, but passaging them by mechanical dissociation failed to generate further spheres and remained in culture as irregular aggregates. The spheres also could not be maintained beyond 4 weeks, as they stopped growing with increasing dark centers, suggestive of disintegration. This technique was abandoned since the spheres could not be expanded and cultured long-term.

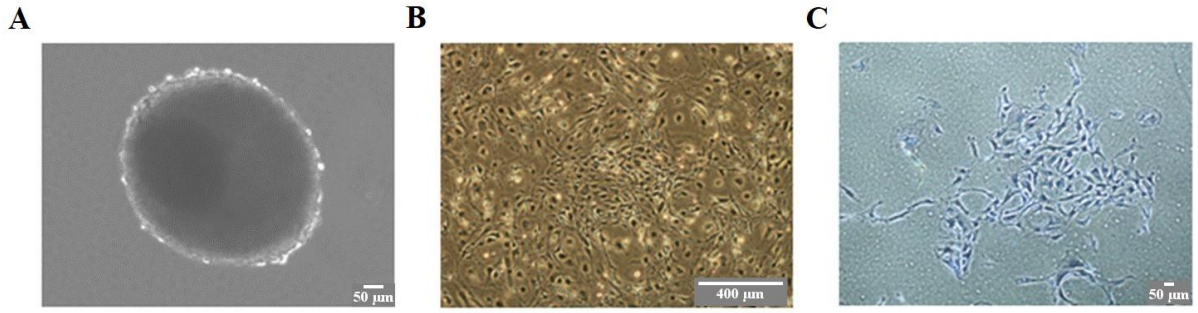

Figure 12. Monolayer culture most effective for TM stem cell isolation. (A) Maximum size of spheres after one month in suspension culture. (B) TM cells were dispersed on feeder culture and had mixed morphology. (C) Colonies of cells with homogenous morphology were derived when plated as a monolayer.

Feeder culture with mouse embryonic fibroblast (MEF) is used to maintain ESC and was tested with TM cells to assess if they support TM stem cell growth. Besides MEF, a transgenic 3T3 fibroblast cell line, designed by Dr Frank McKeon's group at the Genome Institute of Singapore, which promotes the growth of stem cells was also tested as a feeder layer. Feeder cells were treated with mitomycin C to inhibit cell cycle and plated at a confluent density a day prior to seeding cells dissociated from the TM. TM cells were observed to be dispersed on both feeder types instead of forming colonies as was expected (Fig. 12B). Moreover, although cells with compact cell body and large nucleus, both characteristics of stem cells were seen, at least two other different cell morphologies were evident on the superficial layer. So, isolation of TM stem cells was difficult with this method as it failed to propagate a pure population of stem cells.

Monolayer culture with human TM cell culture media used by Gonzalez et al., 2005 [116], Junglas et al., 2008 [152], and McCartney et al., 2005 [153] were studied. The latter two media were unable to support sufficient cell growth. Medium adapted from Gonzalez and colleagues resulted in the formation of colonies within two weeks of seeding (Fig. 12C). The colonies consisted of cells with small cell body, prominent nucleus and few cell processes. Some dispersed cells were evident which were either thin and elongated or polygonal. Selection of colonies by picking and further expansion at a cell density of 3000 cells/cm^2 resulted in a fairly homogenous population which could be maintained up to p15, with senescence becoming noticeable around p8.

The monolayer technique seemed to selectively promote the proliferation of cells with stem cell morphology and was pursued further to test its effectiveness, which was later found to retain stemness and phenotype of stem cells. Thus, monolayer culture of cells isolated from the TM tissue is the culture method utilized for expanding TM stem cells for this study.

3.1.3 Monolayer Culture Cells are of Trabecular Meshwork Origin

To assess whether the cells propagated by the monolayer technique originated from the TM tissue, they were tested for the expression of known TM markers. To date no one gene is known to be uniquely expressed in the TM tissue. Several genes known to be highly expressed in the tissue, namely ankyrin G (*ANK3*), low density lipoprotein receptor (*LDLR*), chitinase 3-like 1 (*CHI3L1*), human milk fat globulin 1 (*HMFG1*), matrix metallopeptidase 1 (*MMP1*) and aquaporin 1 (*AQP1*) are collectively used as markers to identify the TM. RT-PCR anaylsis of the cells showed the expression of these genes (Fig. 13A). Stem cell related marker, ATP-binding cassette sub-family G member 2 (*ABCG2*) was also expressed in the cells. Immunofluoresence confirmed expression at the protein level in nearly 100% of the cells for ANK3, ABCG2, HMFG1 and AQP1 (Fig. 13B). This shows that the isolated cells originated from the TM tissue.

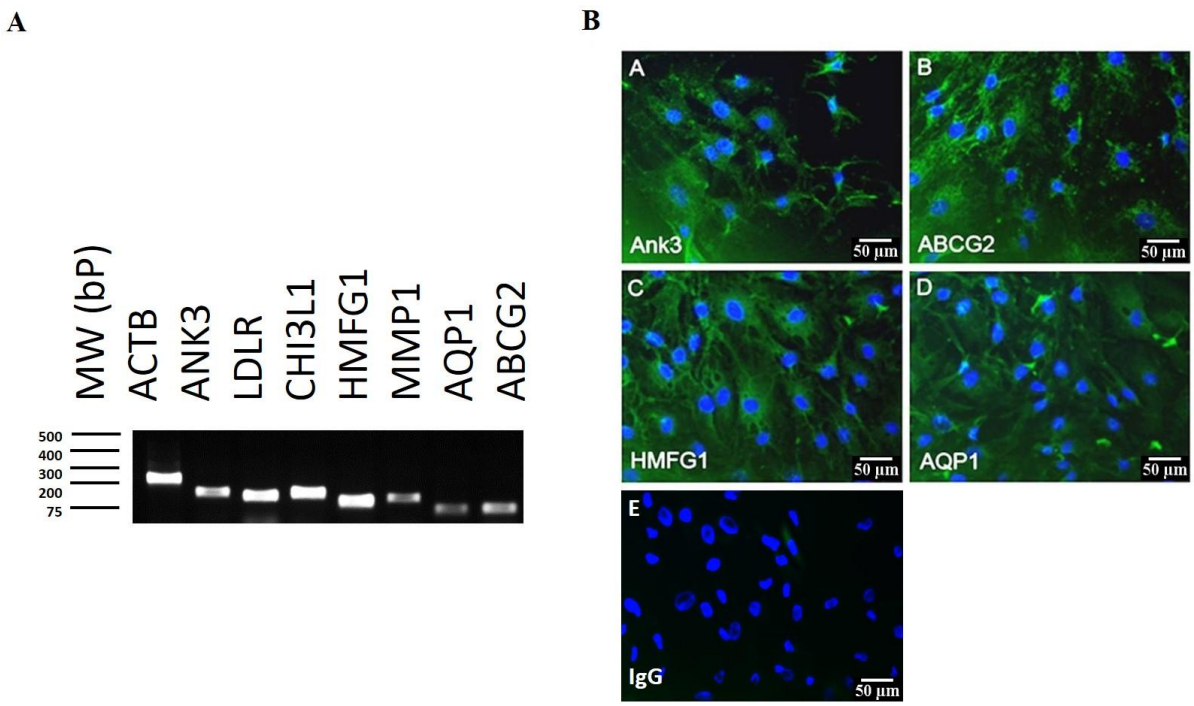

Figure 13. Monolayer culture propagated cells are of TM origin. (A) RT-PCR showed the expression of TM markers (*ANK3*, *LDLR*, *CHI3L1*, *HMFG1*, *MMP1*, *AQP1*) and stem cell related marker (*ABCG2*) in the cells. Amplicons were between 50 – 250 bp. (B) Immunofluorescence confirmed ANK3, ABCG2, HMFG1 and AQP1 protein expression. IgG control showed no signal under 495 nm excitation.

3.1.4 Monolayer Culture Cells Exhibit Stem Cell Phenotype

The ability of the propagated cells from the TM to form colonies when seeded at a sparse density indicate that they might be clonogenic, a property of stem cells. In addition, these cells also have a large nucleus: cytoplasmic ratio which is typical of stem cells. These phenotypes are suggestive of the cells as stem cells, but requires further characterization to confirm this. Expression of stem cells markers is an often utilized to identify potential stem cell populations.

So, expression of several common stem cell markers was analyzed. From the RT-PCR result, they were found to express v-myc myelocytomatosis viral oncogene homolog (*MYC*), nanog homeobox (*NANOG*), octamer-binding protein 4 (*OCT4*), kruppel-like factor 4 (*KLF4*), reduced expression protein 1 (*REX1*) and nestin (*NES*) (Fig. 14A). Sex determining region Y-box 2 (*SOX2*) was absent, which is common in some adult stem cells like MSC at late passage [154]. Immunofluorescence for NANOG and OCT4 showed them to be present in

almost the entire population (Fig.14B). This further confirms the propagated cells as stem cells.

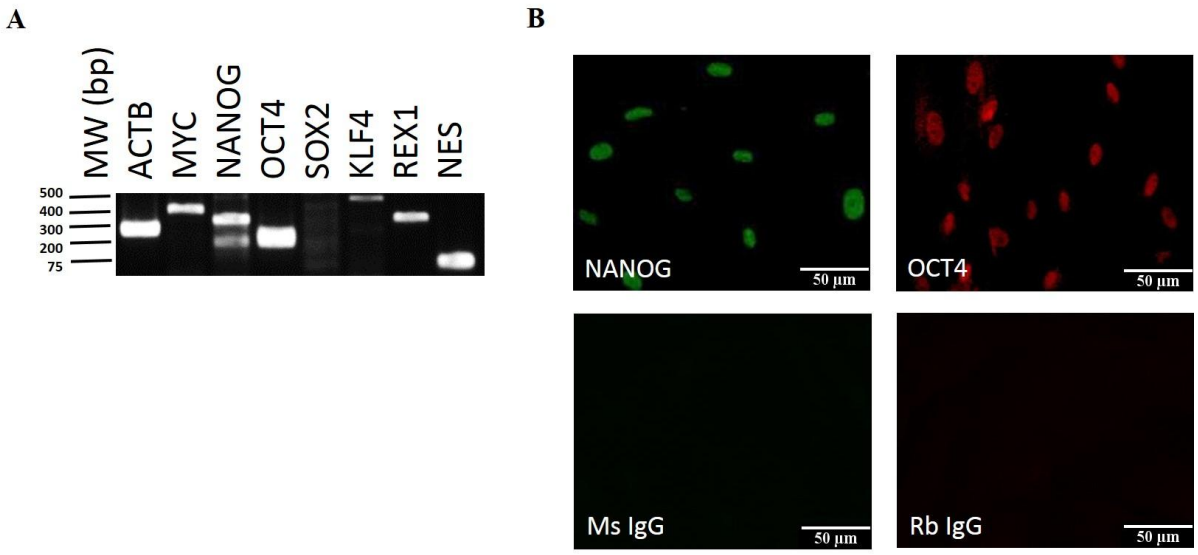

Figure 14. Monolayer culture propagated cells express stem cell markers. (A) The cells were positive for stem cell markers *MYC*, *NANOG*, *OCT4*, *KLF4*, *REX1* and *NES*, but lacked *SOX2*. Size of the amplicons were from 50 – 500 bp. (B) NANOG and OCT4 expression was also demonstrated by immunofluorescence. IgG controls showed no signal under 495 nm absorbance.

Colony forming units-fibroblast (CFU-F) is a method to quantify the frequency of stem/ progenitor cells within a cell population. To assess the proportion of clonogenic cells, i.e. stem cells, among the cells harvested from the TM, CFU-F was performed. Freshly isolated cells from the TM were plated at a low density of 1500 cells/cm^2 and colonies were generated by 14 days, indicative of proliferative cells within the population. The mean frequency of CFU-F formation for the six biological samples tested was 0.15 ± 0.02 SEM (Fig. 15A).

The average for young (< 40 years) and old (> 40 years) samples were compared to assess whether age of the donor affects the stem cell population, but no difference in CFU-F formation frequency was found (p=0.46, t-test) between the two groups (Fig. 15B), indicating the stem cell number is fairly constant throughout life.

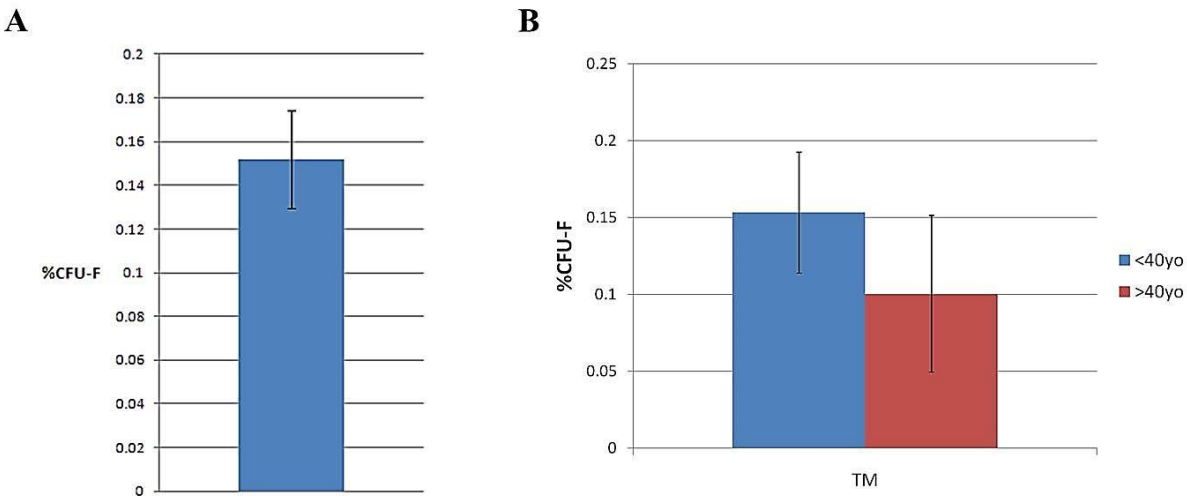

Figure 15. Clonogenic potential assessment of cells isolated from the TM. (A) CFU-F assay quantified the mean frequency of CFU-F formation as 0.15% ± 0.02 SEM across 6 biological samples. (C) No variation in CFU-F formation frequency was detected between the old and young samples.

Taken together, the data shows that about 0.15% of cells harvested from the TM are clonogenic and they display stem cell markers as well as morphology akin to adult stem cells. They are strongly indicative of the population being stem cells.

3.1.5 Trabecular Meshwork Stem Cell Culture Free of Contaminating Cells

The TM marker and stem cell marker expression profile, together genotypically indicate the cells to be TM stem cells. To ensure the isolation and propagation methodology was not promoting growth of cells from peripheral tissues of the cornea and sclera, the tissues were dissected and cultured separately under the same culture condition as TM stem cells. The resulting cells were morphologically distinct from the TM stem cells. The corneal and scleral cells were more elongated without much cell processes and formed a swirl pattern, characteristic of fibroblasts (Figs. 16A-C). Moreover, the TM markers *LDLR*, *CHI3L1*, *MYOC* and *MMP1* were downregulated in them compared to TM stem cells according to qRT-PCR analysis (Fig. 16D), indicating the cornea and sclera alone could not have contributed to the culture.

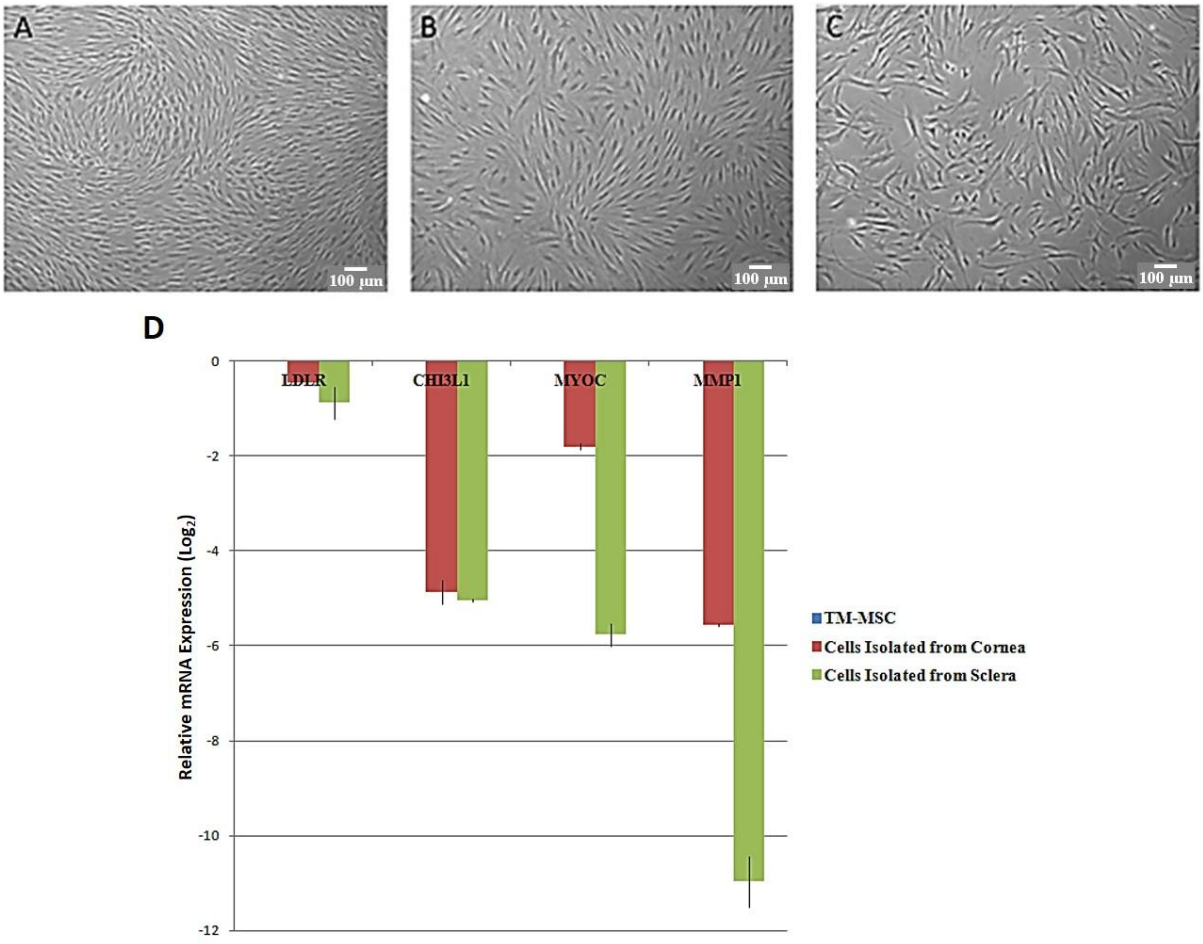

Figure 16. Propagated cells were derived from the TM and not from the cornea or sclera. (A) Corneal cells and (B) scleral cells derived using the TM stem cell isolation technique were morphologically different from the (C) TM stem cells. (D) TM markers *LDLR*, *CHI3L1*, *MYOC* and *MMP1* were lower in expression in the corneal and scleral cells relative to TM stem cells as quantified by qRT-PCR.

There is a possibility of detached epithelial, endothelial or cells of neural crest origin from other parts of the eye getting trapped in the porous TM tissue and contaminating the culture. To ensure no such contamination of culture is present, cultured cells were analyzed for the expression of epithelial markers [cytokeratin 3 (*KRT3*), cytokeratin 12 (*KRT12*), α9-integrin (*ITGA9*)], vascular endothelial markers [von willebrand factor (*VWF*), platelet-endothelial cell adhesion molecule (*CD31*), vascular-endothelial cadherin (*VE-Cad*)], as well as neural crest progenitor marker *p75*. All markers were absent in the population (data not shown), excluding contamination by the Schlemm's canal endothelial cells, corneal endothelial cells, corneal epithelial cells, corneal keratocytes and other such cells types in the eye. Hence, the culture is a fairly pure population of stem cells derived from the TM.

From the various stem cell culture techniques tested, we have developed an optimal method for TM stem cell isolation. Monolayer culture of enzymatically dissociated cells from the TM after size selection formed colonies, picked for expansion and generated a relatively homogeneous population of cells. These cells were evaluated and found to be of TM origin, had clonogenic potential and expressed stem cell markers, confirming them as TM stem cells. The culture was also free from contamination by other ocular cells and deems this technique suitable for TM stem cell isolation and expansion.

3.2 Characterization of Trabecular Meshwork Stem Cells as Mesenchymal Stem Cells

Characterization of TM stem cells as MSC will be presented in this chapter. Resemblance of TM stem cells to MSC in terms of morphology and proliferation, led us to hypothesize that they are MSC. This was tested by assessments for MSC phenotype using specific markers and differentiation potential into several mesenchymal lineages which found the TM stem cells to possess both. Gene expression profiling also demonstrated their similarity to MSC from various sources and mesenchyme-derived tissues. Overall, the data confirms TM stem cells as MSC.

3.2.1 Trabecular Meshwork Stem Cells Resemble Mesenchymal Stem Cells

TM stem cells morphologically resembled mesenchymal stem cells (MSC) with their small cell body, few cell processes and large, round nucleus with prominent nucleolus. MSC are also long and thin, and capable of forming colonies when grown on tissue culture plastic, similar to TM stem cells. To assess the extent of morphological similarity between TM stem cells and MSC under the same culture conditions, MSC derived from human adipose tissue (Ad-MSC) were grown in the same culture medium as TM stem cells. Their morphological resemblance to TM stem cells was evident, with both cell types displaying slightly elongated cells with compact cell body and sizeable nucleus (Fig. 17 A-B). Real-time quantification of proliferation rate of TM stem cells and Ad-MSC measured by the xCELLigence system at p4 showed them to proliferate at a similar rate (Fig. 17C). Their growth curves overlapped substantially and they have the same average doubling time of 70 h. The morphological and proliferative correspondences between TM stem cells and Ad-MSC led to my hypothesis that TM stem cells are MSC which was investigated.

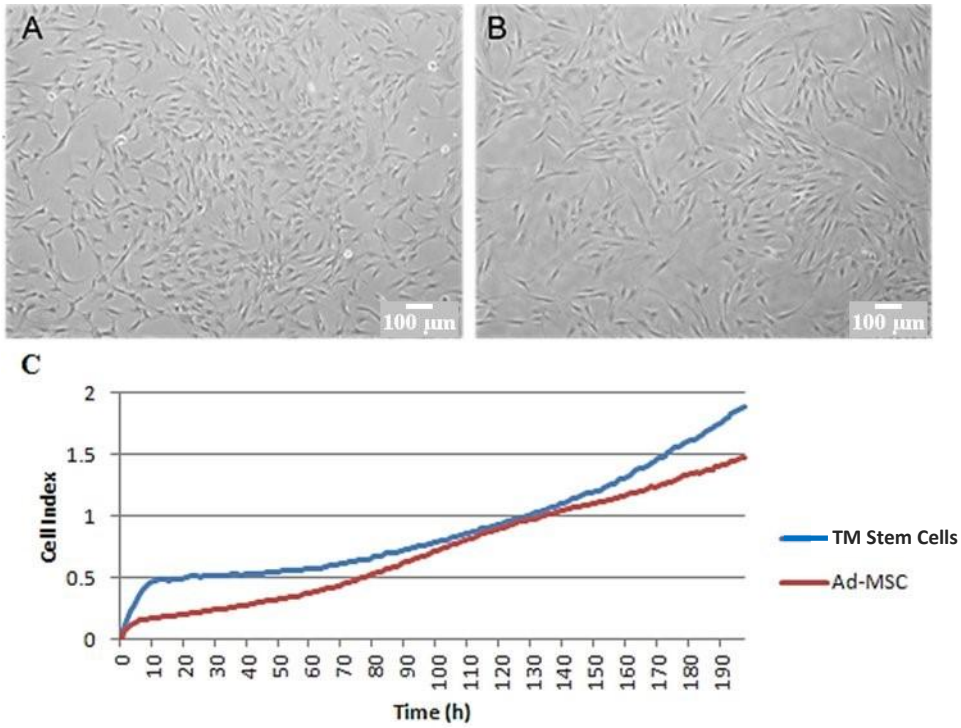

Figure 17. TM stem cells resemble MSC in morphology and proliferation. Both (A) TM stem cells and (B) Ad-MSC are compact, slightly elongated with some cell processes and large nucleus. (C) Real-time quantification of proliferation found them to share similar growth profile and proliferative rate in TM stem cell culture medium.

3.2.2 Criteria for MSC Characterization

In order to characterize a cell type as MSC, certain criteria have to be met other than morphological evidence. Different groups have used dissimilar means of characterizing the cell type from definition to markers, and there was no right or wrong. The wide disparaging use of the term 'MSC' led to the establishment of the minimal set of standard criteria to define MSC by the Mesenchymal and Tissue Stem Cell Committee of the International Society for Cellular Therapy (ISCT) (Table 1) [155]. According to this set of minimal criteria, MSC must be plastic-adherent under standard culture conditions. They must also possess the expression of surface antigens, CD105, CD73 and CD90, and not express the pan-hematopoietic lineage marker (CD45), hematopoietic stem cell marker (CD34), leukocyte markers, (CD14 or CD11b), B-cell markers (CD79α or CD19) and major histocompatibility antigen (HLA-DR). More than 95% of the population is expected to display this phenotype. In addition, they must differentiate *in vitro* into the mesenchymal

lineages of osteocytes, adipocytes and chondrocytes as shown by staining to demonstrate their multipotency.

Table 1. Summary of minimal criteria to identify MSC		
1. Adherence to plastic in standard culture conditions		
2. Phenotype	Positive (≥ 95% +)	Negative (≤ 2% +)
	CD73	CD34
	CD90	CD45
	CD105	CD14 or CD11b
		CD79α or CD19
		HLA-DR
3. *In vitro* differentiation into osteocytes, adipocytes and chondrocytes (demonstrated by staining)		

Table 1. Summary of minimal criteria to identify MSC proposed by the ISCT. Table adapted from Dominici et al., 2006.

This set of criteria to identify MSC has been utilized in this study to explore whether TM stem cells could be MSC. TM stem cells can attach to uncoated tissue culture plastic, thus satisfying the first condition for MSC characterization. In order to fulfil the remaining two criteria, TM stem cells were tested further for MSC phenotype and differentiation potential.

3.2.3 Trabecular Meshwork Stem Cells Display MSC Marker Expression Profile

MSC highly express cell-surface antigens, *NT5E* (*CD73*), *THY-1* (*CD90*) and endoglin (*CD105*). They are used as positive markers of MSC. Certain genes expressed in specific blood cell types, such as hematopoietic stem cells, leukocytes, B-cells and T-cells, but not expressed by MSC are *CD34*, *CD45*, *CD11b*, *CD79α* and *HLA-DR*. Collectively, they are taken to be negative markers of MSC. Hence, expression of the positive markers and absence of the negative ones distinguish MSC.

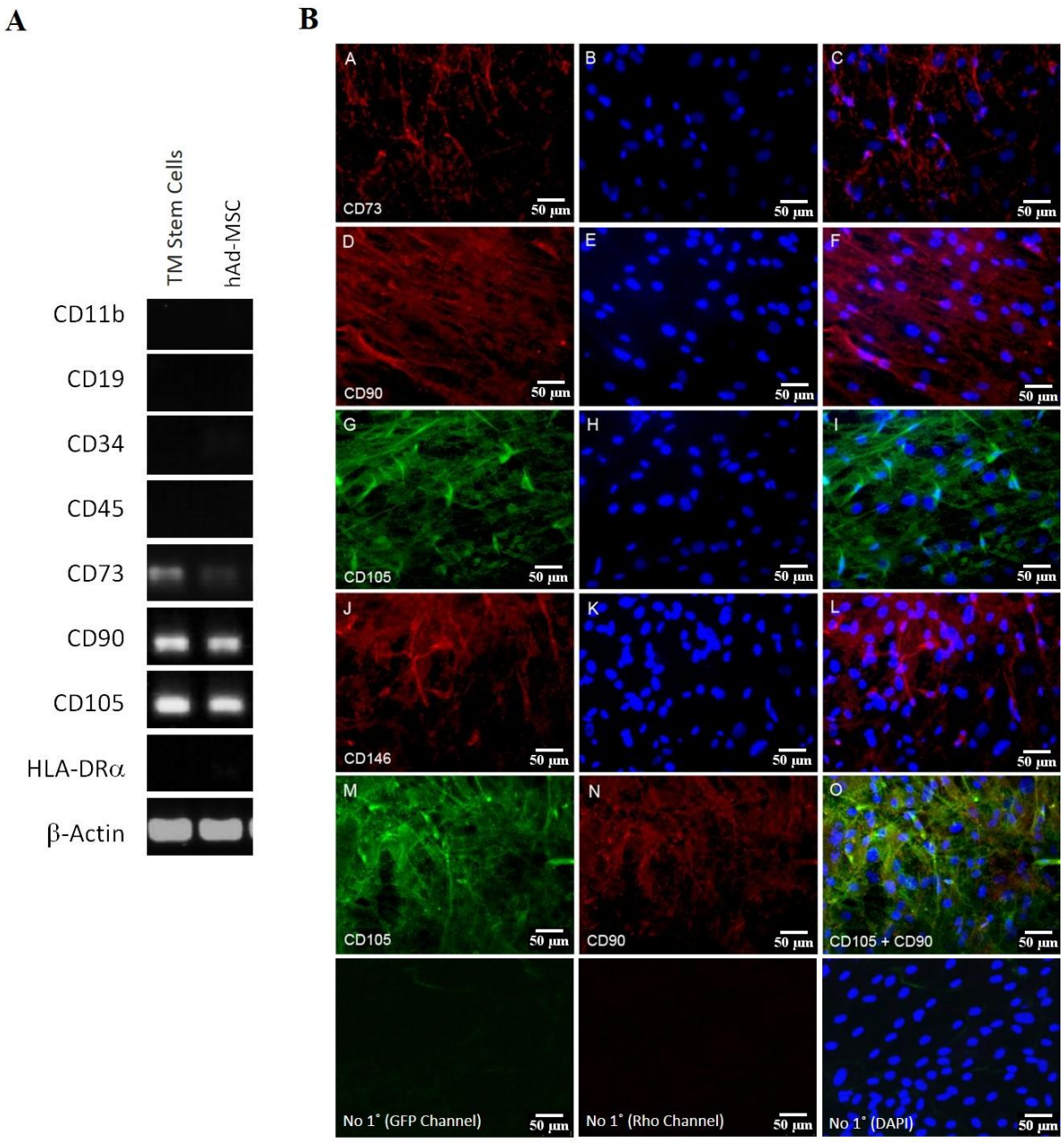

Figure 18. Cultured TM stem cells display MSC marker expression profile. (A) RT-PCR indicated the presence of positive MSC markers and lack of negative MSC markers in the population, similar to Ad-MSC. (B) Immunofluorescence showed the expression of the positive MSC markers, CD73, CD90, CD105 and CD146. The cells were double-positive for CD105 and CD90. (Negative control: no primary antibody).

RT-PCR found TM stem cells to express the positive markers, *CD73*, *CD90* and *CD105*, while lacking the expression of all the negative markers (Fig. 18A). Ad-MSC had the same expression profile, albeit with expression of *CD34* which is common in some MSC subtypes. Immunofluorescence confirmed the expression of CD73, CD90, CD105 and CD146, another accepted marker of MSC (Fig. 18B). The antigens were observed to be uniformly expressed

across the cell surface by majority of the population. Double staining for CD90 and CD105 showed the cells to be positive for both antigens, confirming co-expression of the genes.

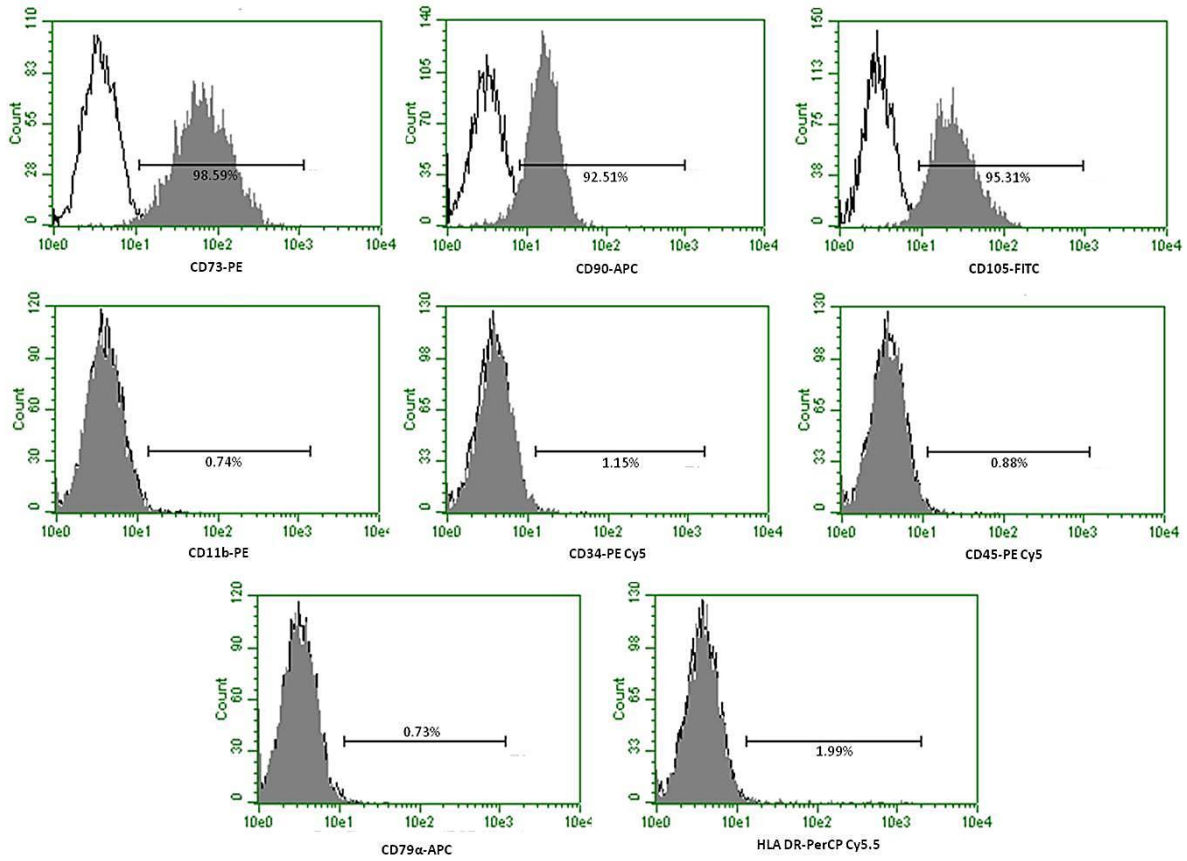

Figure 19. Flow cytometric analysis of MSC markers. The investigation revealed > 92% of the population expressed the positive MSC markers and < 2% had the expression of the negative markers.

Further expression analysis of the markers by flow cytometry revealed more than 92% of the population expressed the positive MSC markers, and less than 2% presented the negative markers (Fig. 19). Thus, the population of TM stem cells is a homogeneous culture of MSC-like cells. Taken together, the results demonstrate the TM stem cells to satisfy the expression phenotype required of MSC and constitute a homogenous population of such cells.

3.2.4 Trabecular Meshwork Stem Cells are Multipotent

MSC have the capacity to differentiate into the various mesenchymal lineages of osteoblasts, chondrocytes, adipocytes, myoblasts, stromal cells and ligament fibroblasts. As a standard,

differentiation into the three mesenchymal lineages of adipocytes, osteocytes and chondrocytes is adopted as another defining characteristic of MSC. To investigate whether TM stem cells are able to differentiate into these cell types, low passage TM stem cells (p2 – p4) were subjected to adipogenic, osteogenic and chondrogenic inducing conditions.

After adipocyte differentiation [156], the cells were stained with Oil Red O to detect adipocytes. Clusters of Oil Red O-positive cells were observed (Fig. 20A). The adipocytic markers, peroxisome proliferator-activated receptor gamma (*PPARγ*), fatty acid binding protein 4 (*FABP4*) and lipoprotein lipase (*LPL*) were also upregulated in the differentiated cells, compared to undifferentiated control as analyzed by qRT-PCR (Fig. 20B). The data demonstrates that TM stem cells can differentiate into adipocytes.

Under conditions promoting osteocytic differentiation [157], the cells gave rise to Alizarin Red-positive cells when stained with the dye which is an indication of intracellular calcium deposits (Fig. 20C). In addition, qRT-PCR found the osteocytic markers, runt-related transcription factor 2 (*RUNX2*) and osteocalcin, to be upregulated in these cells compared to the control (Fig. 20D). So, the TM stem cells are also capable of differentiating into osteocytes.

Chondrocytic differentiation of TM stem cells as an aggregation culture in chondrocyte-inducing medium [139], [140] led to cells that stained for type II collagen, a marker of chondrocytes (Fig. 20E). The staining was more intense in the core of the pellet than the outer region, indicating a higher proportion of differentiated cells in the inner region than the exterior. The result demonstrates the ability of TM stem cells to differentiate into chondrocytes too.

In conclusion, TM stem cells are multipotent as demonstrated by their *in vitro* differentiation into adipocytes, osteocytes and chondrocytes. They, thus, meet the final minimum criterion needed to characterize them as MSC.

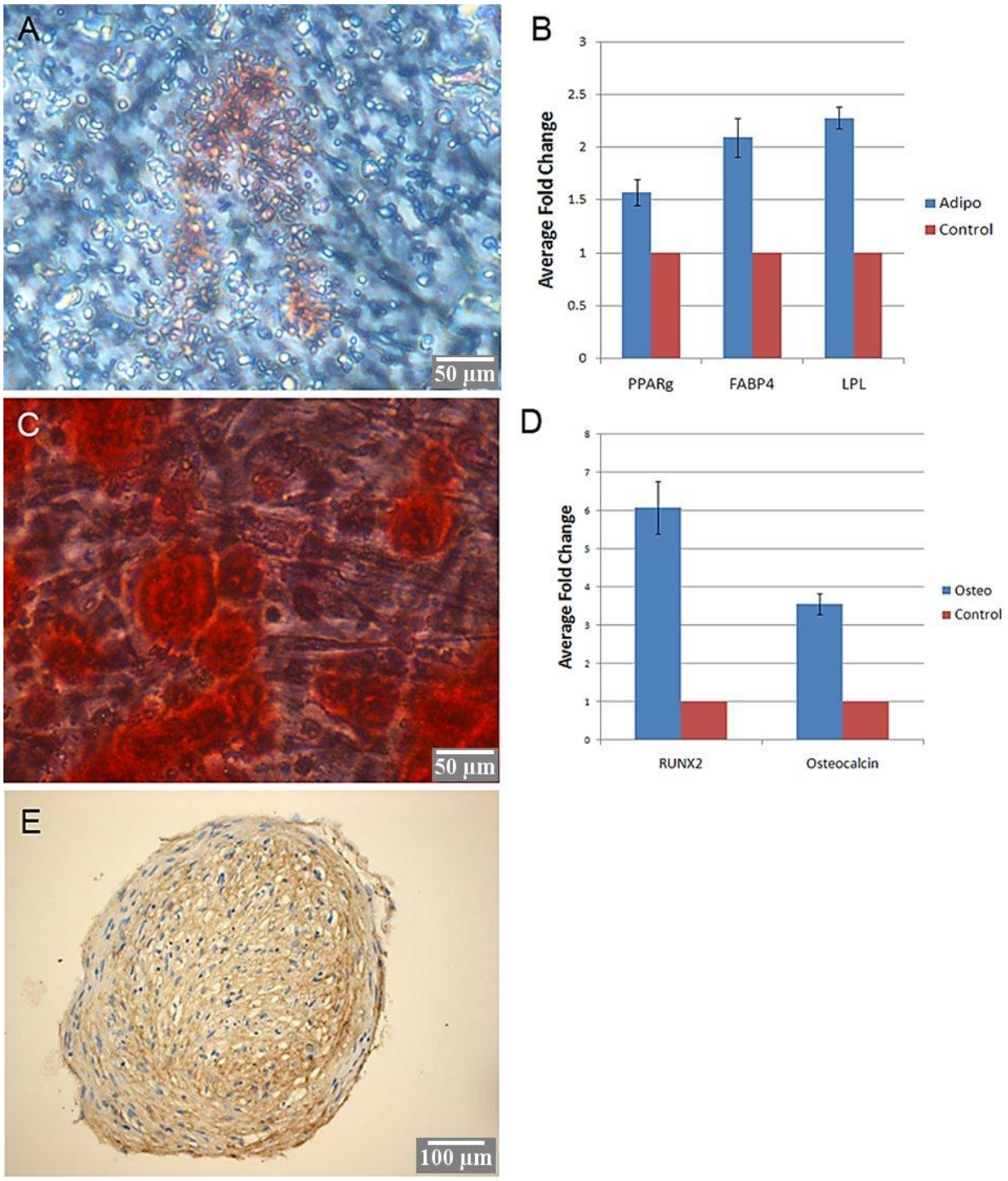

Figure 20. TM stem cells differentiated *in vitro* into adipocytes, osteocytes and chondrocytes. (A) Oil Red O staining was observed under adipogenic differentiation, as well as (B) upregulation of the adipogenic markers relative to undifferentiated control in qRT-PCR analysis. (C) Under osteogenic differentiation condition, the cells were stained by Alizarin Red, indicative of calcium deposits. (D) qRT-PCR showed upregulation of the osteocytic markers. (E) Chondrogenic induction promoted staining for type II collagen, a chondrocytic marker.

3.2.5 Trabecular Meshwork Stem Cells Share Similarities with Mesenchymal Derivatives

Characterization of TM stem cells for MSC properties listed by the ISCT found them to fulfill the criteria to define them as MSC. So, from here on TM stem cell propagated by our group will be termed as trabecular meshwork-derived mesenchymal stem cells (TM-MSC). To further assess how similar they are to MSC and different from other cell types, particularly in the context of the eye, gene expression profiling by microarray was performed.

The cell types included in this microarray study besides TM-MSC are Ad-MSC, corneal fibroblasts, corneal endothelial cells, corneal stroma, scleral fibroblasts, retinal pigmented epithelial cells (RPE), human embryonic stem cells (hESC), neurons differentiated from hESC, neural progenitor cells (NPC) and human umbilical vein endothelial cells (HUVEC). hESC, RPE and HUVEC were expanded from commercially purchased lines, while the rest were isolated/ differentiated in our lab and used for gene expression profiling. Hierarchical clustering of the gene sets according to similarity of gene expression found TM-MSC to be clustered together with Ad-MSC and scleral fibroblasts (Fig. 21A). This shows the similarity of TM-MSC with MSC despite different source and to the scleral cells probably due to common origin from the mesenchyme.

An additional microarray study was performed on the TM-MSC data set by comparing it using gene set enrichment analysis (GSEA) with that of several other cell types published by other groups (Fig. 21B). Both stem and somatic cells were included in the study consisting of bone marrow-derived MSC (BM-MSC), mesenchyme-derived tissues, stem cells from various sources, cells or tissues derived from the eye and several other cells/ tissues of endoderm and ectoderm origin. From the 23 gene sets compared, 8 were found to be significantly enriched in the TM-MSC data set ($p < 0.05$) (Fig. 21B). They were all 3 sets of BM-MSC and mesenchyme-derived tissues, specifically cortical bone, periosteum, articular cartilage and scleral tissue. Olfactory mucosa-derived stem cells were found to be similar to TM-MSC as well probably due to common developmental origin. The data shows the similarity of TM-MSC to BM-MSC despite their different sources, and also to tissues of MSC origin. This adds more support to our hypothesis of TM stem cells being MSC. Interestingly, gene sets related to the eye were not enriched in the TM-MSC data set, perhaps

because the former are all mature cell types and hence are significantly different from the progenitor state of TM-MSC.

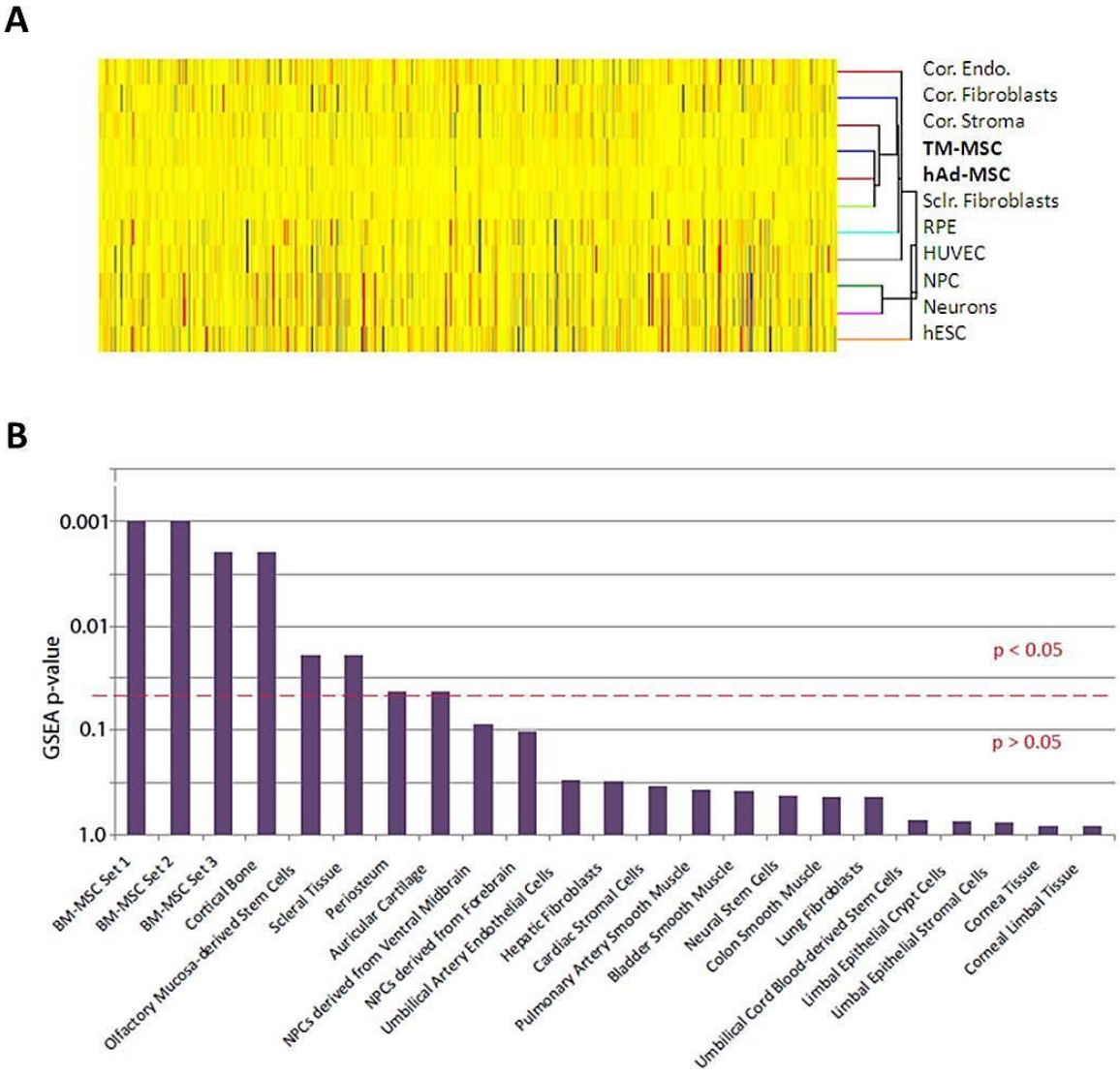

Figure 21. Gene expression profiling demonstrates the similarity of TM-MSC with MSC from different sources and cell types derived from the mesenchyme. (A) Hierarchical clustering of data sets of TM-MSC and several other cell types from the eye, cells of endoderm and ectoderm origins, found them to cluster with Ad-MSC and scleral fibroblasts. (B) GSEA comparison of TM-MSC gene set with that of cell types from diverse tissues showed their closeness to MSC and mesenchyme-derived tissues.

Both set of microarray analyses clearly show the divergence of TM-MSC from cell types arising from the other germ layers in terms of gene expression profile. Importantly, they demonstrate the closeness of TM-MSC to MSC from various sources, and to other cell types of mesenchyme origin. So, they corroborate our finding that TM stem cells are MSC.

In summary, it can be established that the TM stem cells are MSC from their ability to adhere onto tissue culture plastic, possession of MSC marker expression profile and multi-lineage differentiation potential. Furthermore, the microarray studies confirmed their similarity to MSC and tissues derived from MSC. Characterizing the TM stem cells as MSC is particularly important for this study of cell-based therapy for POAG. It shows the multipotency of the cells which will most likely allow the cells to differentiate into mature TM cells, capable of restoring function to the glaucomatous TM by executing essential functions of the TM.

3.3 Identification of Novel Trabecular Meshwork Differentiation Markers

The ultimate objective of the project was to derive functionally mature TM cells that are applicable for POAG treatment. TM-MSC being stem cells of the TM should have inherent potential to differentiate into mature TM cells. A differentiation protocol has to be designed to attain this. But this task is challenged by the lack of differentiation markers necessary to track TM differentiation. It is not clear whether markers used to identify TM origin are differentially expressed between the progenitor and mature populations of the TM. So, their validity as TM differentiation markers is questionable. Hence, the identification of suitable differentiation markers of TM lineage is imperative. To qualify as good differentiation markers, the genes have to be (1) differentially expressed between TM-MSC and mature TM cells and (2) ideally specific to the TM in the anterior segment of the eye. This chapter discusses how the TM differentiation markers were established.

3.3.1 Gene Expression Profiling of TM-MSC and Trabecular Meshwork Tissue

Genes differentially expressed between the TM-MSC and mature TM cells can be used as TM differentiation markers. Efforts to culture differentiated cells from the TM tissue were unsuccessful. So, *ex vivo* TM tissue comprising mostly of differentiated TM cells was utilized here to represent the mature TM cells. To find differentially expressed genes, gene expression profiling by microarray analysis was performed on the TM tissues and TM-MSC from 3 different donors each of the same age group (50 – 70 years). Signal intensities were normalized by the method of centralization and TM vs TM-MSC entity list was generated with one-way ANOVA corrected *p*-value set as ≤ 0.05 (t-test unpaired) and fold change cut-off of 2. Benjamini-Hochberg multiple testing correction was also applied to remove false positives.

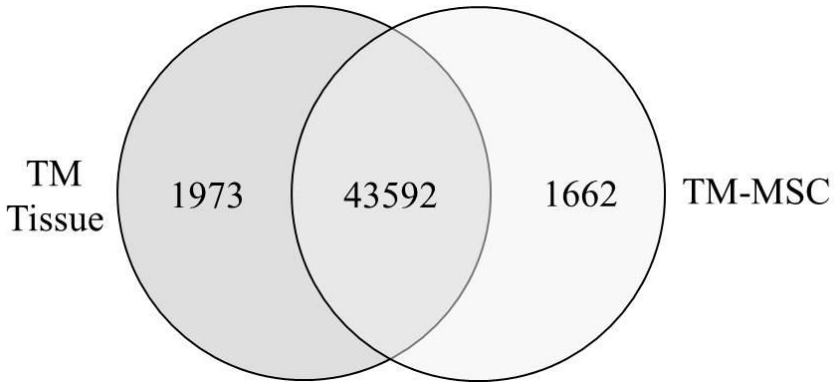

Figure 22. Venn diagram of number of genes upregulated in the TM tissue and TM-MSC as determined by gene expression profiling.

The resultant entity list had considerable number of probes differentially expressed between the two specimens, with 1973 and 1667 genes upregulated in the TM tissue and TM-MSC respectively as compared to the other (Fig. 22). *MYOC* and angiopoietin-like 7 (*ANGPTL7*), two genes first discovered in the TM, were the most highly expressed in the TM tissue with a fold difference of more than 1000 compared to TM-MSC. The top 20 genes upregulated in the TM are listed in Table 2A. These genes code for proteins from different compartments of the cell, like intracellular proteins (*PCP4*, *KRT13*, *KRT5*, *MYH11*, *HBB*, *FAM107A*), the cell surface proteins (*CDH23*, *HLA-DRα*, *VCAM1*, *CXADR*, *TACSTD2*), and secreted proteins (*MYOC*, *ANGPTL7*, *CCL3L3*, *SERPINA3*, *APOD*, *FCGBP*, *PTGDS*, *C2ORF40*). *H19*, a non-protein coding gene functioning as a tumor suppressor, was also upregulated.

Interestingly, *HLA-DRα* which was absent in TM-MSC was highly expressed in the mature cells. *THY-1* (*CD90*), present in TM-MSC, was downregulated in the TM. TM-MSC expressed alpha-kinase 2 (*ALPK2*) and lysyl oxidase (*LOX*) at the greatest level compared to the TM tissue at 138 and 70 times more respectively. Other genes highly downregulated in the TM are listed in Table 2B. Further investigation will disclose which of these differentially expressed genes are specific enough to be applicable as differentiation markers of TM lineage.

Table 2A. Top 20 genes highly expressed in the TM tissue compared to TM-MSC

Symbol	Definition	Fold change (TM/ TM-MSC)
MYOC	Myocilin, trabecular meshwork inducible glucocorticoid response	1373
ANGPTL7	Angiopoietin-like 7	1144
PCP4	Purkinje cell protein 4	656
KRT13	Keratin 13	459
SERPINA3	Serpin peptidase inhibitor, clade A (alpha-1 antiproteinase, antitrypsin), member 3	443
MYH11	Myosin, heavy chain 11, smooth muscle	425
CDH23	Cadherin-like 23	419
HLA-DRA	Major histocompatibility complex, class II, DR alpha	354
PTGDS	Prostaglandin D2 synthase 21kDa (Brain)	300
FAM107A	Family with sequence similarity 107, member A	274
HBB	Hemoglobin, beta	258
C2orf40	Chromosome 2 open reading frame 40	239
FCGBP	Fc fragment of IgG binding protein	231
APOD	Apolipoprotein D	230
CXADR	Coxsackie virus and adenovirus receptor	218
TACSTD2	Tumor-associated calcium signal transducer 2	215
H19	H19, imprinted maternally expressed transcript (non-protein coding)	210
KRT5	Keratin 5	209
CCL3L3	Chemokine (C-C motif) ligand 3-like 3	205
VCAM1	Vascular cell adhesion molecule 1	193

Table 2B. Top 20 genes highly expressed in the TM-MSC compared to TM tissue

Symbol	Definition	Fold change (TM-MSC/TM)
ALPK2	Alpha-kinase 2	138
LOX	Lysyl oxidase	70
FOXD1	Forkhead box D1	66
STS1	Cbl-interacting protein Sts-1	60
STC2	Stanniocalcin 2	58
CD151	CD151 molecule (Raph blood group)	54
KCNK2	Potassium channel, subfamily K, member 2	49
KIAA0101	KIAA0101	47
RPLP0	Ribosomal protein, large, P0	45
MELK	Maternal embryonic leucine zipper kinase	44
MARCH4	Membrane-associated ring finger (C3HC4) 4, E3 ubiquitin protein ligase	43
TXNRD1	Thioredoxin reductase 1	42
TMEM132D	Transmembrane protein 132D	40
THY1 (CD90)	Thy-1 cell surface antigen	39
TNFRSF11B	Tumor necrosis factor receptor superfamily, member 11b	38
FN1	Fibronectin 1	36
WDR1	WD repeat domain 1	36
KDELR3	KDEL (Lys-Asp-Glu-Leu) endoplasmic reticulum protein retention receptor 3	36
TSPO	Translocator protein (18kDa)	35
RAB3B	RAB3B, member RAS oncogene family	34

Table 2. Top 20 genes upregulated in the TM tissue (Table 2A) and TM-MSC (Table 2B) compared to the other.

In order to decipher the differences between the TM stem cells and mature cells in a comprehensive manner of the fairly large gene sets, biological processes differentially regulated between them were identified. Functional annotation clustering by DAVID [146] with an enrichment score cut-off of 1.3, equivalent to 0.05 on non-log scale, and *p*-value ≤ 0.05 found diverse biological processes to be enriched in the TM tissue compared to TM-MSC (Table 3). Biological adhesion was the greatest enriched process which is expected due to the structural complexity of the tissue with ECM and cell junctions that are missing in the monolayer culture of TM-MSC. Mesenchyme development and certain organ developments were also upregulated, indicating the differentiated state of the TM cells and perhaps common signalling pathways involved in their development. Of particular interest were sensory perception to mechanical stretch, homeostasis of number of cells and phagocytosis which was significantly upregulated with 11 contributing genes ($p = 0.007$) and it came under the parent term, endocytosis. All three functional characteristics have been demonstrated in the mature TM cells and are essential for TM function. Pigmentation was also enriched in the mature cells (13 genes; $p = 0.004$), and could potentially be used as a phenotypic assessment of TM differentiation.

Cell motion, a controversial function TM cells are believed to have, was also enriched. In addition, negative regulation of growth (15 genes; $p = 0.027$) under the term regulation of growth, and negative regulation of cell size were augmented relative to TM-MSC, confirming growth arrest of the mature TM cells. Defense response and response to wounding were also higher, probably due to injury from the extraction procedure at post-mortem and/ or TM dissection. Other processes augmented in the TM include gene expression, response to organic substances, membrane organization, several metabolic and biosynthetic processes.

Similar gene ontology (GO) analysis of genes upregulated in the TM-MSC relative to mature cells *ex vivo* found a wide range of biological processes enriched in the TM-MSC (Table 4). Protein localization, intracellular transport and proteolysis with more than 130 responsible genes upregulated for each were the top three upregulated processes. Cell cycle was also among the highly augmented processes, and together with upregulated cell division, indicates the proliferative state of TM-MSC. Nucleotide, ribonucleotide, DNA, RNA (mRNA and ncRNA), ribonucleprotein complex and protein metabolic processes, which biosynthesize these essential constituents of the cells are upregulated. Organizational processes of cytoskeleton, membrane, mitochondria and macromolecule are also enriched. These

biosynthetic and organizational processes further corroborate the growth capacity TM-MSC possess, but the mature TM cells lack. Death is also enriched, but it accounts for both anti-apoptotic and apoptotic processes that counteract each other.

Table 3. Biological processes enriched in the TM tissue.

Biological Process	Number of Genes	*P*-Value
Biological adhesion	117	3.80E-12
Response to organic substance	90	3.70E-04
Positive regulation of nitrogen compound metabolic process	82	3.80E-04
Positive regulation of biosynthetic process	81	5.00E-03
Positive regulation of gene expression	74	7.60E-04
Defense response	70	1.50E-02
Positive regulation of RNA metabolic process	64	5.90E-04
Response to wounding	64	6.10E-03
Positive regulation of transcription, DNA-dependent	63	8.00E-04
Cell motion	58	7.30E-03
Neuron differentiation	54	8.00E-03
Cellular component morphogenesis	52	2.80E-03
Membrane organization	48	8.60E-03
Skeletal system development	44	2.40E-03
Immune system development	41	8.60E-04
Regulation of growth	41	3.00E-02
Embryonic development ending in birth or egg hatching	39	5.00E-02
Sensory organ development	38	1.60E-04
Embryonic morphogenesis	37	3.90E-02
Tube development	33	2.60E-03
Endocytosis	33	2.60E-03
Embryonic organ development	28	1.80E-03
Extracellular structure organization	25	7.10E-03
Cellular amino acid derivative metabolic process	22	5.10E-02
Urogenital system development	19	6.30E-03
Sensory perception of mechanical stimulus	18	7.10E-03
Respiratory system development	17	2.40E-02
Homeostasis of number of cells	16	2.50E-02
Secondary metabolic process	15	7.50E-03
Negative regulation of cell size	15	4.60E-02
Mesenchyme development	14	3.80E-04
Odontogenesis	14	5.60E-04
Pigmentation	13	4.20E-03

Table 3. Biological processes enriched in the TM tissue. Gene ontology (GO) analysis was performed using DAVID functional annotation terms (subset: GOTERM_BP_FAT) on the set of genes enriched in the TM tissue relative to TM-MSC. Descendant GO terms are represented by the parent term.

Table 4. Biological processes enriched in the TM-MSC.

Biological Process	Number of Genes	*P*-Value
Protein localization	157	3.50E-13
Intracellular transport	141	5.80E-19
Proteolysis	130	8.40E-03
Macromolecule catabolic process	119	2.60E-06
Cell cycle	119	1.90E-06
Vesicle-mediated transport	108	1.30E-10
Macromolecular complex subunit organization	107	1.40E-05
Death	99	1.10E-03
Cellular protein catabolic process	91	6.50E-05
Negative regulation of macromolecule metabolic process	91	2.40E-02
Positive regulation of molecular function	84	6.80E-04
Cellular macromolecule localization	83	9.40E-10
Protein complex biogenesis	82	1.20E-05
RNA processing	80	5.20E-04
Cytoskeleton organization	74	7.10E-06
Regulation of cellular protein metabolic process	73	2.00E-04
DNA metabolic process	71	3.20E-03
Membrane organization	65	2.30E-05
Regulation of phosphorus metabolic process	61	5.00E-02
Nitrogen compound biosynthetic process	56	6.90E-05
Cell division	53	3.60E-05
mRNA metabolic process	53	7.50E-03
Negative regulation of molecular function	48	1.00E-02
Positive regulation of protein metabolic process	47	1.60E-05
Ubiquitin-dependent protein catabolic process	44	1.40E-04
Actin filament-based process	41	9.50E-04
ncRNA metabolic process	41	3.60E-04
Purine nucleotide metabolic process	39	1.50E-05
Organelle fission	39	1.30E-03
Negative regulation of protein metabolic process	38	3.90E-05
Microtubule-based process	38	1.20E-02
Regulation of protein kinase cascade	37	1.50E-02
Ribonucleoprotein complex biogenesis	35	2.00E-04
Ribonucleotide metabolic process	33	1.80E-05
Nuclear transport	31	4.30E-04
Posttranscriptional regulation of gene expression	31	3.10E-02
Protein modification by small protein conjugation or removal	27	9.00E-03
Organelle localization	26	2.40E-06
Nucleoside triphosphate metabolic process	26	1.20E-03
Mitochondrion organization	25	5.10E-03
Aminoglycan biosynthetic process	7	2.30E-02
Establishment of cell polarity	6	4.30E-02

Table 4. Biological processes enriched in the TM-MSC. Gene ontology (GO) analysis was performed using DAVID functional annotation terms (subset: GOTERM_BP_FAT) on the set of genes enriched in the TM-MSC compared to TM tissue. Descendant GO terms are represented by the parent term.

Increase in gene expression regulation through RNA processing, posttranscriptional and translational regulation, and elevation of energy production by means of polysaccharide metabolism were noted and they show the active state of TM-MSC (Table 4). Several signalling pathways such as I-kappa B kinase/ NF-kappa B cascade and protein kinase cascade were upregulated too.

Taken together, the data confirms the differences between the TM-MSC and mature TM cells not only in terms of gene expression, but also as inherent functional states, albeit indirectly. GO analysis confirmed the mature TM cells to be in a differentiated state, enriched with biological processes important for its function, while biological processes augmented in the TM-MSC overall showed their active and proliferative state, as expected of stem cells. Importantly, gene expression profiling of both cell types has determined the genes differentially expressed between them and they have the potential to be used as TM lineage markers.

3.3.2 Several Known Markers Differentially Expressed between TM-MSC and TM Tissue

Over 1000 genes were found to be highly expressed in the mature TM cells relative to TM-MSC by gene expression profiling and they may be applicable as differentiation markers of TM lineage. The decisive task was to identify those genes that are specific and robust enough to track TM differentiation. Expression studies by other groups have identified several genes highly expressed in the TM, which are collectively used as markers of the TM (Table 5). Specificity of two of these genes (*CHI3L1* and *MGP*) to the TM has been shown in the anterior segment of the human eye by reporter activity [119], [120]. To assess whether these TM markers were differentially expressed between the mature TM cells and TM-MSC, in particular significantly higher in expression in the TM tissue, they were searched for in the TM vs TM-MSC entity list.

Some TM markers were present in the entity list, being upregulated in the TM tissue relative to TM-MSC. *MYOC* and *MGP* were robustly upregulated in the TM at 1373 and 66 folds respectively. *ANK3, AQP1* and *MMP1* were all about 4 fold higher in the TM compared to TM-MSC. The remaining markers, *CHI3L1*, *LDLR* and *ELAM1* were not found in the list.

Further investigation was done to determine whether the differentially expressed markers are specific to the TM in the anterior segment.

Table 5. Common TM markers as identified by other groups.

Gene	Method of Identification	Reference
CH3L1	Gene expression profile analyses between human primary cultured TM and SC cells	Liton et al., 2005
MGP	Gene expression profile of human TM cDNA library	Gonzalez et al., 2004, Gonzalez et al., 2000; Tomarev et al., 2003
ANKG	Gene expression profile analyses between human primary cultured TM, SC cells and fibroblasts	Challa et al., 2003
AQP1	RT-PCR and immunofluorescence in human cultured TM cells	Stamer et al., 1995
MMP1	Gene expression profile analyses between human primary cultured TM, SC cells and fibroblasts	Challa et al., 2003
LDLR	Uptake of fluoresceinated native LDL, A-LDL or AA-LDL	Chang et al., 1991
MYOC	Sequence cloned first in human TM	Nguyen et al., 1998
ELAM1	Identified as an inflammatory marker in TM cells under oxidative stress	Wang et al., 2001

Table 5. Common TM markers as identified by other groups. Genes highly expressed in the TM discovered by various expression techniques. They are used in combination as TM markers.

3.3.3 Gene Expression Profiling of Cornea and Sclera

Corneal stroma, corneal endothelial cells, Schlemm's cannal endothelial cells and sclera all originate from the paraxial mesenchyme like the TM. They are also in close proximity to the TM, making it likely that some of these cell types may be derived from a common stem cell niche as the TM. If this is the case, the isolated TM-MSC, as a shared progenitor, may be capable of giving rise to some of the other cell types too. So, markers that track TM differentiation alone, and not those of corneal and scleral cell types, have to be identified.

To elucidate such markers, it is necessary to find genes uniquely expressed in the TM in the context of the anterior segment of the eye. For this purpose, TM, corneal and scleral tissues derived from three corneoscleral specimens were subjected to microarray analysis and the resulting gene expression data was processed into two entity lists of TM vs cornea and TM vs

sclera, employing a *p*-value ≤ 0.05 and fold change ≥ 2. A limited number of genes were found to have varying expression, with 47 genes in TM vs cornea and 160 in TM vs sclera data sets. Both entity lists were merged to find genes differential in expression in the cornea and sclera with respect to the TM (i.e. TM vs cornea/ sclera), and 22 genes were identified (Fig. 23). 20 genes were significantly higher in expression in the TM and 2 lower, in comparison to the cornea and sclera (Table 6). Table 6 comprises genes that distinguish the TM from the two peripheral tissues.

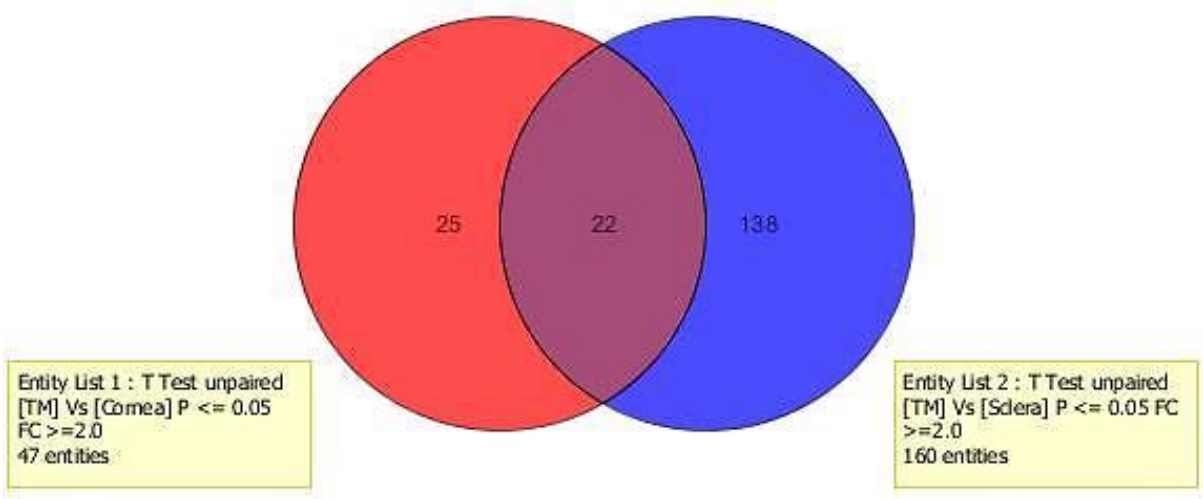

Figure 23. Venn diagram of the merged TM vs cornea and TM vs sclera entity lists. 22 genes were differentially expressed in common in the cornea and sclera with respect to the TM.

Surprisingly, none of the TM markers differentially expressed in the TM vs TM-MSC data set were seen in the merged TM vs cornea/ sclera data set, and it indicates that they are not specific to the TM. So, these markers are not relevant as differentiation markers of TM lineage as they are common to corneal and scleral cells too. Hence, our approach was modified to discover novel markers from this list which were also differentially expressed between the mature TM cells and TM-MSC. This will identify genes that are both 'TM-specific' and robust enough to trace TM differentiation *in vitro* and *in vivo*.

Table 6. List of genes differentially expressed in the cornea and sclera with respect to TM.

	TM / Cornea		TM / Sclera	
Gene	**Fold Change**	**Regulation**	**Fold Change**	**Regulation**
F5	29	up	44	up
NEB	27	up	28	up
CALB2	26	up	31	up
SORCS1	18	up	7	up
BDNF	18	up	21	up
KCNAB1	16	up	8	up
TMEM178	14	up	10	up
SPP1	12	up	8	up
FGF9	12	up	14	up
HEY1	10	up	6	up
CD1D	9	up	10	up
CDH23	9	up	5	up
CDH2	8	up	14	up
MGC33846	7	up	6	up
ZBTB46	6	up	3	up
LOXL3	6	up	4	up
SLC16A10	5	up	9	up
SYTL4	4	up	3	up
FAIM2	4	up	5	up
RAPGEF1	2	up	4	up
SLC7A2	3	down	3	down
ITPA	2	down	2	down

Table 6. Genes differentially expressed in the cornea and sclera with respect to the TM. 20 genes were upregulated and 2 downregulated in the TM relative to cornea and sclera.

3.3.4 Identification of Trabecular Meshwork 'Specific' Markers

A marker highly expressed in the TM in relation to the anterior segment could not be found among known markers of the TM. Novel markers, thus, have to be identified based on the criteria of (1) differential expression between the TM and TM-MSC and (2) specificity to TM in the anterior segment background. We strived to find them by analyzing the gene sets generated by means of microarray for TM-MSC, TM, corneal and scleral tissues.

Overlap of the three entity lists (TM vs TM-MSC, TM vs cornea and TM vs sclera) was performed to find TM unique genes. Fold change cut-off was adjusted to 10 for the TM vs TM-MSC data set to find strongly deviating genes. Hierarchical clustering showed the tissues

to be cluster together apart from TM-MSC, with the TM closer in similarity to sclera than cornea (Fig. 24A). It confirms the divergence of the differentiated cells in the tissues from the progenitor state of TM-MSC. 13 genes were differentially expressed in the TM tissue compared to TM-MSC, cornea and sclera (Fig. 24B). 12 genes are upregulated and one is downregulated in the TM tissue, compared to the other samples. The details of the genes, fold change and regulation are presented in Table 7.

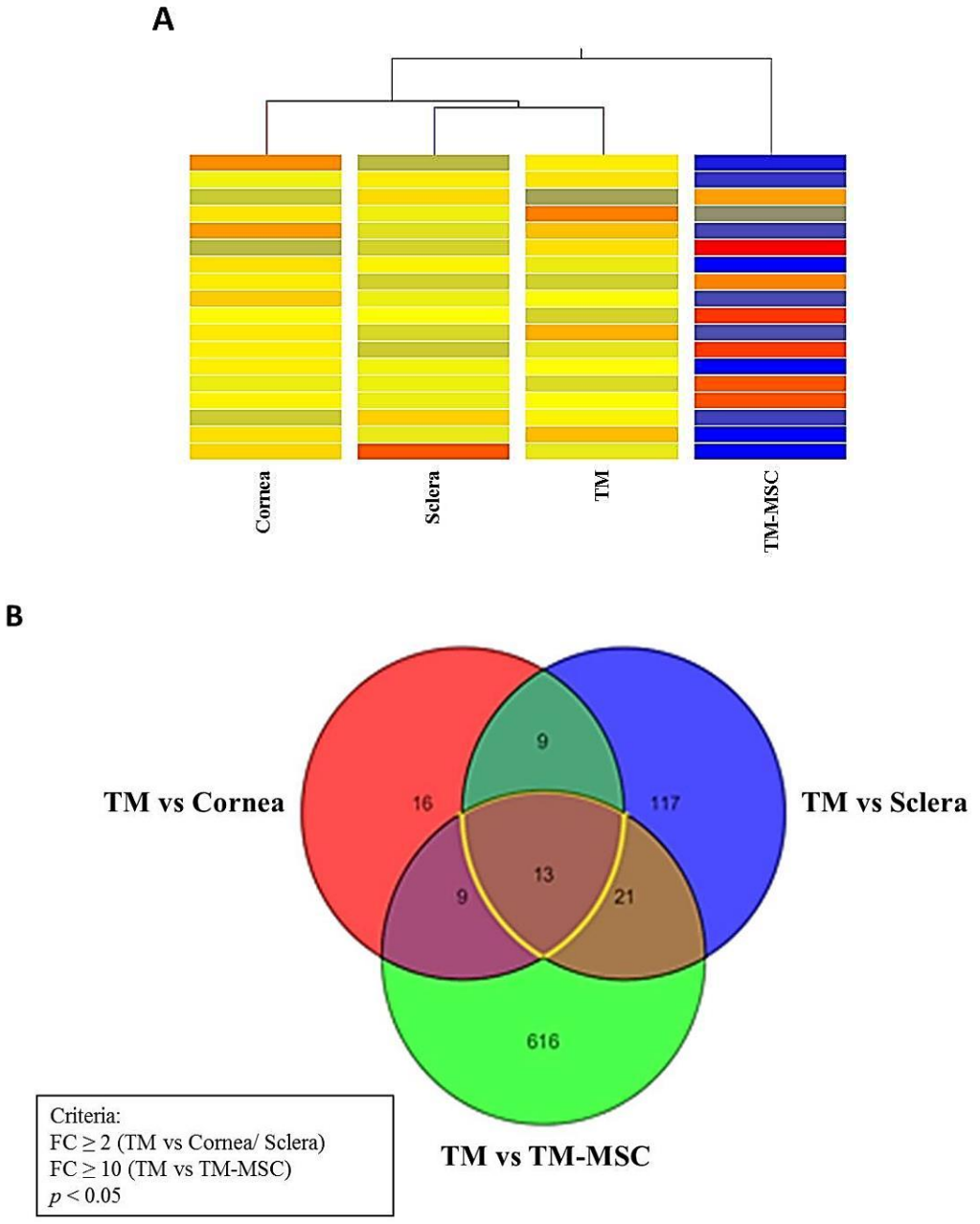

Figure 24. Gene expression profiling of TM-MSC, TM, corneal and scleral tissues. (A) Hierarchical clustering showed the tissues to cluster together, separated from TM-MSC. (B) Venn diagram of merged entity lists found 13 genes differentially expressed in the TM relative to other samples.

	TM-MSC		Cornea		Sclera	
Symbol	Fold Change	Regulation	Fold Change	Regulation	Fold Change	Regulation
CDH23	419.49	up	8.91	up	4.93	up
SLC16A10	87.16	up	4.50	up	9.15	up
SPP1	84.28	up	12.32	up	7.55	up
F5	66.02	up	28.57	up	44.33	up
KCNAB1	54.09	up	15.87	up	8.05	up
MGC33846	41.64	up	6.82	up	5.59	up
FGF9	40.09	up	11.79	up	13.92	up
TMEM178	39.45	up	13.66	up	10.07	up
HEY1	35.81	up	9.72	up	5.52	up
NEB	34.94	up	26.67	up	27.60	up
SORCS1	26.24	up	18.48	up	6.76	up
CD1D	10.14	up	8.94	up	9.52	up
BDNF	12.57	down	18.02	up	21.11	up

Table 7. List of genes differentially expressed in the TM compared to TM-MSC, cornea and sclera. Genes highlighted were shortlisted for further characterization.

Half the genes upregulated in the TM were selected for further analysis based on most divergence in expression from cornea and sclera, and availability of antibodies. Cadherin-related 23 (*CDH23*), secreted phosphoprotein 1 (*SPP1*), coagulation factor 5 (*F5*), potassium voltage-gated channel, shaker-related subfamily, beta member 1 (*KCNAB1*), fibroblast growth factor 9 (*FGF9*), hairy/enhancer-of-split related with YRPW motif 1 (*HEY1*) were chosen as TM differentiation markers (Table 7). Brain-derived neurotropic factor (*BDNF*), downregulated in the TM tissue relative to TM-MSC, was chosen as a TM-MSC marker (i.e. negative differentiation marker). The result was attained from the expression data of three biological replicates and is expected to be tangible. But due to the nature of study, there is a slight chance for false positives. So, verification by other means of expression analysis is necessary to affirm the result.

3.3.5 Verification of Candidate Differentiation Markers

As a standard, genes selected for further study from microarray results are validated by qRT-PCR for their differential expression. So, expression of the shortlisted differentiation markers was analyzed by this technique. The tissues were obtained from three new donors and three other TM-MSC lines were used. Deriving the samples from three new biological replicates increases the reliability of the study by eliminating donor-specific variations.

qRT-PCR result confirmed the downregulation of the differentiation markers in the cornea and sclera compared to TM tissue (Fig. 25A). *F5* was the lowest expressed in the two peripheral tissues at log fold change less than -2. The rest were also greatly downregulated with log fold changes between -2 and -0.5. This ascertains high expression in the TM relative to the cornea and sclera as detected by microarray.

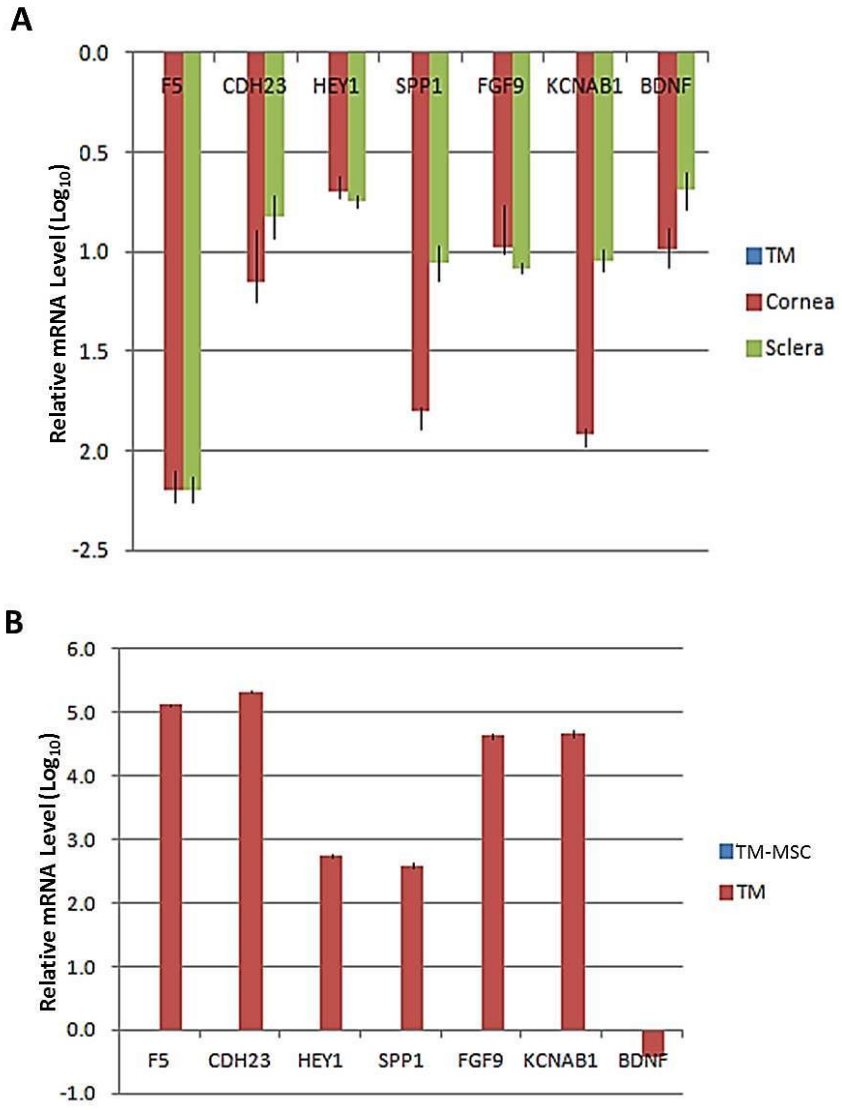

Figure 25. Verification of shortlisted marker gene expression by qRT-PCR. (A) Downregulation of the markers in the cornea and sclera normalized to the TM. (D) The positive markers were all highly expressed in the TM, while BDNF, a negative marker, was low in expression relative to TM-MSC.

Next, in comparison to TM-MSC, the positive differentiation markers were all highly expressed in the TM, while *BDNF* was low in expression (Fig. 25B). The positive markers were more than 2 times higher with *F5* and *CDH23* beyond 5 fold higher in the TM relative

to TM-MSC on log scale. *BDNF* was substantially low at -0.5 fold in the TM on log scale. This confirms their differential expression in the two cell types as identified by microarray. So, according to mRNA expression analysis, the markers: are specific to the TM relative to the cornea and sclera; are differentially expressed robustly between the TM and TM-MSC; thus satisfy both criteria the markers should possess.

Immunofluorescence of corneoscleral tissue cryosections was also performed to ensure the markers are highly expressed in the TM compared to the rest of the anterior segment. Tissue staining using standard protocol proved to be particularly hard as high background and low real signal was observed even with the IgG control. Several fixation techniques were tested before or after sectioning. After much optimization, fresh tissues that were cryosectioned and fixed when necessary was found to yield high signal to noise ratio and was adopted for tissue staining. Minimal dilution of the antibodies for staining was also determined and used for the procedure.

SPP1 and FGF9 were expressed highly in the TM and absent in the surrounding tissues at the dilutions tested (Fig. 26). Other positive markers of TM differentiation, KCNAB1, CDH23, F5 and HEY1 were also highly expressed in the TM, but some signal was detected in the peripheral tissues, particularly in the sclera and in some cases in the Schlemm's canal. BDNF which is upregulated in the TM relative to the cornea and sclera according mRNA level, was also of higher intensity in the TM compared to the surrounding tissues, but not as much as the positive markers. As a TM-MSC marker, BDNF should have been expressed most intensely in the insert portion of the TM, but this was not apparent in this case probably due to the extremely small number of stem cells (~ 1%) in the TM. The immunofluorescence data in general has demonstrated the positive markers to be most highly expressed in the TM tissue in the anterior segment background and implies them as good markers of TM differentiation. It is best to use them collectively to ensure robust differentiation, although a minimal combination of these may work just as fine.

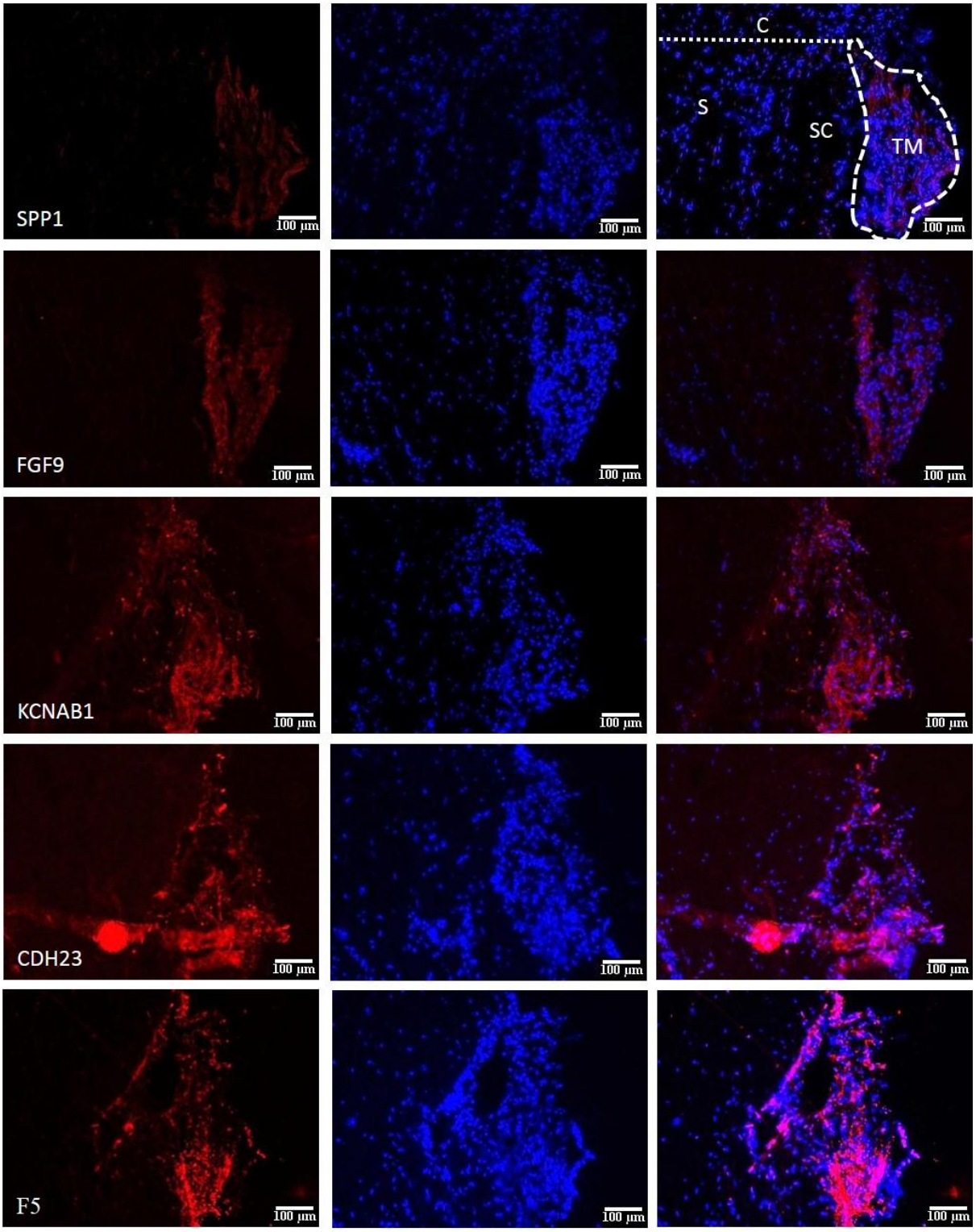

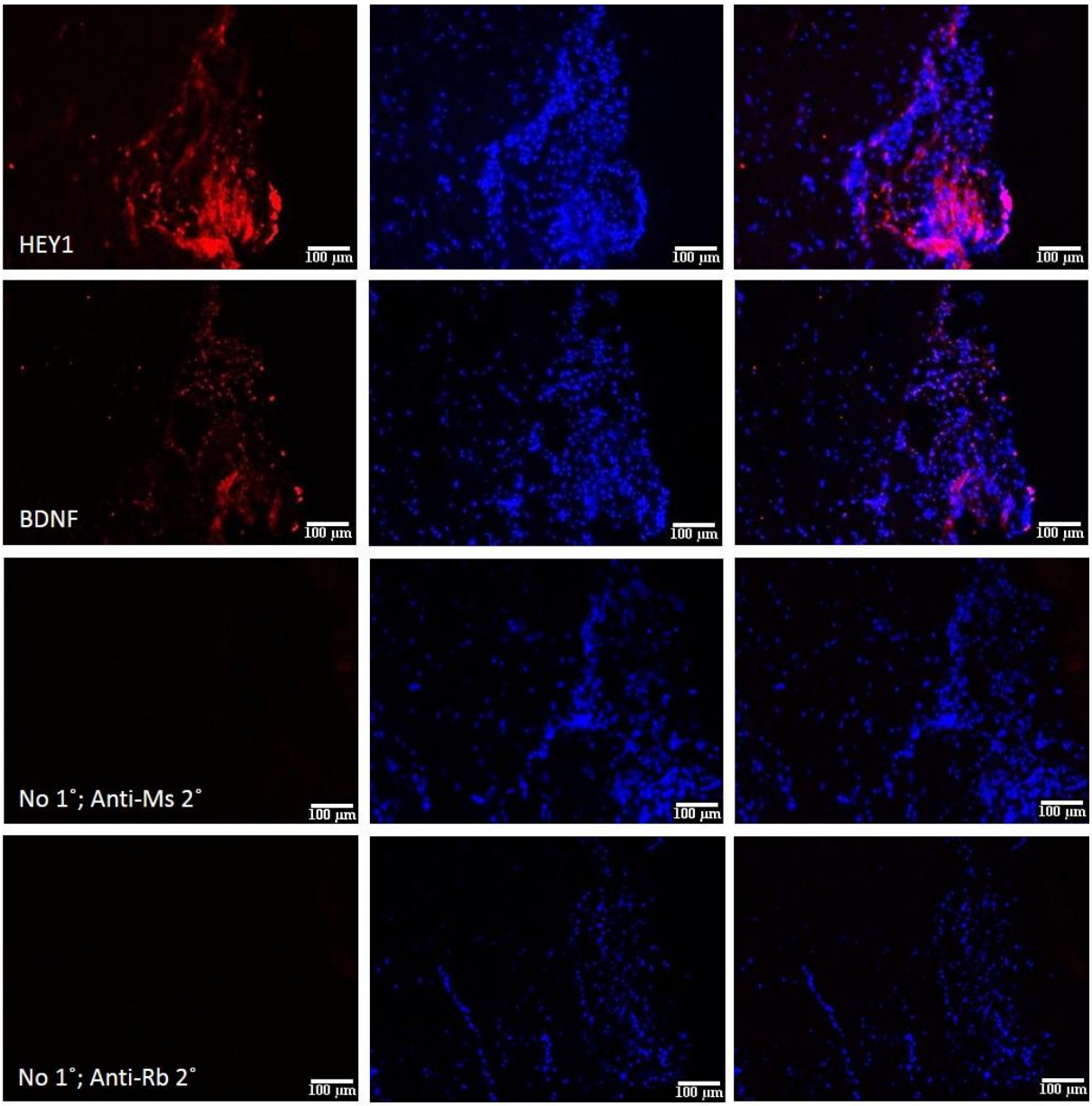

Figure 26. Immunofluorescence of TM differentiation markers on the corneoscleral tissue sections. The positive markers were all highly expressed in the TM compared to the rest of the anterior segment. Components of the anterior segment are annotated as follows: TM, cornea (C), sclera (S) and Schlemm's canal (SC). The negative marker, BDNF, was also slightly more intense in the TM relative to peripheral tissues. Conditions with no primary antibody and incubated with the respective secondary antibody were used as negative controls.

Our study has identified markers of TM differentiation, both positive and negative ones, by gene expression profiling. They have been verified for their differential expression in the TM tissue and TM-MSC, as well as 'specificity' to the TM in the context of the anterior segment of the eye. Upon successful differentiation of TM-MSC into TM lineage, the positive markers (TM markers) are expected to be upregulated, whereas BDNF being a negative marker (TM-MSC marker) ideally should be downregulated. Besides tracing TM differentiation, they can also serve dual function as TM markers to identify cells of TM origin.

3.4 Generation of Mature Trabecular Meshwork Cells

The search for a cell-based therapy for POAG requires a TM differentiation methodology to generate differentiated cells for transplantation purpose. To date, no directed TM differentiation protocol has been established. So, at this juncture, it was necessary to find conditions that could induce TM differentiation of TM-MSC. To this end, small molecules targeting signalling pathways, epigenetic modifiers and coating substrates were tested. Several small molecules, a culture condition and a differentiation medium were identified as inducers of TM differentiation. The newly established TM differentiation markers were used for the differentiation assessment. Upregulation of the positive markers (termed TM markers) and downregulation of the negative marker (termed TM-MSC marker) were considered as an indication of TM induction. Details of the screening, differentiation inducing conditions and verification procedures are presented in this chapter.

3.4.1 Growth Factors Upregulated in the Trabecular Meshwork

Signalling molecules are differentially expressed in differentiated cells and their progenitors, and more often than not, they are able to induce differentiation as shown by many studies. To find signalling molecules upregulated in the mature TM cells, gene ontology by protein class was performed on the TM vs TM-MSC data set using Panther classification system [147]. In the mature cells, 78 signalling molecules were enriched of which 12 were growth factors (Fig. 27).

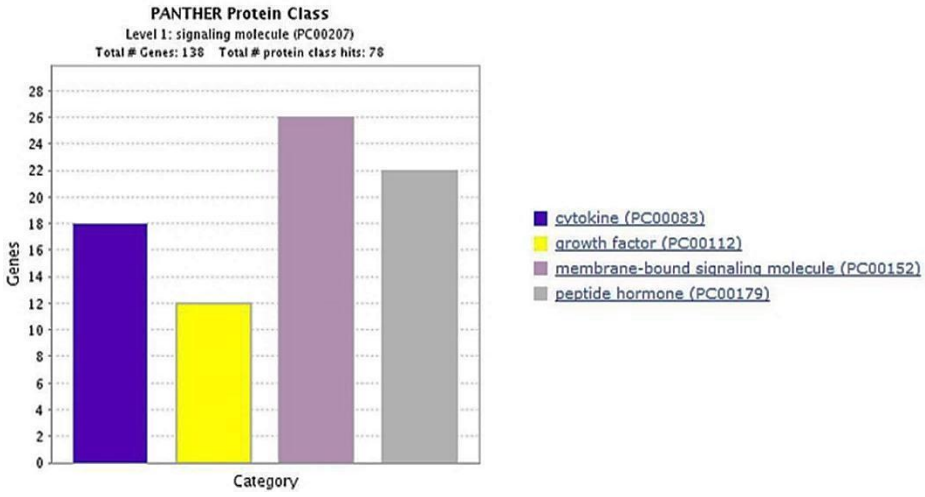

Figure 27. Gene ontology of TM vs TM-MSC expression data set by protein class (signalling molecules).

Growth factors enriched in the TM are betacellulin (*BTC*), bone morphogenetic protein 2 (*BMP2*), fibroblast growth factor 9 (*FGF9*), *FGF13*, *FGF18*, glial cell derived neurotrophic factor (*GDNF*), left-right determination factor 2 (*LEFTY2*), leucine rich repeat neuronal 1 (*LRRN1*), platelet-derived growth factor beta polypeptide (*PDGFB*), *PDGFD*, phosphoinositide-3-kinase interacting protein 1 (*PIK3IP1*) and transforming growth factor beta 3 (*TGFβ3*). *TGFβ, BMP2*, *FGF9* and *PDGFD* had an upregulation of more than 10 folds in the TM and hence were of particular interest. These growth factors may be involved in TM differentiation or at least in the maintenance of the differentiated cells and were selected for further analysis.

3.4.2 Small Molecules Tested for TM Induction Potential

Gene ontology of TM vs TM-MSC data set found 12 growth factors to be highly expressed in the TM in relation to TM-MSC. *TGFβ, BMP2*, *FGF9* and *PDGFD* were the most differentially expressed among them. To study whether these enriched signalling pathways in the differentiated TM cells could induce TM differentiation of TM-MSC, small molecules targeting these pathways were tested. Other pathways known to be involved in the differentiation of various cell types were also included in the study (Table 8A). Where feasible both agonists and antagonists of the pathways were tested at the highest recommended concentration. In some cases only agonist or antagonist was available. In addition, epigenetic modifiers stipulated in several differentiation protocols were studied for their TM induction potential (Table 8B).

Table 8A. List of small molecules targeting signalling pathways.

Pathway	Agonist	Antagonist
BMP	Simvastatin	Dorsomorphin
TGFβ	IDEI IDEII	SB431542
PDGF	Isoproterenol	Lycopene
FGF	BCI	PD173074
EGF	AMG9810	CI-1033
GDNF	XIB4035	
SHH	Purmorphamine	Cyclopamine
Integrin		ROCK Inhibitor
Wnt	GSK3i	XAV939
Adenylate Cyclase	Forskolin	
L-type Ca^{2+} Channel	R(+) Bay K 8644	
Ras		SC1
Ribosomal S6 Kinase		BI-D1870

Table 8B. List of epigenetic modifiers.

Target	Type	Molecule
Glucocorticoid receptor	Agonist	Dexamethasone
RAR-RXR-coactivator complex	Agonist	Retinoic Acid
HDAC	Antagonist	Trichostatin A
DNA Methylase	Antagonist	2-Axacytidine
Histone de-methylase	Antagonist	Tranylcypromine Hydrochloride
Histone Methylase	Antagonist	BIX01294

Table 8. Classification of small molecules tested for TM induction potential. (A) Small molecules targeting signalling pathways upregulated in the TM and other pathways known to be involved in differentiation. (B) Epigenetic modifiers used in the study.

TM-MSC were treated with the small molecules individually to assess whether they are capable of inducing TM differentiation. Cells were harvested at various time points of 3 days, 1 week and 2 weeks from start of treatment and checked for marker expression by qRT-PCR. A positive indication of differentiation would be upregulation of ideally all the TM markers and decline in BDNF expression upon treatment. In some cases, most of the TM markers increased in expression while some remained fairly constant and BDNF was unchanged. So, we revised the criteria of differentiation assessment by marker analysis as (1) significant upregulation of most of the TM markers and (2) decrease/ no change in TM-MSC marker. So, small molecules that met these two standards were adopted as potential TM differentiation inducers and explored further.

3.4.3 Small Molecules that Failed to Promote TM Differentiation

TM differentiation is expected to be accompanied by the upregulation of all or at least most of the TM markers, while BDNF (TM-MSC marker) is downregulated. Most of the small molecules were unsuccessful in modulating the markers in the 'right trend', suggesting they were not inducing TM differentiation. They were agonist and antagonist of BMP, TGFβ, EGF, SHH and Wnt pathways (Fig. 28A); activator of PDGF pathway and inhibitor of FGF and integrin signalling (Fig. 28B). As for epigenetic modifiers, inducers of glucocorticoid receptor and RAR-RXR-coactivator complex, in addition to inhibitors of DNA methylase, histone demethylase and histone methylase, failed to induce TM differentiation (Fig. 28C). Fortunately, some small molecules were identified to modulate the markers in the 'desired trend' which will be elaborated upon later.

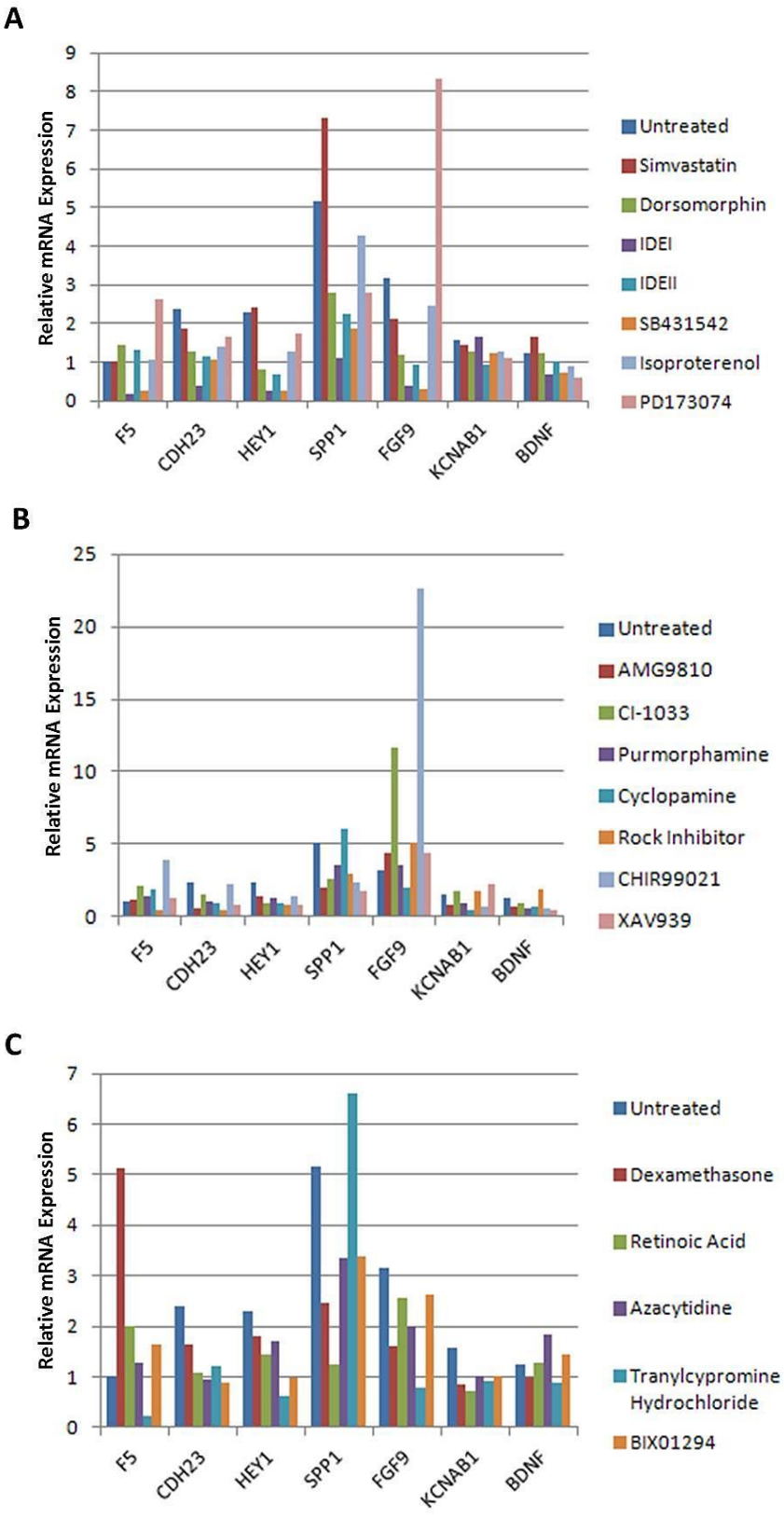

Figure 28. Most small molecules tested failed to induce TM differentiation. (A & B) qRT-PCR result of signalling factors that did not result in the desired regulation of differentiation markers. (B) qRT-PCR analysis of epigenetic modifiers which had the same effect.

3.4.4 Trichostatin A Induces TM Differentiation

One of the small molecules that strongly modulated marker expression was Trichostatin A (TSA), a histone deacetylasae (HDAC) inhibitor. TM-MSC incubated with 10 µM TSA changed morphology within 3 days of treatment after being plated at the same cell density as untreated cells. Under treatment, the compact cell body became enlarged and elongated (Fig. 29A). qRT-PCR analysis at this time point showed the upregulation of all TM markers and downregulation of *BDNF* in the treated cells compared to untreated samples, which was statistically significant ($p < 0.05$) (Fig. 29B). Expression of TM markers increased by 1.5 to 3 folds, while *BDNF* decreased by – 0.5 fold on log scale upon TSA treatment. Thus, it presents the ideal pattern of marker regulation expected of a good TM differentiation factor.

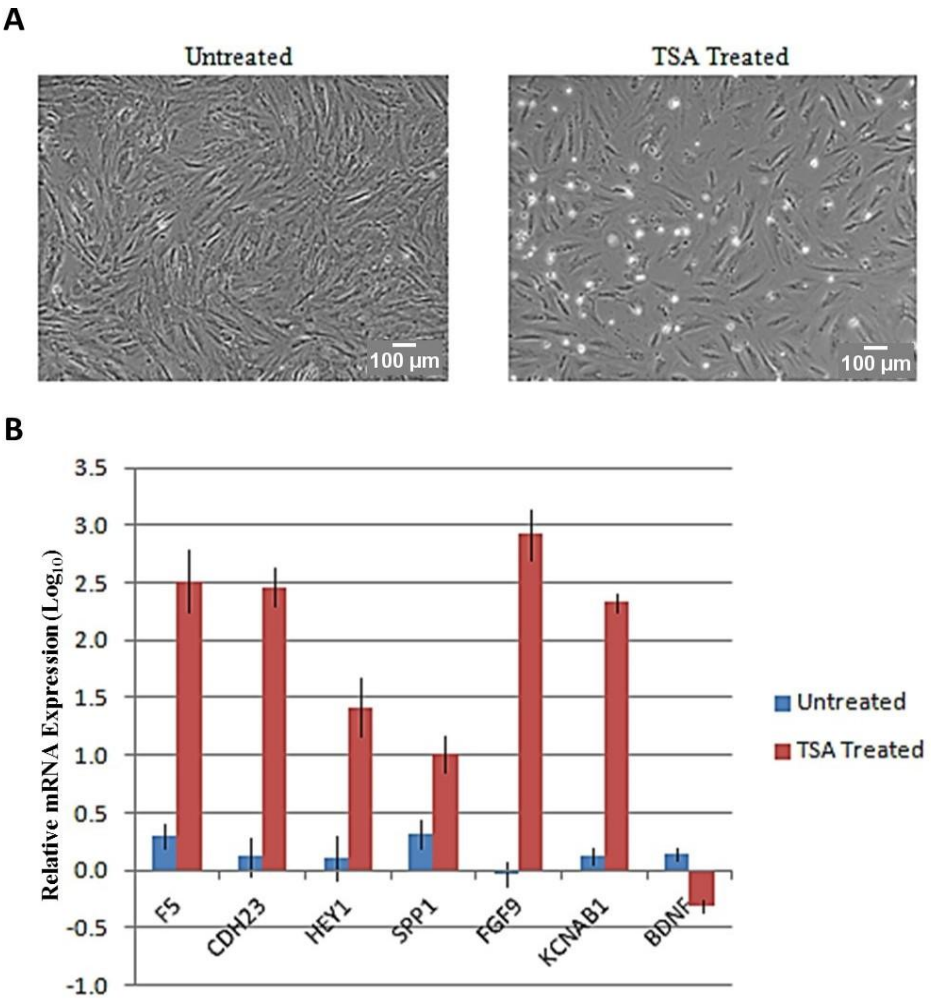

Figure 29. TSA induces TM differentiation. (A) TSA treated TM-MSC are larger and more elongated compared to untreated control. (B) qRT-PCR analysis found the TM markers to be robustly upregulated, whereas BDNF decreased in expression in the treated cells relative to untreated samples.

The marker modulation was also observed at the protein level by immunofluorescence of CDH23 and SPP1, as well as BDNF (Fig. 30). Signal from the two TM markers was more intense in the treated samples than the control. BDNF staining was converse, being stronger in the untreated cells in relation to the treated ones. Although majority of the cells presented increased expression of CDH23/ SPP1 and decreased level of BDNF, there were a considerable number of cells with expression still similar to untreated control. So, the population is heterogeneous, consisting of both differentiated and undifferentiated cells. The expression data provides evidence of TM differentiation in TM-MSC promoted by TSA.

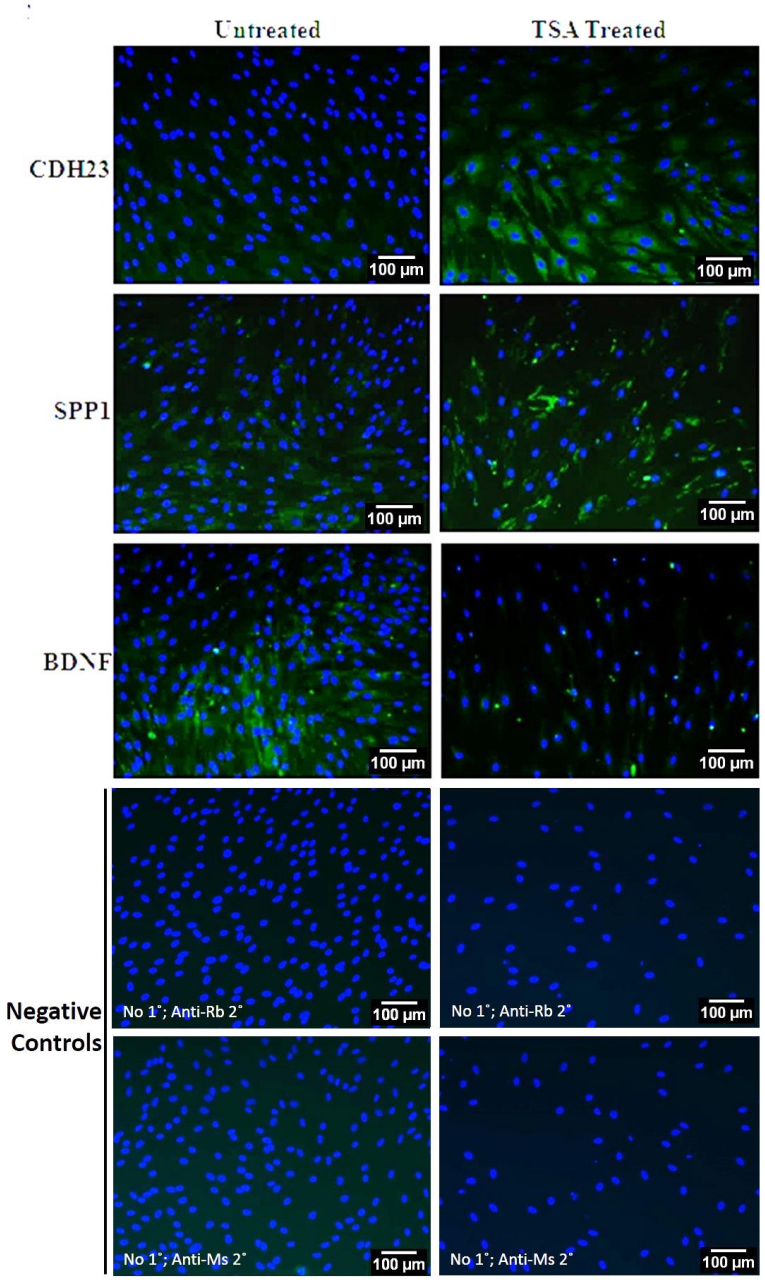

Figure 30. TSA modulates the differentiation markers at the protein level. Immunofluorescence for CDH23 and SPP1 were more intense after treatment. The converse was true for BDNF.

TSA treatment resulted in the detachment of a substantial number of cells (Fig. 29A). Quantification of cell number by xCELLigence system over the course of treatment illustrated a decrease in attached cells with time (Fig. 31A). By day 3, approximately only about 50% of the seeded cells remained bound to the plate which is suggestive of cell toxicity. The detached cells were able to be stained with trypan blue and indicate cell death (data not shown). To assess if the attached cells were viable, qRT-PCR analysis was done for the proliferative marker *PCNA*, anti-apoptotic marker *BCL2*, and apoptotic markers *TP53* and *CASP3* (Fig. 32B). *BCL2* and *CASP3* expression was unchanged, while *TP53* was slightly downregulated although not significantly upon treatment. *PCNA* was upregulated in the treated cells relative to control ($p < 0.05$). So, the adherent cells retain viability and are proliferative, albeit at a slower extent than control cells.

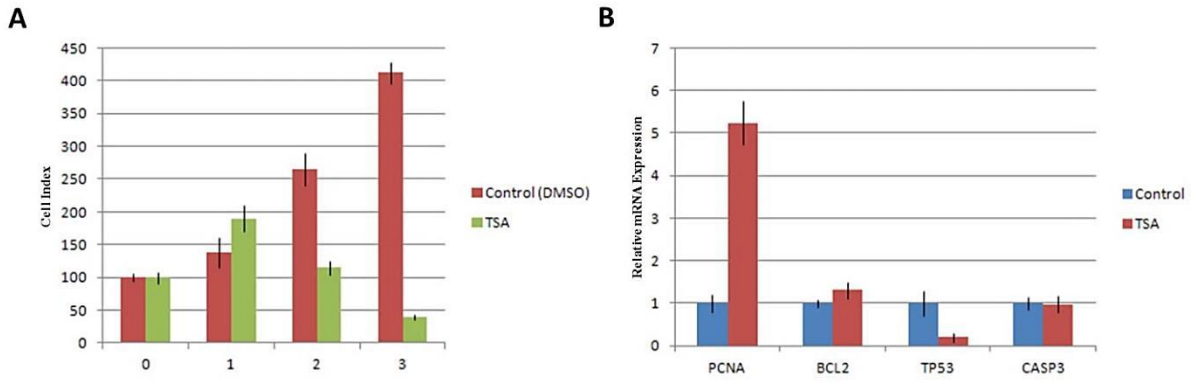

Figure 31. Attached TSA-treated cells are viable and proliferative, although significant detachment was observed. (A) TSA treatment decreased the number of cells attached to the plate over time as measured by real-time quantification of proliferation. (B) No change was seen in the anti-apoptotic marker *BCL2*, apoptotic markers *TP53* and *CASP3* levels after treatment, while *PCNA* was upregulated from qRT-PCR analysis.

If TSA is a true regulator of the differentiation markers, it would do so in a dose-specific manner. To test this theory, a dose response assay was set up with increasing concentrations of TSA for 3 days. qRT-PCR analysis normalized to untreated cells at end point found expression of the TM markers to be correlated to dose, meaning expression was higher with increasing dose (Fig. 32). TM-MSC marker, BDNF was inversely correlated to dose. With increasing concentration of TSA, the proportion of cells that acquired TM cell-like morphology grew, but was also accompanied by more cell death. The minimum dose which considerably regulated the markers was 10 µM. The data confirms the dose-specific effect

TSA has on the differentiation markers, indicating it as a modulator of the markers and possibly TM differentiation. The assay also deduced the optimal dosage for treatment.

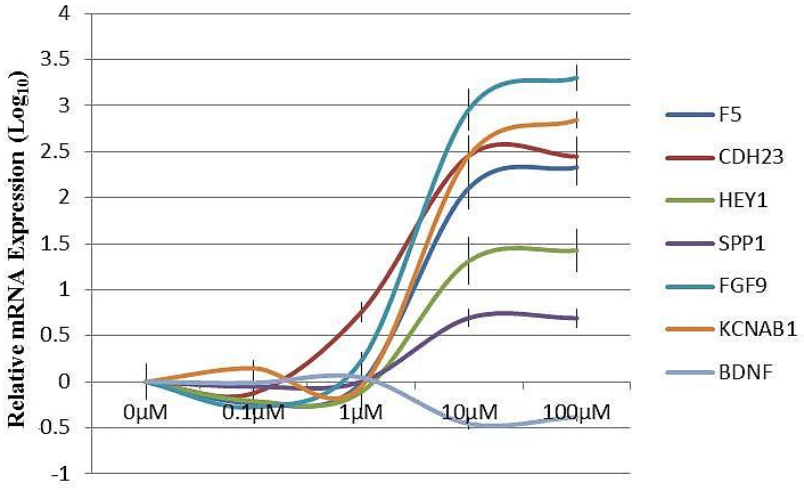

Figure 32. Dose response effect of TSA on TM differentiation markers. The regulation of differentiation markers was correlated to TSA dose as quantified by qRT-PCR after 3 day treatment. 10 μM was determined as the optimal dosage.

TSA treatment led to morphological and marker expression changes which postulate the treated cells to be in a differentiated state. However, investigation for the incorporation of acetylated-LDL, a characteristic of functional TM cells, found the treated cells to be unable to uptake the compound (data not shown). So, it is likely that TSA treatment has induced the cells to differentiate, but only to an intermediate phase, not yet to a fully functional phenotype. Nevertheless, the result is encouraging as the treatment holds promise. It needs to be developed further with other added factors to enhance the differentiation by inducing the transitional differentiated cells farther into mature, functional TM cells.

3.4.5 SC1, BCI, Forskolin and BI-D1870 are Potential TM Differentiation Inducers

Regulation of most differentiation markers in the 'correct' direction is taken to be an implication of differentiation. From the list of small molecules tested, four more factors had the desired effect on the differentiation markers. They are SC1 and BCI which activate Ras signalling and FGF pathway respectively; forskolin, an agonist of adenylate cyclase; and BI-D1870, a ribosomal S6 kinase (RSK) inhibitor.

Treatment of TM-MSC with 1 µM SC1 upregulated all the TM markers within 3 days, while BDNF showed mild increase (Fig. 33A). BCI, forskolin and BI-D1870 modulated the markers at a concentration of 10 µM after 2 weeks of treatment. Both BCI and BI-D1870 upregulated the TM markers and downregulated BDNF. Forskolin increased the expression level of TM markers while BDNF was slightly upregulated. These four small molecules befit the criteria for a TM differentiation factor.

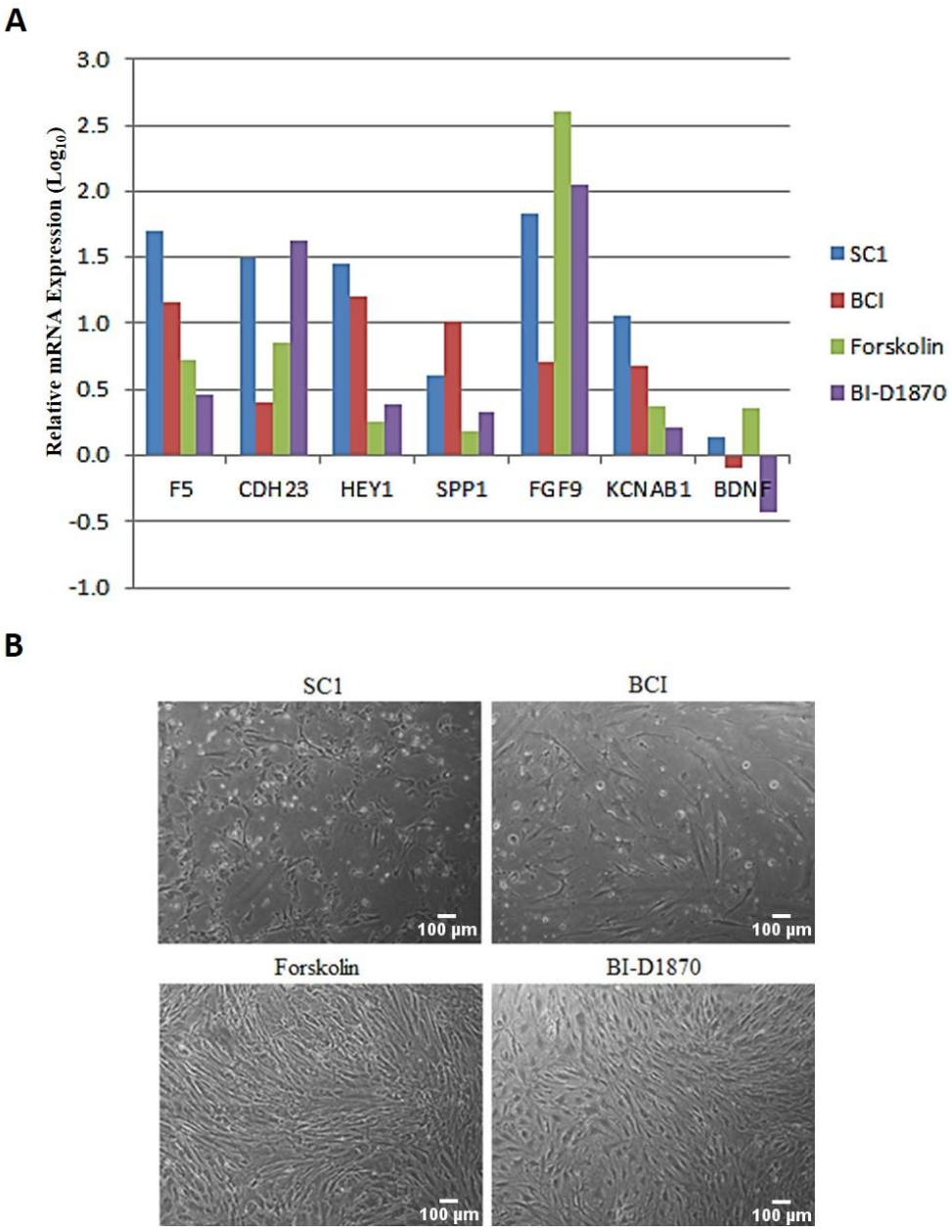

Figure 33. Other small molecules that upregulated the TM differentiation markers. (A) qRT-PCR assessment found SC1, BCI, forskolin and B1-D1870 to upregulate the TM markers. BDNF was downregulated by BCI and BI-D1870, but not with SC1 and forskolin. (B) Change in morphology was evident after SC1, BCI and BI-D1870 treatment.

SC1 and BCI treatment detached a large number of cells (Fig. 33B). Morphologically, TM-MSC incubated with SC1 were still compact as either polygonal or elongated cells. This was also observed with BCI treatment, together with some elongated and larger cells. Forskolin and BI-D1870 applications did not affect cell density, and led to a heterogeneous population in terms of cell size.

These small molecules were tested as a cocktail and in various combinations together with TSA to assess whether they could improve differentiation. qRT-PCR showed increase in expression of the TM markers and decline in BDNF in all conditions that contained TSA (Fig. 34). The combination without TSA only had modest effect. Removal of other small molecules from the cocktail overall did not affect most of the marker expression relative to cocktail. Hence, the result suggests that the other small molecules were unsuccessful in augmenting the effect of TSA. So, BCI, forskolin, BI-D1890 and SC1 were not studied further.

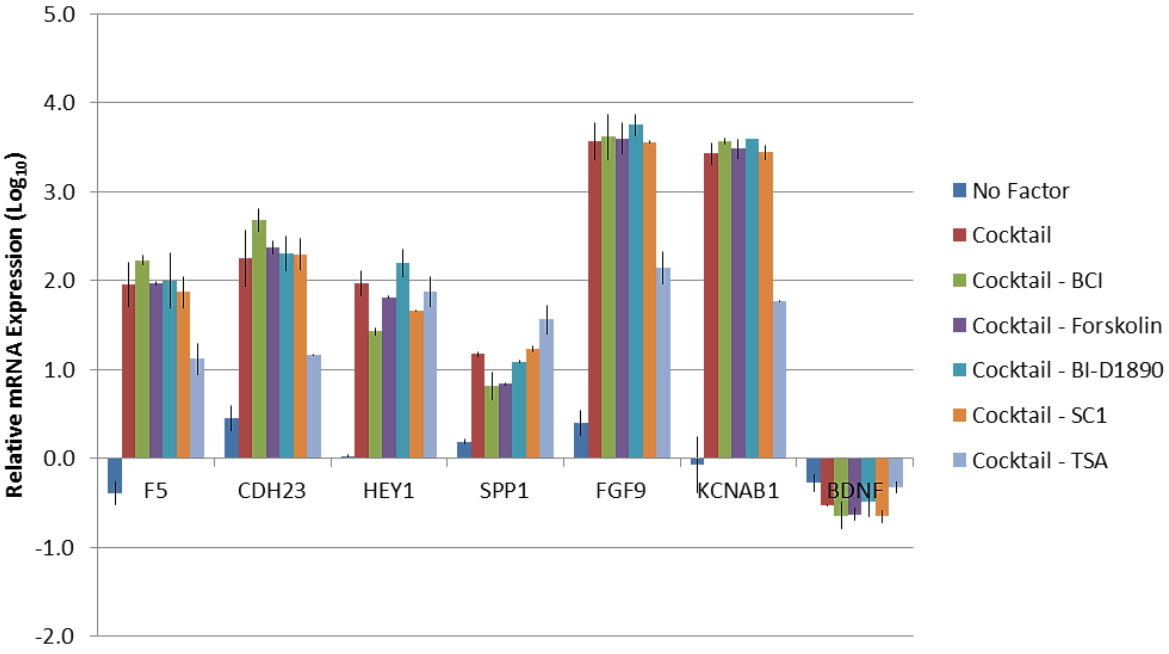

Figure 34. BCI, forskolin, BI-D1890 and SC1 failed to augment the effect of TSA. qRT-PCR analysis of cells treated with the cocktail of factors and various combinations, showed conditions with TSA generally performed better. Removal of other factors did not affect the expression much, unlike TSA withdrawal, relative to cocktail.

3.4.6 Aggregation of TM-MSC Promotes TM Differentiation

Different matrices such as hydrogel and vitronectin were tried to investigate whether they could induce TM differentiation. These coating substrates are used to support the differentiation of certain cell types. However, they failed to induce differentiation of TM-MSC into TM lineage as determined from qRT-PCR for the differentiation markers (data not shown).

Aggregation is another technique employed to differentiate cells and was studied for TM differentiation potential. 2 x 10^5 TM-MSC were force aggregated by centrifugation and the pellet was maintained in growth medium for 3 days (Fig. 35A). qRT-PCR result showed expression of BDNF was unaffected in the pellets, but significantly higher expression was seen for the TM markers, in contrast to cells cultured as a monolayer for the same duration (Fig. 35B). This indicates pellet assay as a suitable matrix for TM differentiation induction.

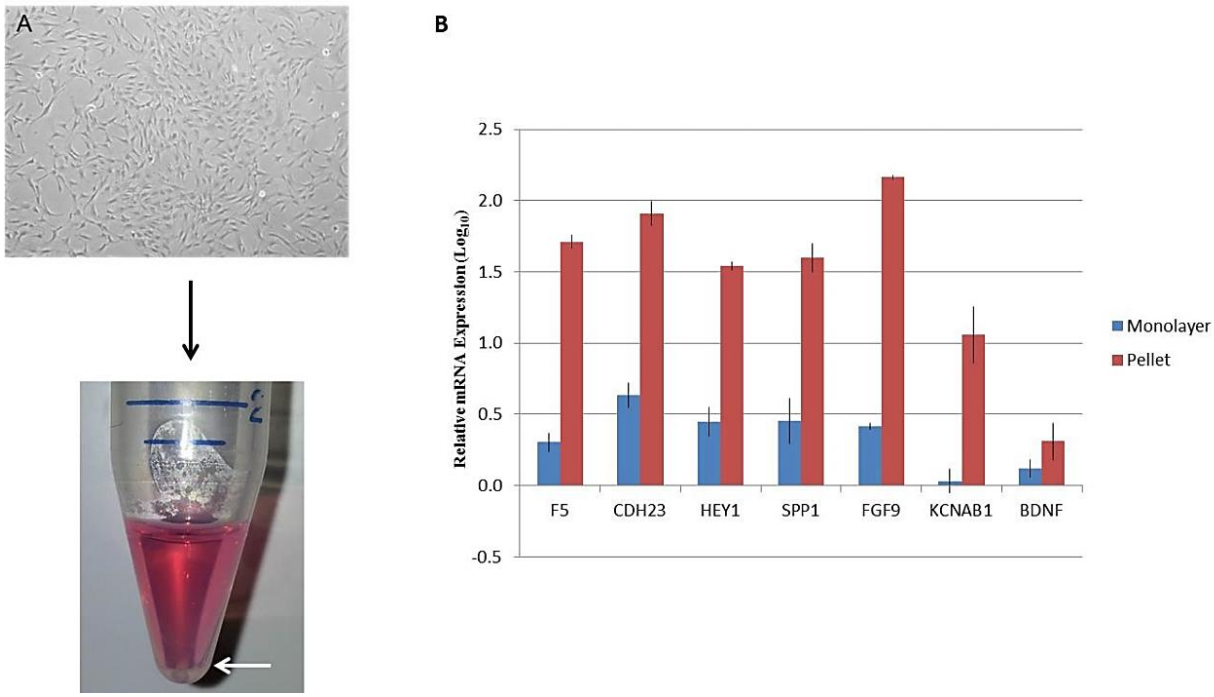

Figure 35. Pellet culture is a suitable condition for TM differentiation. (A) TM-MSC were force aggregated into a pellet and maintained in culture for 3 days. (B) This method significantly increased the TM markers' expression while BDNF was unchanged relative to monolayer control.

3.4.7 Medium TADLIS Induces TM Differentiation

Several chondrocytic markers (*CRTAC1*, *FOXC1*, *CLEC2d*, *SOX9* and collagen X) and numerous growth factors (*BMP1*, *BMP2*, *FGF9*, *FGF13*, *FGF18*, *TGFβ3*, *PDGFD* and *PDGFB*) known to induce chondrogenesis were upregulated in the TM vs TM-MSC entity list. In fact, these growth factors make up two-third of the growth factors that are enriched in the TM. None of the other mesenchymal lineages examined shared this similarity with the TM. It may be possible that TM cells and chondrocytes being derived from the mesenchyme may have a common intermediate phase during their differentiation before they diverge into distinct cell types. If this is the case, chondrogenic medium may have the potential to induce TM differentiation. This hypothesis was explored by treating the TM-MSC with the chondrogenic medium we had previously utilized to evaluate the differentiation potential of the cells (section 3.2.4). The medium consists of **T**GFβ3, **a**scorbic acid, **d**examethasone, **l**inoleic acid, **I**TS and **s**odium pyruvate in low-glucose DMEM. The medium was termed TADLIS, using the first letter of the constituents.

Culturing TM-MSC in the TADLIS medium noticeably changed the morphology of the cells (Fig. 36A). The cells became enlarged, elongated and slightly irregular-shaped, similar in morphology to primary TM cells. qRT-PCR analysis at 1 week and 2 weeks after treatment initiation demonstrated the TM markers to be consistently upregulated with time (Fig. 36B). At the end point, most markers were more than 5 times higher than pre-treated cells on log scale. Moreover, the TM-MSC marker, *BDNF* declined in expression by 1 week and was maintained at this downregulated level at 2 weeks of treatment. This ideal pattern of marker expression is expected of an optimal differentiation condition, and thus suggests the condition to be suitable as a TM differentiation method.

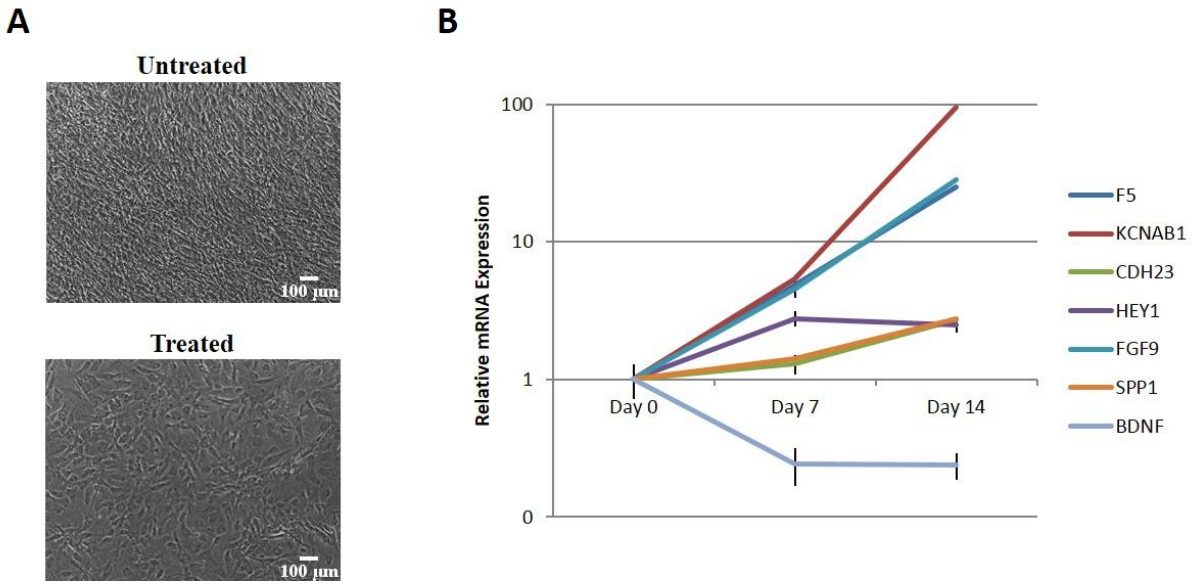

Figure 36. TADLIS medium promotes TM morphology and marker expression. (A) Treatment resulted in larger and irregular-shaped cells, typical of primary TM cells. (B) Expression of all TM markers increased with time, while BDNF declined as quantified by qRT-PCR.

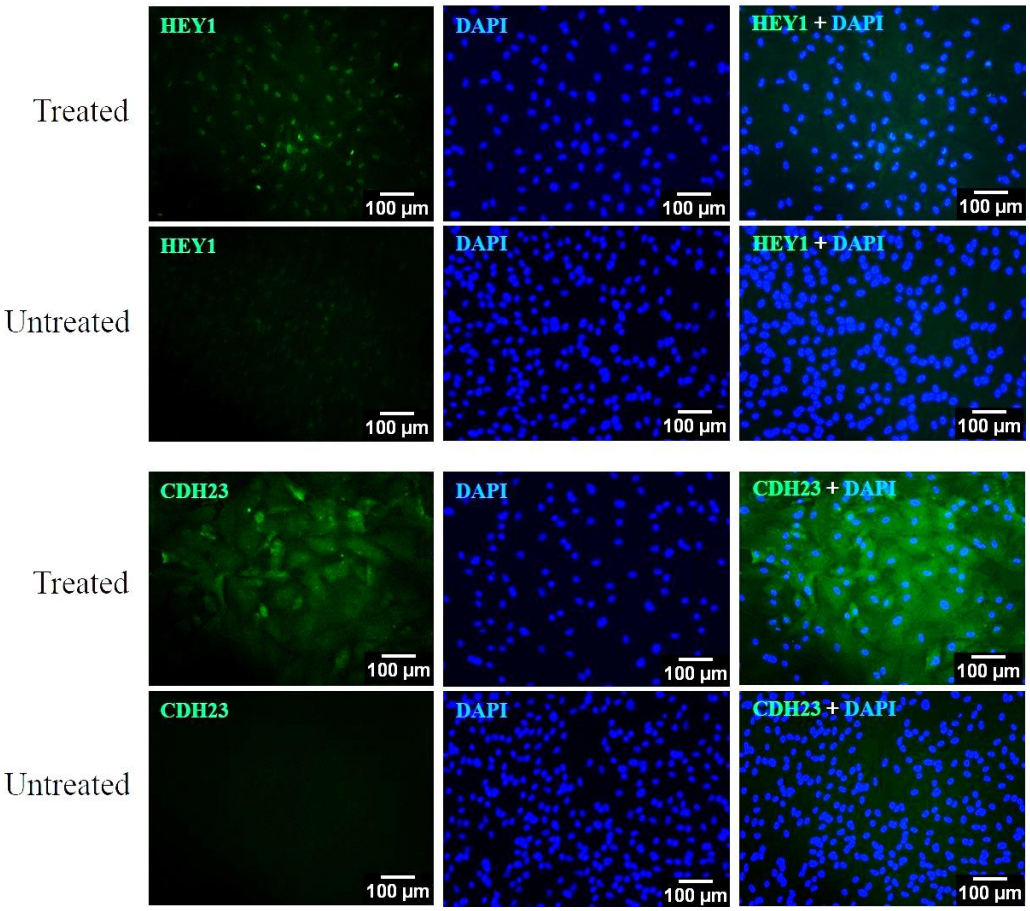

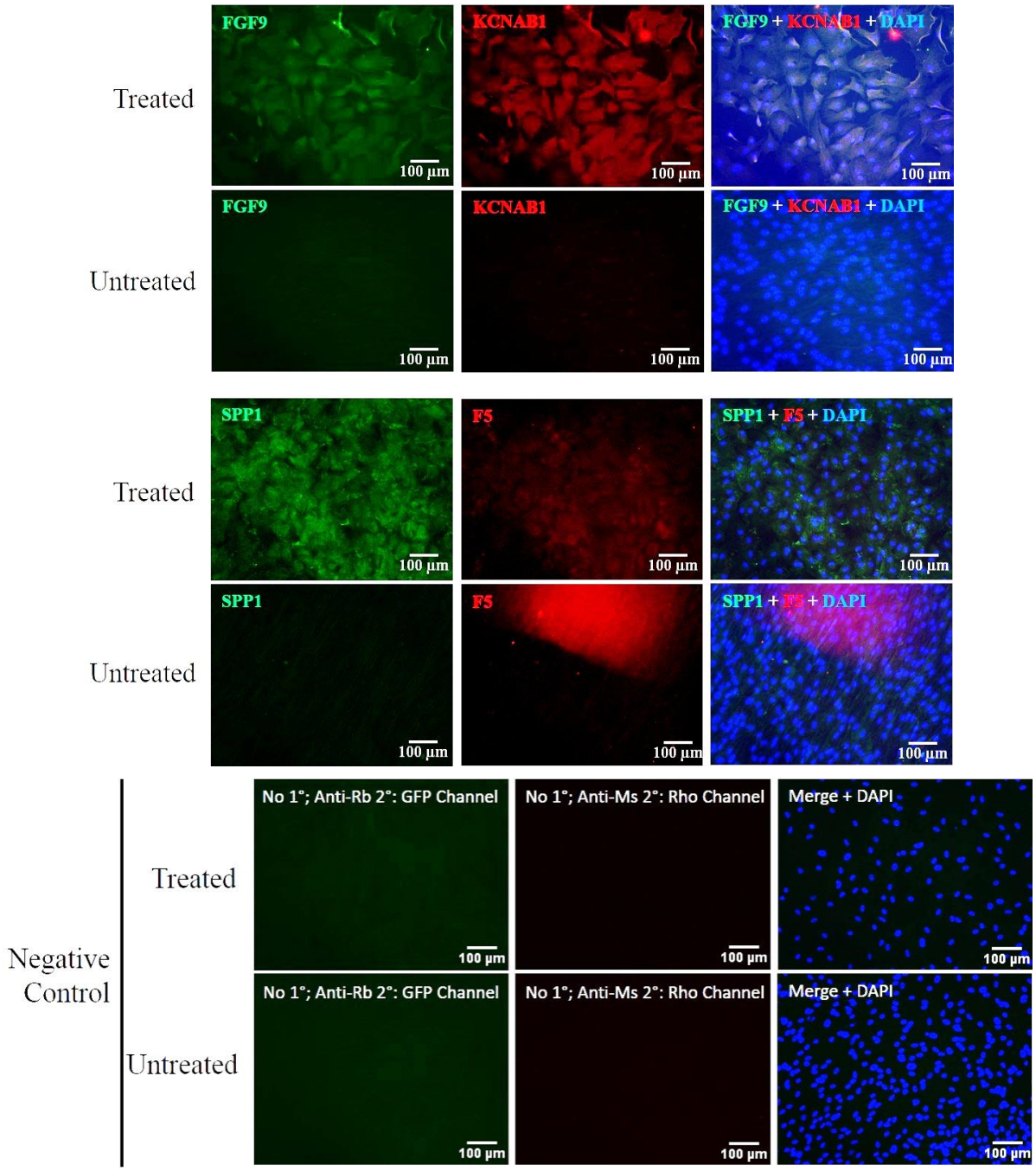

Figure 37. TADLIS medium induced upregulation of the TM markers at the protein level. Double immunofluorescence for some of the antigens showed the treated cells to co-express them.

Immunofluorescence for the TM markers confirmed their increase in expression at the protein level after treatment with the TADLIS medium (Fig. 37). Almost 100% of the treated cells had a much higher signal intensity compared to the control cells. Untreated cells had negligible expression of most markers as is expected, but very low expression of HEY1 and SPP1 was detected in them. The untreated cells have been maintained in culture for the same duration as treated cells and spontaneous differentiation may have occurred that could have

contributed to the expression of these markers in the control. Double staining (FGF9/ KCNAB1 and SPP1/ F5) found the treated cells to co-express the antigens, thus confirming a relatively homogeneous population of differentiation cells upon induction.

TADLIS medium induced TM morphology and marker expression profile in TM-MSC as verified by RNA and protein expression studies. The next task was to determine if the differentiated cells were functionally mature. Uptake of modified LDL is a property mature TM cells can perform, but not evident in TM stem cells. This assay was employed to assess the functionality of the differentiated cells. Treated cells incubated in medium containing labelled acetylated-LDL (Ac-LDL) incorporated the compound into their cytoplasm but control cells were not able to (Fig. 38A). Much of the treated cells were labelled and flow cytometric analysis quantified approximately 86% of the treated cells had incorporated the compound, signifying their functionality (Fig. 38B). Untreated cells at day 14 and day 0 remained unlabelled. Thus, factors in the TADLIS medium have induced TM-MSC to differentiate into mature, functional cells at a high efficiency. It is necessary to elucidate the minimal factors in this medium essential for differentiation in order to optimize differentiation, but at this stage it remains known.

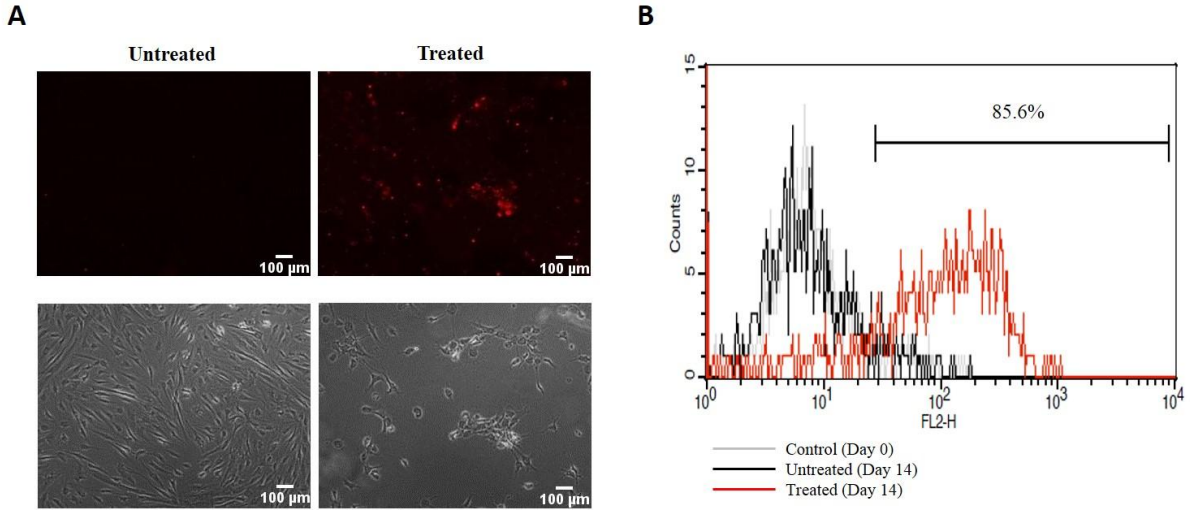

Figure 38. TADLIS medium induced TM-MSC to differentiate into functional TM cells at a high efficiency. (A) Treated cells incorporated labelled Ac-LDL unlike untreated cells. (B) Flow cytometry showed about 86% of the treated cells were labelled.

In summary, from the numerous small molecules and coating substrates tested, several conditions were identified to promote TM differentiation of TM-MSC. TSA, an epigenetic modifier, was the most promising candidate among the small molecules as observed by its induction of TM morphology and TM marker expression profile, although it could not fully differentiate the cells into functional cells. Aggregation was also found to be a suitable culture condition since it increased TM marker expression, denoting differentiation. Treatment of TM-MSC with the TADLIS medium was the most optimal of all these conditions, as it not only induced TM phenotype, but also rendered the cells functional with high differentiation efficiency. So, several appropriate means of TM differentiation have been presented. In addition, the ability of TM-MSC to differentiate into mature TM cells has been demonstrated, reinforcing them as progenitors of the TM. This capacity of stem cells to generate cells of the tissue they were derived from is essential to assert their source. Importantly, this study has identified means of producing an expandable source of mature TM cells for regenerative medicine to treat POAG. Efforts to optimize the differentiation procedure by identifying essential components of the TADLIS medium and combination with TSA are underway.

3.5 Age-Correlated Gene Expression Study of the Trabecular Meshwork

Structural changes in the TM with age have been well documented including significant decline in cell number and trabecular thickening. This coincides with rising IOP noticed with aging. In addition, POAG is detected only beyond the 50s and indicates increased susceptibility in the older population to the disease. Age-related modifications in the TM could be contributing to IOP increase and vulnerability to POAG in the older segment of the population. Gene expression variation between the young and aging TM could reveal the intrinsic differences between them at a cellular level which may explain the structural differences and increased vulnerability. It will also advance understanding of aging in general in the TM. To this end, gene expression profiling was done on the two sample age groups which identified biological processes differentially regulated between them. This chapter discusses the genetic study and how these processes were deciphered. To our knowledge, this is the first report of age-correlated expression study on the TM.

3.5.1 Age Groups Selected and Donor Information

POAG is an aging disease, manifesting in the population commonly beyond 50s. Some groups claim it can be detected as early as 40 years of age. But often the diagnosis is made when the affected individual becomes aware of it in its advance stage, which usually occurs in the 50s and beyond. So, clearly some abnormality in the TM is rendering it susceptible in the later part of a person's lifetime. To understand the genetic level differences that could contribute to the increased susceptibility with age, it is critical to designate the proper age groups for this study in order to derive meaningful data. The age groups were restricted as < 30 years for young and ≥ 50 years for the old samples, leaving a gap of two decades between them. The selected sample age groups are relevant to study the age-related modification in TM and aging in general. Omission of the middle age group is necessary to avoid overlapping of data sets as individuals are known to age at varying rates. Details of the donors are presented in Table 9, including age, ethnicity and cause of death.

Table 9. Donor information.

Tissue ID	Age (Yrs)	Gender	Ethnicity	Cause of Death
#2701/2702	9	F	Black	Acute cardiac crisis; Cerebral palsy
#2377/2378	22	F	Black	Sepsis; Pneumonia
#2653/2654	25	M	Caucasian	Accident
#0733/0734	50	F	Caucasian	Found down
#0771/0772	52	F	Caucasian	Acute cardiac arrest
#0815/0816	60	M	Asian	Acute cardiac arrest; Coronary artery disease

Table 9. Information of donors from whom TM tissue samples were extracted for the age-correlated expression study.

TM samples were derived from both male and female donors who were of diverse ethnicity. So, genetic differences associated with gender and ethnicity should have been avoided. None of the donors had any known eye-related disorders, and TM samples harvested from them were considered as normal. The samples were extracted within the maximum time period of 14 days from death, during which the TM cells are known to be still viable.

3.5.2 Genes Expression Profiling of Young and Old Trabecular Meshwork

Genome-wide expression analysis can disclose differences at the genetic level and has been employed by some groups to study the glaucomatous TM in comparison to healthy TM. But to our knowledge, gene expression profiling of TM tissue with age has not been explored. To understand the genetic differences between the young and old TM, specimens harvested from young and old donors were studied by microarray analysis. RNA harvested from the tissue was amplified into labelled cRNA and two technical replicates for each were hybridized onto microarray beadchips. The raw data generated from beadchip readings were background subtracted and normalized by the method of centralization.

Hierarchical clustering found the biological replicates from each group to cluster together, separated from the other group (Fig. 39A). The closeness of the samples within the same group imply similarity in gene expression among them, while segregation of the two groups suggests some divergence in expression and confirms genetic differences do exist between the young and old TM tissues. The clustering also indicated the predominant differences in expression were due to age of the donors and not sex or ethnicity.

Pearson correlation analysis to measure similarity between any two ages showed that the young and old populations were divergent in gene expression patterns as indicated by relatively lower correlation coefficients (indicated in black) (Fig. 39B). The closeness of the samples within the same group implies similarity in gene expression among them (red colour indicates high correlation), while segregation of the two groups indicates divergence and confirms molecular differences exist between young and old TM tissues and they are likely to be age-regulated.

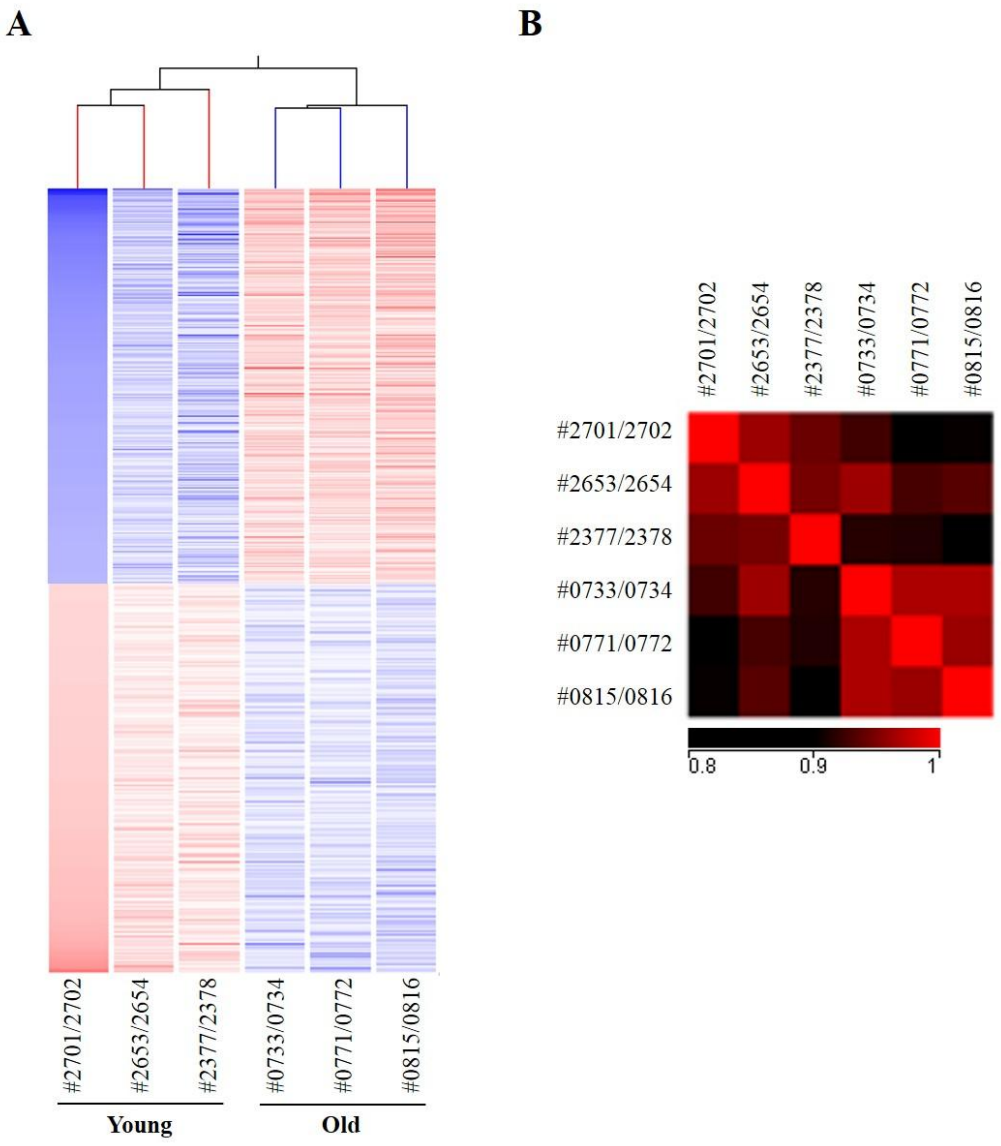

Figure 39. TM specimens of the young and old groups were dissimilar in gene expression. (A) Hierarchical clustering of the global transcriptome profile with age illustrated segregation of the two groups with biological replicates clustering together. A modest set of genes were differentially expressed between them (blue: downregulation; red: upregulation). (B) Pearson's correlation coefficient compared the degree of similarity between the sample groups. The analysis showed the homogeneity in expression profile within the age groups (red indicates high correlation) and generally reduced similarity between the groups (black indicates reduced correlation).

3.5.3 Genes Differentially Expressed between Young and Old Trabecular Meshwork

Additional processing of the young and old gene sets to find gene expression variation generated a young vs old entity list that passed the one-way ANOVA *p*-value ≤ 0.05 (student's t-test unpaired) and fold change ≥ 2. False positives were omitted with benjamini-hochberg multiple testing correction. About 4.5% of the probes detected differential expression between the young and old specimens with statistical significance. 1737 of the probes corresponded to protein-coding genes and the remaining 404 probes detected hypothetical proteins, pseudogenes and non-coding RNA genes. Most expression differences were between 2 – 5 fold (82%), while 3.6% genes changed more than 10-fold (Fig. 40A). Overall, 699 genes were upregulated and 1442 were downregulated with age (Fig. 40B).

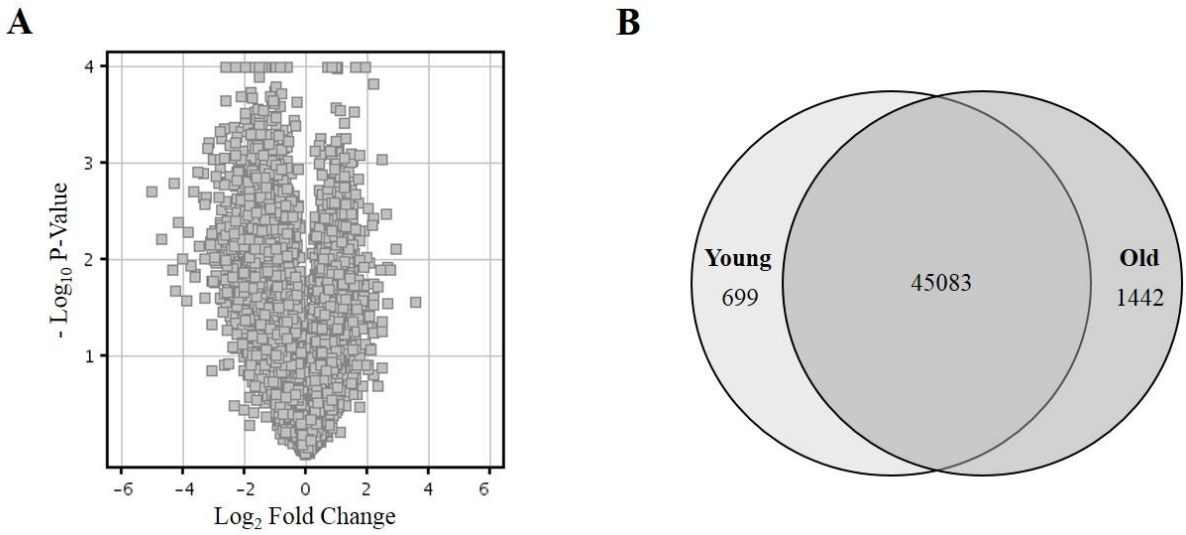

Figure 40. Relative distribution of genes differentially expressed between the young and old TM samples. (A) Volcano plot of genes across the various fold differences and significance. Most genes were within 2 – 5 fold difference (82%) while a limited number had more than 10-fold variation (4%) at p ≤ 0.05. (A) Venn diagram of genes differentially expressed between young and old TM samples. The list includes protein-coding genes for well-characterized proteins and predicted proteins, as well as pseudogenes and RNA genes.

LOC441310, encoding a predicted protein similar to FLJ00290 was the mostly highly expressed in the old TM samples relative to young ones. Members of the CXC chemokine family, *IL8*, *CXCL1*, *CXCL2*, involved in inflammation were also among the top few genes enriched in the old samples. Other high ranking genes encode proteins expressed under cellular stress, specifically transcriptional repressor *MAFF*, growth/ apoptosis regulators

GADD45G and *SLC25A24*. *CYP4B1* and *DHGH*, associated with metabolism of xenobiotics, were among the top 25 genes upregulated in the aged TM too. The enrichment of considerable number of proteins related to inflammation, cellular stress and metabolism of xenobiotics among the highly upregulated genes in the older TM are suggestive of their cells experiencing some form of stress. It could culminate in the loss of cells as has been observed *in vivo*. Another gene of interest part of the highly enriched genes was *TFP12*, a serine protease inhibitor, which suggests that matrix remodelling could be compromised in the aging TM. Details of the 25 genes highly expressed in the old samples relative to young ones are presented in Table 10A.

Table 10A. List of top 25 genes highly expressed in the aged TM relative to young ones.

Symbol	Definition	Fold Change (Old/ Young)
LOC441310	PREDICTED: similar to FLJ00290 protein (LOC441310), mRNA	79
MIR302C	microRNA 302c	36
ARC	Activity-regulated cytoskeleton-associated protein	32
MAFF	V-maf musculoaponeurotic fibrosarcoma oncogene homolog F (avian)	29
HOMER1	Homer homolog 1 (Drosophila)	27
HBEGF	Heparin-binding EGF-like growth factor	26
CCRN4L	CCR4 carbon catabolite repression 4-like (S. cerevisiae)	23
RRAD	Ras-related associated with diabetes	22
MIR155HG	MIR155 host gene (non-protein coding)	21
CXCL2	Chemokine (C-X-C motif) ligand 2	20
NPC1L1	NPC1 (Niemann-Pick disease, type C1, gene)-like 1	20
CYP4B1	Cytochrome P450, family 4, subfamily B, polypeptide 1	20
IL8	Interleukin 8	19
PRG2	Proteoglycan 2, bone marrow (natural killer cell activator, eosinophil granule major basic protein)	19
CXCL1	Chemokine (C-X-C motif) ligand 1 (melanoma growth stimulating activity, alpha)	19
FAM171B	Family with sequence similarity 171, member B	19
CA2	Carbonic anhydrase II	18
SLC25A24	Solute carrier family 25 (mitochondrial carrier; phosphate carrier), member 24 (SLC25A24), nuclear gene encoding mitochondrial protein	18
TFPI2	Tissue factor pathway inhibitor 2	18
MSC	Musculin (activated B-cell factor-1)	18
HAUS8	HAUS augmin-like complex, subunit 8	17
GADD45G	Growth arrest and DNA-damage-inducible, gamma	17
DHDH	Dihydrodiol dehydrogenase (dimeric)	16
THOC6	THO complex 6 homolog (Drosophila)	16
LOC100190939	Hypothetical LOC100190939 (LOC100190939), non-coding RNA	15

Table 10B. Top 25 genes enriched in the young TM compared to old ones.

Symbol	Definition	Fold Change (Young/ Old)
LYVE1	Lymphatic vessel endothelial hyaluronan receptor 1	27
MS4A4A	Membrane-spanning 4-domains, subfamily A, member 4	18
CD163	CD163 molecule	14
C1QB	Complement component 1, q subcomponent, B chain	13
XLKD1	Extracellular link domain containing 1	12
CSF1R	Colony stimulating factor 1 receptor, formerly McDonough feline sarcoma viral (v-fms) oncogene homolog	11
SCARNA2	Small Cajal body-specific RNA 2 (SCARNA2), guide RNA.	11
F13A1	Coagulation factor XIII, A1 polypeptide	10
DLK1	Delta-like 1 homolog (Drosophila)	10
RNASE6	Ribonuclease, RNase A family, k6	9
	BX393727 Homo sapiens NEUROBLASTOMA COT 25-NORMALIZED Homo sapiens cDNA clone CS0DC001YP02 5-PRIME, mRNA sequence	9
ABCA6	ATP-binding cassette, sub-family A (ABC1), member 6	8
CLEC14A	C-type lectin domain family 14, member A	8
SNORD3C	Small nucleolar RNA, C/D box 3C (SNORD3C), small nucleolar RNA	8
MS4A6A	Membrane-spanning 4-domains, subfamily A, member 6A	8
CHN2	Chimerin (chimaerin) 2	7
TEK	TEK tyrosine kinase, endothelial (venous malformations, multiple cutaneous and mucosal)	7
KBTBD11	Kelch repeat and BTB (POZ) domain containing 11	7
VAV3	Vav 3 guanine nucleotide exchange factor	7
	Homo sapiens mRNA; cDNA DKFZp686I0981 (from clone DKFZp686I0981)	7
NCAM1	Neural cell adhesion molecule 1	6
FCGR3B	Fc fragment of IgG, low affinity IIIb, receptor (CD16b)	6
RAPGEF5	Rap guanine nucleotide exchange factor (GEF) 5	6
ST6GALNAC3	ST6 (alpha-N-acetyl-neuraminyl-2,3-beta-galactosyl-1, 3)-N-acetylgalactosaminide alpha-2,6-sialyltransferase 3 (Alpha-N-Acetyl-Neuraminyl-2,3-Beta-Galactosyl-1,3)-N-Acetylgalactosaminide ST6 alpha-2,6-Sialyltransferase 3	6
SLCO2B1	Solute carrier organic anion transporter family, member 2B1	6

Table 10. Top 25 genes upregulated in the aged (Table 10A) and young (Table 10B) TM compared to the other.

Among the genes highly downregulated in the aged TM in comparison to young samples are those involved in regulation of cell growth and differentiation, host defense, cell adhesion and glycoprotein turnover (Table 10B). Majority of the top 25 downregulated genes were associated with cell maintenance, specifically *LYVE1*, a gene which is most prominently downregulated, *CSF1R*, *DLK1*, *CHN2*, *TEK* and *VAV3*. This suggests that the young TM is able to maintain itself and this ability may be lost in the aging TM. Those involved in cell defense were *CD163*, *C1QB*, *RNASE6*, *FCGR3B* and *TEK* which are anti-inflammatory, indicating the young samples probably experience less cellular stress, unlike the old TM. Cell adhesion molecules highly downregulated were *CLEC14A* and *NCAM1*, which are essential in maintaining the structural integrity of the tissue.

Matrix remodelling is an important function performed by the TM and a component of this process is glycoprotein turnover, which may be downregulated considering *CLEC14A* and *ST6GALNAC3*, genes involved in the latter were among the highly downregulated genes. So, matrix remodelling may be affected in the aging TM. Taken together, the result implies that cell maintenance, structural integrity of the tissue, cellular defense and matrix remodelling are downregulated in the aging TM relative to young samples. Whether these processes are enriched statistically significantly in the gene sets will be investigated later.

The expression data of genes greatly differentially expressed between the old and young samples indicate the aging TM to be under stress, with increased expression of genes involved in inflammation and cellular stress response. Normal functioning of the old TM may be also affected as deduced from the downregulation of genes responsible for cell maintenance, host defense, cell adhesion and matrix remodelling. Such gene expression changes could result in phenotypic modifications seen in the aging TM.

3.5.4 Biological Processes Differentially Regulated with Age in the Trabecular Meshwork

Dissimilarities in the biological processes taking place in the young and old TM specimens became evident upon looking at the set of highly differentially expressed genes. In order to have a comprehensive view of the entire data set to verify the aforementioned biological processes as well as identify other processes that are disparate, gene ontology (GO) was performed. Functional annotation clustering through DAVID [146] with the enrichment score ≥ 1.3, equivalent to 0.05 on non-log scale, and $p \leq 0.05$ found a diverse range of biological pathways differentially regulated with age in the TM.

The GO analysis identified and confirmed most of our observations from the gene expression profile. Biological processes most enriched in the aged TM does include those related to cell death, and stress response (Table 11). Specifically, regulation of cell death, growth (negative), cell component size (comprising negative regulation of cell size) and cell proliferation (negative) were all upregulated in the old TM samples relative to young ones, indicating increased cell death in the aged samples. Stress response related processes, such as response to wounding, abiotic stimulus and bacterium were also enriched, together with the downstream inflammatory response and cytokine response, especially that of *TNF*. ER stress

response was also high likely due to unfolded proteins as suggested by its increased response. So, overall the cells in the aging TM seem to experience cellular stress, which could account for their marked cell death.

Table 11. Biological processes enriched in the aged TM.

Biological Process	Number of Genes	*P*-Value
Regulation of transcription	220	1.20E-08
Regulation of RNA metabolic process	138	1.80E-03
Intracellular signaling cascade	108	8.80E-05
Regulation of cell death	90	1.50E-08
Positive regulation of macromolecule metabolic process	79	1.10E-04
Phosphorus metabolic process	79	4.30E-03
Proteolysis	79	2.70E-02
Regulation of cell proliferation	79	5.80E-06
Death	77	8.80E-07
Macromolecule catabolic process	76	2.60E-05
Positive regulation of nitrogen compound metabolic process	68	5.70E-06
Negative regulation of macromolecule metabolic process	67	5.40E-04
Macromolecular complex subunit organization	67	2.10E-04
RNA processing	55	1.80E-04
Positive regulation of molecular function	52	4.30E-03
Negative regulation of biosynthetic process	52	2.70E-03
Regulation of transferase activity	48	8.50E-07
Regulation of cell cycle	46	1.80E-07
Negative regulation of nitrogen compound metabolic process	46	7.50E-03
Response to wounding	46	1.10E-02
Protein complex biogenesis	45	7.60E-03
Regulation of growth	40	7.10E-05
Negative regulation of molecular function	38	2.10E-04
Response to abiotic stimulus	37	2.40E-03
RNA biosynthetic process	35	1.90E-04
Chromatin organization	34	1.80E-02
Microtubule-based process	30	5.60E-04
Regulation of cellular component size	29	3.30E-03
inflammatory response	29	3.20E-02
Positive regulation of developmental process	28	8.70E-03
Positive regulation of multicellular organismal process	25	1.10E-02
Regulation of locomotion	24	1.10E-03
Response to extracellular stimulus	23	1.20E-02
Response to bacterium	19	4.00E-02
Regulation of translation	18	3.30E-03
Taxis	18	1.50E-02
Response to unfolded protein	15	6.50E-05
Response to cytokine stimulus	11	1.90E-02
Response to endoplasmic reticulum stress	10	1.30E-04
ER-nuclear signaling pathway	9	8.70E-04

Table 11. Biological processes enriched in the aged TM. GO analysis was performed using DAVID functional annotation terms (subset: GOTERM_BP_FAT) on the set of genes enriched in the old TM samples relative to young ones. Descendant GO terms are represented by the parent term.

Genes associated with the regulation of transcription were the most enriched in the older specimens with 220 responsible genes upregulated (Table 11). This together with the other

affected processes of translational regulation, RNA biosynthesis/ metabolism as well as processing and protein complex biogenesis could be due to a compensatory mechanism to the increased proteolysis identified in the aging TM. Certain organizational processes of chromatin, macromolecular complex subunit, and multicellular organismal process were also upregulated together with intracellular signalling (particularly through protein kinase activity) and ER-nuclear signalling. In the aging TM, both biosynthetic and molecular functions were also negatively regulated as seen in the GO analysis (Table 11), and signify the less than optimal state of the aged TM. Moreover, migration associated processes of microtubule-related process, locomotion regulation and taxis were augmented in the older samples indicating increased migration of the TM cells probably upon some stimulus in the aging TM. TM cell loss attributed to migration has been hypothesized by some groups, but never proven *in vivo*.

Similar GO analysis of genes downregulated in the old TM samples, in comparison to young samples, found far fewer biological processes enriched in the young samples (i.e. down in the old samples). Lipid associated processes of lipid biosynthesis and glycerolipid metabolism were weaker in the aged TM, as well as organophosphate metabolism (Table 12). The significance of these processes in terms of TM structure/ function is unknown. Unexpectedly, processes related to cell maintenance, defense and matrix remodelling, which were initially speculated to be affected in the older sample set, as assessed from the highly downregulated genes, were not significantly enriched in the GO analysis. So, it can be taken that mechanisms governing cellular defense and homeostatic regulation of matrix components are still functioning normally in the aged TM. In addition, phagocytosis (parent term: endocytosis) and sensory perceptions of mechanical stretch, both essential processes of the TM were not downregulated in the older samples. The data, taken together, shows the young and old TM are mostly functionally equal, at least in the unstimulated state.

Table 12. Biological processes enriched in the young TM.

Biological Process	Gene Number	*P*-Value
Lipid biosynthetic process	19	3.50E-03
Glycerolipid metabolic process	11	1.40E-02
Organophosphate metabolic process	11	4.90E-02

Table 12. Biological processes enriched in the young TM. GO analysis was performed using DAVID functional annotation terms (subset: GOTERM_BP_FAT) on the set of genes enriched in the young TM samples relative to old ones. Descendant GO terms are represented by the parent term.

Gene expression profiling followed by GO analysis showed that the aging TM is functionally equivalent to young samples in the unstimulated state. Processes relevant to TM function and structural integrity were not deregulated between the two age groups, but various responses related to stress and inflammation were significantly enriched in the aging TM. This is supported by the augmentation of cell death related processes, which could account for the loss of TM cells observed with age. In addition, locomotion associated processes were increased in the older sample set, indicating migration of TM cells from the tissue may also be contributing to the cell loss. The data, taken together, shows that many key functions of the TM are maintained, though additional and potentially pathological activities are gained with aging.

4. Discussion

The exact pathophysiological mechanisms causing POAG are not completely understood. But the association of TM dysfunction with POAG, as characterized by structural changes in the TM, has been well established. TM is a critical component of the major outflow pathway and increased resistance posed by the pathological changes in the tissue impedes aqueous humour exit from the anterior chamber. Consequently, buildup of aqueous in the chamber elevates IOP and the excessive pressure exerts strain on the optic nerve, damaging the RGC responsible for transferring visual information to the brain. As a result, visual field is compromised in a slow and progressive manner. Hence, the structural/ functional integrity of the TM is indispensable in maintaining normal IOP and in turn healthy vision.

Regenerative medicine is promising in a number of diseases such as myocardial infraction [158], type I diabetes [159] and brain injury [160], [161] among many others, where function of the affected tissue has improved with stem cell transplantation. Extensive research for cell-based therapy to treat POAG is undergoing to replace the lost RGC but only limited success has been achieved [102]–[108]. Though no group has been able to regenerate the RGC *in vivo* due to the restricting nature of the retina, protective means have been found for RGC survival through neurotropic factors [109]–[112]. Replacement of TM cells is little ventured although the diseased TM seems to be the root cause of POAG. The lack of an expandable source of TM cells *in vitro* for such study is a reason. Mature TM cells have limited propagation *in vitro*, and stem cells of the TM, although proven to exist *in vivo*, had not been isolated.

The ultimate goal of the project was to establish a source of expandable TM cells, applicable for translational research as well as *in vitro* mechanistic studies of the TM. However, TM stem cell isolation technique, TM differentiation markers and differentiation method were all unknown and challenged the project. These were taken as objectives to address and were successfully identified. More importantly, expandable pools of stem cells and mature cells of the TM have been established.

A wide variety of animal models are used for the study of POAG, in particular for TM examination. They include rodents, rabbits, dogs, cats, monkeys and several other species. There is no ideal model of POAG due to the complexity of the disease and structural

differences in the TM. Primates have high homology and similar TM anatomy with humans, but their large size, expense and difficulty in handling them deter their use in TM study. In non-primates, TM is less trabecular than in humans and they have intrascleral plexus in place of the schlemm's canal [162], [163]. They also experience perfusion volume-dependent rise in the outflow facility termed as "washout" which is not observed in human meshwork. Moreover, they have very small globes which make TM extraction hard. So, no good and affordable animal model is available. Hence, we decided to use TM tissue harvested from human cadaveric eyes for this study. Study of human samples avoids other species-specific variations too.

Human TM can be attained from whole globe or corneoscleral rim. We chose the latter as our source of TM since it is easier to process. The TM tissue is feasible for research for up to 3 weeks. Tissues that were within two weeks from death were utilized for this study to ensure viability. Basic study of TM is normally performed on tissue sections and cultured cells. Upon confirmation of data, the more complex organ culture system is employed for further research. So, cultured cells and *ex vivo* tissue were used for hypothesis testing in this study.

Previous groups have attempted to isolate the elusive TM progenitors using various techniques. Primary TM culture with TM explants gave rise to a small subpopulation expressing stem cell markers, *MUC1* and *ANK3* [124]. Another group cultured primary human TM cells as free-floating spheres on suspension culture plates, which they believed were TM progenitors [116]. These methods were tried, in addition to other adult stem cells propagation techniques. However, they failed to give rise to a pure population of TM progenitors.

Monolayer culture of enzymatically dissociated cells from the TM incubated in a modified TM culture medium [116] yielded colonies of compact cells which were picked for further propagation. This led to a relatively homogenous population of cells with high nucleus to cytoplasmic ratio. These TM-derived cells expressed stem cell markers, had clonogenic potential and were of TM origin, implying them as TM stem cells. Size selection with 40 µm cell strainer prior to plating cells dissociated from the TM tissue, culture in the presence of embryonic stem cell (ESC) culture qualified serum and selective expansion of colonies could have favoured growth of the small progenitors over differentiated cells. Moreover, lack of expression of endothelial, epithelial and neural crest markers in the cultured cells excluded

the possiblity of contamination from other cell types in the vincity of the TM tissue. Thus, we have devised a method for TM stem cell isolation and propagation which is efficient and specific in culturing TM stem cells.

The morphological resemblence of the isolated TM stem cells to MSC prompted us to study them for MSC characteristics. Different approaches have been used to characterize MSC. As a standard, the ISCT has proposed the minimal criteria to define human MSC [155]. Tests for the three MSC properties found the TM-derived cells to: (1) Adhere to tissue culture plastic; (2) Express MSC markers' expression profile; (3) Differentiate into the mesenchymal lineages of adipocytes, osteocytes and chondrocytes *in vitro*. Thus, they meet the standard criteria for MSC characterization, confirming them not only as MSC, but also multipotent and were termed TM-MSC. Their propensity to differentiate can allow them to be differentiated into mature TM cells.

GSEA of TM-MSC gene set with that of other stem cells and cell types published by other groups found TM-MSC to be very similar to MSC from the bone marrow and adipose tissue, and to some extent to several mesenchyme-derived cell types. The close expression similarity of TM-MSC with BM-MSC and Ad-MSC further corroborates them as MSC. Our findings on the isolation and characterization of TM stem cells as MSC have been published in stem cells and development [164].

A similar work by Du and group published around the same time also isolated a multipotent stem cell population arising from the human TM [165]. They were purified either by fluorescence associated cell sorting (FACS) or clonal growth from explant culture and enzymatically dissociated TM cells respectively. These cells expressed markers of mesenchymal stem cells (*ABCG2*, *CD73*, *CD90*, *CD166*, and *BMI1*) and pluripotent stem cells (*NOTCH1* and *OCT4*). They differentiated into neural, adipose and corneal lineages *in vitro*, proving their multipotential property. The authors concluded the population as somatic stem cells of the TM. Although they did not define them as MSC, our study corroborates their results, with the antigen profiling of similar markers and demonstration of multipotency. Comparable techniques of TM stem cell isolation also boosts the reliability of our method. In fact, this group holds a patent (US 20120237485) for methods of obtaining an isolated population of TM stem cells and claims for a kit applicable for glaucoma cellular therapy.

A later work by Nadri et al. also confirmed the cell type of TM progenitors as MSC [166]. The group adopted an isolation procedure similar to our technique which gave rise to fibroblast-like cells that were positive for MSC markers (CD105, CD90, CD44 and CD166). These cells were capable of differentiation toward mesenchymal lineages. In addition, they differentiated into photoreceptor cells on amniotic membrane in the presence of induction medium. So, they demonstrated the MSC phenotype and multi-lineage differential potential of the TM stem cells, adding support to our findings.

TM stem cells expressed several pluripotent stem cell markers, which is interesting considering that they are multipotent adult stem cells. It is not so surprising as MSC derived from the bone marrow and adipose tissue have been known to retain expression of some of these markers [167]. Of the 84 genes profiled by qRT-PCR, 58 were expressed in one or both the cell samples. So, expression of the stem cell markers, other than the MSC markers, can also be used to identify them as a stem cell population.

TM stem cells characterized as MSC is of prime significance in our effort for cell-based therapy for POAG. MSC have been reported to be an optimal source of cells for clinical application by numerous groups. Friedenstein was the first to document MSC as a cell type derived from the bone marrow and their capacity to differentiate into osteocytes in 1976 [168]. Since then, immense progress has been made in understanding their characteristics and potential for translation. MSC can be isolated from a wide range of tissues such as bone marrow, adipose, umbilical cord and dental pulp [169], [170]. They can also be derived from organs like heart, spleen and thymus [171], [172]. MSC have the ability to differentiate into the cell types of connective tissues (osteocytes, chondrocytes, adipocytes, endothelium, myocytes and cardiomyocytes). In addition, they can transdifferentiate into cells of ectodermal (neuronal) and endodermal (pancreatic, hepatic and respiratory epithelium) origins, indicating their multi-lineage potential.

MSC are also known for their immunomodulatory effects as they can inhibit cytotoxic T cells and natural killer (NK) cells [173], [174]. MSC secrete antagonists of T cell development and proliferation to inactivate them. They also express human leukocytes antigen (HLA) class I proteins which deter their recognition by NK cells. The anti-inflammatory property of MSC has been demonstrated to confer immunoprotection *in vivo* in the case of autoimmune diseases.

It remains to be known whether TM-MSC are capable of immunoprotection which will be immensely beneficial in treating inflammatory glaucomas where the anterior chamber segments including the TM are inflammed. This maybe favourable in the case of POAG as well since inflammatory and immune environment is suspected to be compromised [175].

Based on their multipotency and protective effects, numerous groups have investigated their potential in mediating tissue and organ repair, and confirmed their efficacy in transplantation through local and systemic administration. MSC delivered intravenously have been shown to home and engraft into the diseased liver, bone and lungs [176], [177]. The studies demonstrate the ability of MSC to migrate, transverse through the endothelium and reach the injured tissue to stimulate regeneration. MSC also secrete trophic factors like growth factors and chemokines which have been found to ameliorate the survival of damaged cells and promote repair at the injury site in a range of tissues [178], [179]. Neuroprotection presented by MSC delivered intravitreally improved the survival of RGC via secreted trophic factors in animal models of glaucoma although no significant integration of MSC was apparent [105]. Intravenous delivery, however, did not confer this protective effect. So, depending on the tissue, MSC repair damaged tissues by directly integrating into the injured tissue to generate newly differentiated cells and/ or indirectly through expression of trophic factors which ameliorate survival of the damaged cells. Both modes of repair are likely to be beneficial for repairing the diseased TM, but the exact mechanism inducible by TM-MSC needs to be elucidated to optimize a treatment strategy for clinical application.

Clinical studies have proven MSC as beneficial for treating various diseases including but not limited to musculoskeletal, cardiovascular and neurodegenerative diseases. There are currently over 400 clinical trials worldwide using MSC in a diverse range of translational purposes as estimated from the public clinical trials database (http://www.clinicaltrials.gov). Majority of the trails showed no detrimental effect of utilizing MSC for therapeutic application and confirmed safety of the approach [180]. Both autologous and allogenic MSC transplantations have been evaluated for efficacy and safety. The safety of MSC therapy demonstrated by previous trails makes us anticipate that transplantation of TM-MSC to regenerate the diseased TM will plausibly not have harmful effects. Again, only an actual trail can confirm this.

In this study, we have identified the TM as another novel source of MSC. It is tempting to extrapolate that TM-MSC also have the beneficial properties as MSC, specifically capacity to

home to site of injury, differentiate into mature cells, secrete trophic factors which stimulate repair of damaged cells and block inflammation. Although these capabilities have not been investigated in TM-MSC, they are expected to possess them just as MSC from various sources have. So, transplantation of TM-MSC will likely help to repair and regenerate the dysfunctional TM in POAG. Autologous and allogenic approaches may be considered, but allogenic MSC may be more effective, given the genetic predisposition of the disease. Administration of MSC would have to be locally into the anterior chamber due to the avascular nature of the tissue.

In fact, another study by Du and group demonstrated the homing potential of human TM stem cells into the mouse TM *in vivo* when transplanted into the normal anterior chamber [136]. Human TM stem cells isolated and expanded in culture were labelled with the fluorescent dye DiO, injected into the mouse anterior chamber and were detected to integrate primarily into the TM. The integrated cells had differentiated as evaluated by TM marker expression. Apoptosis in the TM was very minimal and the integrated cells sustained in the tissue for at least 4 months without eliciting inflammation. Whether the engrafted cells are functional and able to control IOP adequately is not known. But, the study does prove that TM stem cells can home into the TM tissue and highlights the feasibility of regenerative medicine for POAG using TM stem cells.

More transplantation ventures were performed in 2014 with MSC and TM-like induced pluripotent stem cells (iPSC) [181], [182]. Ocularly injected MSC homed to the TM but failed to integrate into the tissue. Yet, they alleviated the IOP increase brought about by laser treatment of the TM [181]. Medium conditioned under hypoxia environment also produced the same effect, indicating the MSC secretum modified by stress is promoting tissue repair. iPSC were differentiated into TM-like cells through formation of embryoid bodies (EB), cultured on TM-derived ECM and maintained in TM cell conditioned medium. The resultant cells also improved outflow facility in a cell loss model [182]. Collectively, these successful transplantation studies prove that the TM is amenable to transplantation.

TM stem cells are hypothesized to be common progenitors to the TM and corneal endothelium (CE) by Yu and colleagues [183]. CE is on the posterior surface of the cornea, adjacent to the TM which surrounds its circumference. It consists of a monolayer of hexagonal-shaped cells attached to the Descemet's membrane on its posterior side and

exposed to the aqueous anteriorly. CE allows the entry of water and solutes into the avascular cornea to nourish, and at the same time actively pumps water from the cornea back into the anterior chamber to maintain a mildly dehydrated state of the cornea for optical transparency. CE and TM are both neural crest in origin, arising from the first wave of neural crest-derived mesenchymal cells. Cell density is higher in the periphery than in the center of the CE [184], [185] and when corneas stripped of CE were grafted in rats with excised corneas, repopulation of the transplanted cornea with endothelial cells was observed [186]. The studies postulate the transition zone (insert region) between the cornea and TM as a common niche of stem cells of the TM and CE. Contribution from the insert region for TM maintenance has already been discussed before. So, Yu termed the insert cells as 'PET cells' (progenitors for endothelium and trabeculum). Moreover, cornea wounding promoted the expression of stem cell markers, OCT4 and WNT1, in the insert region and TM [114]. This work further supports the hypothesis of a common progenitor for the TM and CE.

Recent work by Yu and group on the PET cells confirmed them as bipotent and highly proliferative with similar expression patterns for stem cell markers [187]. Cells harvested from bovine CE and TM were cultured as spheres on suspension culture dishes. Secondary sphere formation found the spheres were proliferative and majority of the cells were positive for Ki67. Differentiation was induced by dissociating the spheres and maintaining them as a monolayer in growth factor-free medium. Differentiation of TM spheres resulted in cells expressing TM markers that have acquired TM function (uptake of Ac-LDL and phagocytosis of melanin). Differentiated cells from CE spheres expressed CE markers and exhibited higher resistance, a characteristic of CE cells. Cells from both types of spheres differentiated into neurons in neural induction medium, identifying them as bipotent. The results, collectively, confirm the PET cells as common progenitors of the TM and CE.

In our effort to find differentiation inducers of TM lineage, several conditions were found to promote hexagonal morphology of the TM-MSC and upon confluence gave rise to a 'cobblestone' monolayer, similar to endothelial cell cultures. This was apparent on hydrogels of higher stiffness and treatment with 5-azacytidine and retinoic acid. Preliminary investigation of these treated cells for CE markers by our collaborators at Singapore Eye Research Institute (SERI) showed the markers to be upregulated. In some cases, the marker expression was almost similar to that of primary CE cells. Our work also supports the notion of the insert cells being shared progenitors of the TM and CE. This work is still in its

preliminary stage and is beyond the scope of the project. So, the data has not been presented here.

The capacity of TM-MSC to integrate into the TM tissue and differentiate has already been demonstrated by Du et al., [136]. So, our focus was shifted to establishing a scalable source of differentiated TM cells *in vitro* from TM-MSC. The TM cells differentiated *in vitro* can also be used for transplantation and may even be more effective given the functionality. This maneuver was hindered by the lack of knowledge of differentiation markers and inducers of TM lineage. A list of genes differentially expressed in the TM-MSC and *ex vivo* TM tissue was generated via gene expression profiling and was examined for genes suitable as TM differentiation markers. The genome-wide expression analysis is first of its kind investigating intrinsic differences between the differentiated cells *in vivo* and the population of cultured stem cells of the TM. It has shown biological processes divergent between the two cell types. Adhesion, negative regulative of growth and development-related processes are enriched in the differentiated cells reflecting structural complexity of the cells interacting in the 3D network of the TM and differentiated state of the cells. Moreover, phagocytosis, migration, homeostasis of cell number, sensory perception of mechanical stimulus and pigmentation are all properties of the differentiated TM cells and they are augmented in them according to the upregulation of their gene sets. It clearly represents the physiological state the TM-MSC need to acquire through differentiation to become functional TM cells. On the contrary, TM-MSC were found to be a population of active and proliferative cells as assessed from the enrichment of cell division associated processes, cell component organizational processes, regulation of gene expression, signalling cascades and metabolic processes in them.

Scattered reports on certain genes differentially expressed in the filtering compartment of the TM and its stem cell niche exist. Through immunocharacterization *in vivo*, Challa reported ANK3 and HMFG1 were highly expressed in the niche, while CHI3L1 is low compared to rest of the TM tissue [124]. The reliability of these genes as differentiation markers is questionable since they have not been tested in actual differentiation studies to deduce whether they are modulated over the course of differentiation. In addition, contradictory to Challa's work, *ANK3* is actually upregulated in the TM compared to TM-MSC as determined through our gene expression profiling. *HMFG1* and *CHI3LI* are not differentially expressed, but several other genes highly expressed in the TM (*MYOC*, *AQP1*, *MGP* and *MMP1*) are higher in expression in the TM relative to TM-MSC. However, they have similar expression

in the cornea and sclera, rendering them non-specific to the TM and hence not applicable as differentiation markers.

MYOC and *ANGPTL7* are the most highly expressed genes in the TM relative to TM-MSC. Serial analysis of gene expression (SAGE) profiling also showed *MYOC* and *ANGPTL7* to be among the 40 most highly expressed sequence tags in the TM libraries [188]. It was tempting to use them as TM differentiation markers but their ubiquitous expression in the ocular tissues made them unsuitable. Besides the TM, MYOC is detected amply in the cornea, sclera, choroid, ciliary body, iris, lamina cribosa, retina and optic nerve as well as in the acellular vitreous and aqueous humour [189]–[192]. ANGPTL7 is highly expressed in the cornea and lens [193]. Its expression in other ocular tissues is not well understood. So, to elucidate robust markers that are to a certain extent specific to the TM, genes enriched in the TM tissue in relation to the cornea, sclera and TM-MSC were identified through further gene expression study and selected candidates were evaluated. Relative mRNA levels measured by qRT-PCR confirmed highest expression in the TM. Immunocharacterization on corneoscleral sections displayed high marker expression in the TM, with some displaying specificity while the rest had greater expression in the TM in the context of the anterior segment of the eye. Thus, the study has identified novel markers of TM lineage.

The newly established positive markers of TM differentiation (TM markers) include secreted proteins F5, SPP1 and FGF9, membrane proteins CDH23 and KCNAB1, and transcription factor HEY1. F5 is a key cofactor for prothrombinase activity which is part of the coagulation process. Its gene has been mapped to the glaucoma locus, GLC1A where MYOC also resides and is known to be downregulated in cultured human TM cells [60]. Similarly, SPP1, a phosphoprotein involved in matrix mineralization through its inhibition of calcification *in vivo*, is also downregulated in human TM cells *in vitro* and highly expressed in the TM tissue [37], [194], [195]. It is also a cytokine that promotes interferon gamma (IFNG) and interleukin 12 (IL12) production. The primary TM cells in these studies will likely contain TM stem cells and their downregulation of both proteins compared to TM tissue support our data. FGF9 regulates proliferation and differentiation of several cell types including neural crest cells from which the TM was derived. The association of these genes with TM function and maintenance is unknown.

CDH23 as a calcium-dependent cell-cell adhesion protein is probably involved in the structural maintenance of the TM. KCNAB1, another cell surface antigen, is part of the voltage-gated potassium channel. Transcriptional repressor, HEY1, is activated by Notch signalling and is important for development. The roles KCNAB1 and HEY1 play in the TM mechanism are yet to be known. TM-MSC marker, BDNF, is a neurotrophin involved in the regulation of survival, differentiation and stress response. It is known to be expressed by both cultured human TM cells and *ex vivo* TM tissue, with the former expressing it at a higher level [196]. *BDNF* polymorphism may also be associated with POAG progression [197], although again its exact pathophysiological mechanism is unclear.

TM-MSC were preferred as progenitor cells to induce TM differentiation. As adult stem cells, they circumvent the ethical and political concerns that challenge ESC research. They could also be more primed to differentiate into TM lineage being derived from it. Du et al., have already shown the TM induction potential of the isolated TM stem cells [165]. TM stem cells cultured in bovine aqueous humour and 10% FBS for 10 days differentiated into mature cells. Both conditions upregulated the genes highly expressed in the TM and decreased some stem cell markers' expression. The cells could phagocytose fluorescent labelled bioparticles almost at the same extent as primary TM cells.

Recently, a report on TM differentiation from iPSC was published [198]. Co-culturing iPSC with primary TM cells in transwells differentiated them into functional TM cells. This implies that the conditioned medium contains the TM secretum which induces TM differentiation. Similar technique adopted by Yu et al. utilized TM-derived ECM and conditioned medium which also had the same effect on TM progenitors cultured as spheres [187]. These are the few known methods of TM differentiation. Though effective, these differentiation protocols are largely nonspecific and probably induced spontaneous differentiation in the cells. Such methods may yield inconsistent results due to batch to batch variation of the aqueous and FBS. Efficacy of conditioned medium could also vary with donor lines. For our study, we are interested in designing a directed differentiation protocol, with defined differentiation factors, that will allow consistent and reliable differentiation into TM cells.

It is unclear whether the TM consists of cells of the same type or multiple cell types. Heat shock protein, crystallin alpha B (CRYAB), has been described to be expressed in the JCT

cells, but absent in cells of the other layers. There may be subtypes of TM cells, but no data has confirmed this. So, for the purpose of our differentiation study, we have taken the TM to contain a single population of differentiated cells.

Gene ontology of TM vs TM-MSC entity list identified signalling pathways enriched in the differentiated cells. Signalling molecules targeting them may potentially induce TM differentiation. Small molecules are considered as an attractive alternative to signalling proteins. They were tested in addition to some known differentiation inducers, including signalling factors and epigenetic modifiers. Small molecules are increasingly playing an integral role in the development of chemically defined media for the differentiation of various cell types. They are relatively inexpensive, xeno-free and exhibit broad selectivity for ligand subtypes, unlike endogenous signalling proteins. They also offer precise temporal control, improving consistency and efficiency of differentiation. This renders them valuable for translational research.

Trichostatin A, a histone deacetylase inhibitor, upregulated all the chosen TM markers (*F5*, *CDH23*, *HEY1*, *SPP1*, *FGF9* and *KCNAB1*) and decreased the expression of TM-MSC marker (*BDNF*), as shown by qRT-PCR and immunofluorescence. Considerable cell detachment was noticed upon treatment, which may be due to the absence of a suitable matrix to support the modified cells. Fibronectin, laminin, collagen types IV and VI are major components of the ECM in the TM tissue [199], [200]. It remains to be known if they could promote better cell attachment during differentiation when utilized as coating substrates. The adherent cells were non-apoptotic, enlarged and elongated, deeming them morphologically distinct from the compact TM-MSC and similar to TM cells, although they did not demonstrate functionality by modified-LDL uptake.

Acetylation of DNA-associated histone and non-histone proteins is one of the epigenetic modifications of chromatin which regulates gene expression [201]–[203]. Acetylation is controlled by histone acetyltransferases (HATs) and histone deacetylases (HDACs) [204]. HAT activity relaxes the chromatin structure allowing transcriptional activation, thereby increasing gene expression, while HDAC in contrast represses transcription. Inhibitors of HDAC block deacetylation, thereby promoting histone acetylation and subsequently gene expression which influences proliferation, differentiation and apoptosis [205], [206]. TSA has the same effect and has been applied in differentiation such as myocardial differentiation of

ESC [207], hepatic differentiation of MSC [208], differentiation and mineralization of pulp-derived cells [209] and astrocytic lineage progression of cortical progenitors [210]. TSA dose used for TM differentiation is relatively high compared to the amount used in other types of differentiation. The high dose suggests that the mode of action in TM differentiation may not be solely through HDAC inhibition. Nevertheless, TSA increases the expression of TM markers, downregulates TM-MSC marker, accompanied by morphological changes which all indicate TM-MSC differentiating into TM cells, at least intermediately since functionality is missing.

SC1, BCI and forskolin which activate the Ras, FGF and adenylate cyclase signalling pathways respectively have the desired effect on the TM differentiation markers. BI-D1870, an antagonist of RSK, also has similar influence. Their mechanisms of action coincide with several pathways enriched in the TM tissue such as FGF signalling activated by BCI; BTC, GDNF and PDGF activate Ras downstream indirectly and SC1 achieves this through Ras-GAP inhibition. Among the small molecules tested, TSA is the most robust differentiation factor as its treatment alone upregulated the markers more than their combined treatments.

Forced aggregation confers 3D patterning of cells which enhances cell-cell contacts and promotes biochemical interactions. Many stem cell differentiation protocols employ it as an induction step like ESC differentiation into hematopoietic [211], cardiac [212] and hepatocytic lineages [213]. In this study as well this technique seems to specify TM differentiation, according to the significant upregulation of TM markers.

Chondrocyte specific markers and growth factors that enhance chondrogenesis are enriched in the TM tissue. TM-MSC cultured in the chondrogenic medium, TADLIS (named after its key components **T**GFβ3, **a**scorbic acid, **d**examethasone, **l**inoleic acid, **I**TS and **s**odium pyruvate) differentiated into mature TM cells expressing the positive differentiation markers and downregulated BDNF as shown by expression analysis. Greater than 80% of the cells had functionality as evaluated by Ac-LDL incorporation. So, this method of differentiation is applicable for TM differentiation.

Constituents of the TADLIS medium are common to the differentiation inducing conditions of adipocytes, osteocytes and chondrocytes, though in different combinations. So, it is plausible that only specific elements in this cocktail are inducing TM differentiation and

efforts to find these minimal factors necessary for differentiation are undergoing. Furthermore, the sequential and combinatorial treatments with TSA are also being tested to determine an optimal differentiation condition. Marker expression analysis for the other mesenchymal lineages may be needed to ensure the differentiation condition is only promoting TM differentiation. Nevertheless, although not perfect, the study has identified a differentiation medium capable of promoting differentiation of TM-MSC into TM lineage. Importantly, it proves the ability of TM-MSC to differentiate into mature TM cells *in vitro* and has established an expandable population of functional TM cells for POAG study and treatment.

Donor-specific variation in the relative expression level of markers under the various differentiation conditions was evident probably due to the diverse background of donors such as age, ethnicity, lifestyle, drug intake, genetics, etc. In fact, the plasticity of MSC is known to decrease with age [214]. Such variations also have to be considered when selecting the donors of TM-MSC to ensure quality of cells suitable for differentiation. MSC from more accessible sources such as adipose and bone marrow could also differentiate into TM cells under our conditions, but this needs to be investigated.

Structural modifications in the TM with age are well-documented. This includes decline in TM cellularity [129], [130], trabecular thickening, trabecular fusion and modification of extracellular matrix material in the JCT [126]. The incidence of POAG is also correlated to age. Age-related changes in the TM could explain the increased susceptibility to the disease with age. Such alterations are usually phenotypic manifestation of age-dependent gene expression changes. Gene expression profiling of young and aging TM specimens was done for a deeper understanding of aging in the TM. To our knowledge, expression analysis on the TM with respect to age has never been investigated before.

From our analysis, cell death and negative growth related processes are enriched in the aging TM. Cellular stress responses and inflammatory response are also augmented. So, it seems likely that cells in the aging TM are experiencing some form of stress that they are not able to cope with, and undergo apoptosis. It could account for the loss of TM cells observed with age. The exact cause of stress is unclear. Constitution of the aqueous humour which supplies and nourishes the TM may be changing with age, such that it may be dwindling in factors

essential for TM cell survival and/ or rising in harmful compounds which could impose stress on the TM cells, resulting in their death.

Zahn and group deciphered the aging signature of human tissues by comparing genome-wide transcriptional profiles of the brain, muscle and kidney [215]. They found expression of cell cycle, complement activation (associated with inflammation), and extracellular matrix genes to increase with age, which were also identified in the aging TM, although the enrichment of the latter as a biological process was not statistically significant. Another gene set enriched in the aging tissues is related to cytoplasmic ribosomal genes. Several of these (*RN5S9*, 18S rRNA and *RPL28* and 28S rRNA) were upregulated with age in the TM. In addition, chloride transport genes and electron transport genes were deduced to decline in expression with age by Zahn et al. Two chloride transport genes (*CLCA1* and *FXYD5*) were found to be downregulated in the aging TM, but none of the electron transport genes were among the age-regulated genes. In general, our gene expression analysis of young and old TM sample sets retains most of the aging signature. Genes of the chloride and electron transport systems may not have been strongly altered in this data set and as result could have been excluded with the stringent cut-off of 2-fold or more.

Despite several similar gene set enrichments in the different human tissues, much of aging is known to be tissue-specific. Cell migration related processes are augmented in the aging TM, but not identified to be upregulated in the other aged tissues. Hogg et al. have shown bovine aqueous humour to stimulate the migration of human and bovine cultured TM cells [216]. They identified fibronectin as a major chemoattractant in the aqueous humour for the cells. Media conditioned by bovine CE and scleral fibroblasts also promote migration of bovine TM cells, with CE having a more prominent effect. It is possible that alterations in the composition of aqueous humour with age created by certain ocular cells could be inducing the TM cells to migrate, and account for the cell loss. Biological processes relevant to phagocytosis were not affected with aging. So, phagocytosis is not contributing to the migration here, although it is known to modulate migration of TM cells.

Cells in the aging TM are believed to retain their functionality as functional processes of the TM are not deregulated with age. Functions of the TM like phagocytosis, stretch response and ECM modulation were among the enriched biological processes in neither the young nor old TM. Only lipid biosynthesis, glycerolipid and organophosphate metabolic processes are

downregulated in the old TM. It is unclear how these processes are associated with aging in the TM. A limitation of expression profiling is structural and chemical changes cannot be detected with gene arrays. One such modification that could contribute to meshwork stiffness is advanced glycation end product (AGE) receptor activity through cross-linking of the meshwork [217]. Probes targeting genes coding for the receptors involved in it, namely receptor for advanced glycation end products (RAGE), macrophage scavenger receptor (MSR), oligosaccharyl transferase-48 (AGE-R1), 80 K-H phosphoprotein (AGE-R2), galectin-3 (AGE-R3) and CD36 among others are present on the array. The GO term, AGE receptor activity, was not affected with aging as deduced from our GO analysis. So, from our expression profiling, it is evident that dysfunctional TM cells are not causing the modifications in the TM since remnant cells retain function, rather they may have resulted from the loss of TM cells via cellular stress and/ or migration.

It is conceivable that changing composition of the aqueous humour is resulting in the cell loss. With declining TM cell number as one ages, regulation of matrix remodelling may be compromised and produces the structural modifications accompanying aging. The changing structure, in turn, could increase susceptibility to POAG through elevation in outflow resistance.

Besides coding genes, noncoding genes, specifically microRNAs are differentially expressed in the old vs young data set. *MIR302C*, *MIR155HG* and *MIR214*, which are tumor suppressors are highly expressed in the aging TM cells. *MIR214* also regulates type I collagen [218]. Function is yet to be annotated to the other microRNAs upregulated in the aging TM. *MIR568* is upregulated in the young TM samples and it inhibits activation and function of T cells [219]. Other than the growth regulatory role most of these microRNAs play, it will be useful to investigate their role in TM function and maintenance, especially with regards to aging.

POAG is perceived to be an exacerbation of the aging process in the TM since TM structural modifications with age including cell loss are also manifested in the glaucomatous TM but in a more pronounced fashion. Hence, we believe cell loss occurring at a greater magnitude in the diseased TM due to elevated aqueous changes create marked modifications in the TM which hinder the outflow facility. The work by Hogg et al., corroborates this idea as aqueous humour derived from glaucomatous patients stimulated the migration of TM cells *in vitro*

more than that from control subjects [216]. TM cells remnant in the diseased tissue are probably still normal and functioning, and the pathology is most likely manifested from excessive TM cell loss.

This study further underscores the importance of cell replacement therapy to treat POAG. Supplementing the diseased tissue with functional TM cells may ameliorate its performance, enough to bring IOP under control and slow or even completely stop the progression of the disease. Though differentiated TM cells can be derived from TM explants, it is limited by the very slow process and low number of cells derived. Hence, primary TM cells may be insufficient for the thorough investigation of the approach. Transformed human TM cell lines are available but since they have been genetically altered to improve proliferation, they are unsafe for therapy for fear of tumor formation. Thus, our methodology for generating mature TM cells in a scalable manner will be extremely beneficial to explore this approach.

In conclusion, the study has isolated, characterized and differentiated TM stem cells for the study and treatment of POAG. Our findings will help in the better understanding of inherent differences between the TM stem cells and differentiated TM cells. We have established methodologies for TM stem cell isolation and their differentiation into TM lineage which will advance the implementation of regenerative medicine for POAG. We have also identified the TM as a novel source of MSC in the process. Furthermore, we have identified novel markers of the TM, applicable both for identifying TM cells and to assess TM differentiation. Hence, the study is of significance in the TM research field. Manuscripts on the identification of novel TM differentiation markers and gene expression study of aging in the TM are being prepared for publication.

5. Future Perspectives

It is promising that mature TM cells can be propagated *in vitro* using our differentiation methodology. While the TADLIS medium is effective, it may not be the most efficient. Minimal factors essential for TM differentiation in the cocktail have to be elucidated in order to avoid components that render no benefit for the differentiation or may even hamper it. This can be achieved by treating the TM-MSC with different combinations of factors to determine the best consolidation that upregulate the TM differentiation markers as well as promote better uptake of Ac-LDL. TSA was very robust in regulating the TM differentiation markers, but the differentiated cells did not seem to have functionality since they were incapable of uptaking the modified LDL. It is necessary to test TSA together with the minimal essential factors as sequential and combinatorial treatments to assess whether it could bolster the differentiation. So, further improvements to the differentiation protocol is required to derive a more efficient differentiation treatment regime.

One means of characterizing the functionality of differentiated TM cells was investigated in this study. More holistic characterization of the cells is vital before transplantation studies. This will include assessment for other TM functions such as phagocytosis and secretion of ECM components. Phagocytosis can be analyzed by the uptake of opsinized labelled-bacterium or bioparticles, while ECM factor secretion could be quantified at the mRNA level via qRT-PCR or through a proteomic approach using ELISA. Pigmentation of TM cells upon differentiation was another characteristic of mature TM cells that TM progenitors lack as determined from our gene expression profiling of the two cell types. Assessment for this phenotype too could be adopted to more thoroughly characterize the differentiated TM cells.

Better understanding of the regulatory mechanisms that govern TM differentiation is another aspect of the field that can be studied. The identification of small molecules that induce TM differentiation provides insight into the possible signalling pathways that regulate the differentiation. Further examination of these pathways by microarray analysis or simply targeting the potential pathways with inhibitors during the course of differentiation will reveal the exact mechanism of TM differentiation.

Expandable pools of TM progenitors and mature cells are available by means of the progenitor isolation technique and differentiation methodology respectively. Moving forward,

transplantation into animal models of POAG can be examined with the two cell types. This will demonstrate which cell type is better suited for the purpose through the analysis of grafting efficiency, interaction between the new cells and host tissue, IOP regulation and inflammatory response. TM progenitors as a stem cell population may be promising with its capacity to self-renew, however, the risk of tumorigenesis is imminent due to uncontrolled proliferation that may lead to tumor formation. TM cells differentiated *in vitro* could be more functionally relevant with the validation of TM characteristics prior to transplantation. Hence, a transplantation study will decide the best type of TM cells for POAG cellular therapy.

Characterization of the TM progenitors as MSC warrants the study of MSC from accessible sources such as adipose or bone marrow. MSC from such alternative sources can be investigated for their differentiation potential into mature TM cells by our differentiation technique or with some modifications, if required. It will be an attractive option for cell replacement for POAG if proven effective, as donor cells can be attained from living donors instead of cadaveric eyes. It also makes the option of autologous treatment possible, but the efficacy of this option has to be determined compared to allogenic transplantation due to the genetic association of the disease. In the near future, allogenic transplantation may be preferred, but it may change with the advent of genome editing and the increasing knowledge of disease locus, patient cells could be modified for autologous treatment. The latter will be challenging and only possible in the remote future, but it will allow ‘customized’ treatment.

Molecular dissection of aging in the TM has revealed several biological processes that are perturbed with age in the tissue. As a continuation to the study, mechanistic examination of young and old TM cells *in vitro* can be conducted to validate our findings as well as understand signalling pathways that contribute to the aging-related cell loss. Some POAG lines could be included in the study to analyze whether these biological perturbations are common between aging and POAG or unique to aging alone. It will facilitate better understanding of the disease and its association with aging.

6. Conclusion

POAG, the most common form of glaucoma, is a neurodegenerative ocular disease believed to manifest from TM malfunction. This study was initiated in an effort to establish an expandable pool of TM cells for regenerative application for POAG. We have isolated and propagated the elusive TM stem cells using a monolayer culture system with certain selection procedures. The technique fostered a relatively homogenous cell population which was verified as TM stem cells and further characterization of these cells found them to be MSC. The TM-MSC were adherent on tissue culture plastic, expressed MSC marker profile, and multipotent, as evaluated for MSC properties. This is the first report of stem cell isolation and characterization from the TM and the TM stem cell isolation method can be adapted for other TM progenitor studies.

The study also identified novel TM differentiation markers that are robustly differentially expressed between the *ex vivo* TM tissue and TM-MSC. In addition, they were specific to some extent to the TM in the anterior segment of the eye. Next, TM lineage inducing conditions were found which include small molecules, aggregation culture and the TADLIS medium. The TADLIS medium efficiently differentiated the TM-MSC into functionally mature TM cells at a high efficiency. Hence, a differentiation method has been devised which can generate a scalable population of mature TM cells for translational research as well as mechanistic study. Further work is necessary to determine the minimal factors in this medium and test the other conditions in combination to optimize differentiation.

Aging in the TM was studied by gene expression profiling to molecularly understand age-related changes in the TM. It identified several biological processes enriched in the aging TM, in particular cell death (possibly arising from cellular stress) and migration. These processes could contribute to the cell loss observed with age in the TM, and indirectly result in the structural changes and increased POAG susceptibility. The finding is the first account of genomic evidence for mechanisms responsible of TM cell loss which have been hypothesized before but not proven.

7. References

[1] H. A. Quigley and A. T. Broman, "The number of people with glaucoma worldwide in 2010 and 2020," *Br. J. Ophthalmol.*, vol. 90, no. 3, pp. 262–7, 2006.

[2] J. Haffmans, "Beiträge zur Kentniss des Glaucoms," *Arch. für Ophthalmol.*, vol. 8, pp. 124–78, 1861.

[3] American Academy of Ophthalmology, "Preferred practice pattern: Primary open-angle glaucoma," *Am. Acad. Ophthalmol.*, 2010.

[4] M. W. Tuck and R. P. Crick, "The age distribution of primary open angle glaucoma," *Ophthalmic Epidemiol.*, vol. 5, no. 4, pp. 173–83, 1998. [published erratum appears in Ophthalmic Epidemiol 1999 Mar;6(1):84].

[5] R. C. Wolfs, P. H. Borger, R. S. Ramrattan, C. C. Klaver, C. A. Hulsman, A. Hofman, J. R. Vingerling, and R. A. Hitchings, "Changing views on open-angle glaucoma: Definitions and prevalences — The Rotterdam Study," *Invest. Ophthalmol. Vis. Sci.*, vol. 41, no. 11, pp. 3309-21, 2000.

[6] S. de Voogd, M. K. Ikram, R. C. Wolfs, N. M. Jansonius, A. Hofman, and P. T. de Jong, "Incidence of open-angle glaucoma in a general elderly population: The Rotterdam Study," *Ophthalmology*, vol. 112, no. 9, pp. 1487–93, 2005.

[7] A. E. Maumenee, "Causes of optic nerve damage in glaucoma," *Ophthalmology*, vol. 90, no. 7, pp. 741–52, 1983.

[8] H. A. Quigley, "Neuronal death in glaucoma," *Prog. Retin. Eye Res.*, vol. 18, no. 1, pp. 39–57, 1999.

[9] M. T. Nicolela and S. M. Drance, "Various glaucomatous optic nerve appearances: clinical correlations," *Ophthalmology*, vol. 103, no. 4, pp. 640–9, 1996.

[10] K. Grødum, A. Heijl, and B. Bengtsson, "Refractive error and glaucoma," *Acta Ophthalmol. Scand.*, vol. 79, no. 6, pp. 560–66, 2001.

[11] L. Xu, Y. Wang, S. Wang, Y. Wang, and J. B. Jonas, "High myopia and glaucoma susceptibility the Beijing Eye Study," *Ophthalmology*, vol. 114, no. 2, pp. 216–20, 2007.

[12] P. Mitchell, F. Hourihan, J. Sandbach, and J. J. Wang, "The relationship between glaucoma and myopia: the Blue Mountains Eye Study," *Ophthalmology*, vol. 106, no. 10, pp. 2010–5, 1999.

[13] A. A. Kuzin, R. Varma, H. S. Reddy, M. Torres, and S. P. Azen, "Ocular biometry and open-angle glaucoma: the Los Angeles Latino Eye Study," *Ophthalmology*, vol. 117, no. 9, pp. 1713–9, 2010.

[14] Y. Suzuki, A. Iwase, M. Araie, T. Yamamoto, H. Abe, S. Shirato, Y. Kuwayama, H. K. Mishima, H. Shimizu, G. Tomita, Y. Inoue, and Y. Kitazawa, "Risk factors for open-angle glaucoma in a Japanese population: the Tajimi Study," *Ophthalmology*, vol. 113, no. 9, pp. 1613–7, 2006.

[15] P. Mitchell, W. Smith, T. Chey, and P. R. Healey, "Open-angle glaucoma and diabetes: the Blue Mountains eye study, Australia," *Ophthalmology*, vol. 104, no. 4, pp. 712–8, 1997.

[16] I. Dielemans, P. T. de Jong, R. Stolk, J. R. Vingerling, D. E. Grobbee, and A. Hofman, "Primary open-angle glaucoma, intraocular pressure, and diabetes mellitus in the general elderly population. The Rotterdam Study," *Ophthalmology*, vol. 103, no. 8, pp. 1271–5, 1996.

[17] I. Dielemans, J. R. Vingerling, D. Algra, A. Hofman, D. E. Grobbee, and P. T. de Jong, "Primary open-angle glaucoma, intraocular pressure, and systemic blood pressure in the general elderly population. The Rotterdam Study," *Ophthalmology*, vol. 102, no. 1, pp. 54 – 60, 1995.

[18] S. de Voogd, R. C. Wolfs, N. M. Jansonius, J. C. Witteman, A. Hofman, and P. T. de Jong, "Atherosclerosis, C-reactive protein, and risk for open-angle glaucoma: the Rotterdam study," *Invest. Ophthalmol. Vis. Sci.*, vol. 47, no. 9, pp. 3772–6, 2006.

[19] B. E. Klein, R. Klein, S. M. Meuer, and L. A. Goetz, "Migraine headache and its association with open-angle glaucoma: the Beaver Dam Eye Study," *Invest. Ophthalmol. Vis. Sci.*, vol. 34, no. 10, pp. 3024–7, 1993.

[20] M. C. Leske, A. M. Connell, S. Wu, L. G. Hyman, and A. P. Schachat, "Risk factors for open-angle glaucoma. The Barbados Eye Study," *Arch. Ophthalmol.*, vol. 113, no. 7, pp. 918–24, 1995.

[21] J. H. Kang, L. R. Pasquale, B. A. Rosner, W. C. Willett, K. M. Egan, N. Faberowski, and S. E. Hankinson, "Prospective study of cigarette smoking and the risk of primary open-angle glaucoma," *Arch. Ophthalmol.*, vol. 121, no. 12, pp. 1762–8, 2003.

[22] D. Gaasterland and C. Kupfer, "Experimental glaucoma in the rhesus monkey," *Invest. Ophthalmol.*, vol. 13, no. 6, pp. 455–7, 1974.

[23] A. J. Weber and D. Zelenak, "Experimental glaucoma in the primate induced by latex microspheres," *J. Neurosci. Methods*, vol. 111, no. 1, pp. 39–48, 2001.

[24] H. A. Quigley and E. M. Addicks, "Chronic experimental glaucoma in primates. I. Production of elevated intraocular pressure by anterior chamber injection of autologous ghost red blood cells," *Invest. Ophthalmol. Vis. Sci.*, vol. 19, no. 2, pp. 126–36, 1980.

[25] H. A. Quigley and E. M. Addicks, "Chronic experimental glaucoma in primates. II. Effect of extended intraocular pressure elevation on optic nerve head and axonal transport," *Invest. Ophthalmol. Vis. Sci.*, vol. 19, no. 2, pp. 137–52, 1980.

[26] D. B. Gould, R. S. Smith, and S. W. John, "Anterior segment development relevant to glaucoma," *Int. J. Dev. Biol.*, vol. 48, no. 8–9, pp. 1015–29, 2004.

[27] G. E. Marshall, A. G. Konstas, and W. R. Lee, "Immunogold ultrastructural localization of collagens in the aged human outflow system," *Ophthalmology*, vol. 98, no. 5, pp. 692–700, 1991.

[28] C. G. Murphy, A. J. Yun, D. A. Newsome, and J. A. Alvarado, "Localization of extracellular proteins of the human trabecular meshwork by indirect immunofluorescence," *Am. J. Ophthalmol.*, vol. 104, pp. 33–43, 1987.

[29] G. E. Marshall, A. G. Konstas, and W. R. Lee, "Immunogold localization of type IV collagen and laminin in the aging human outflow system," *Exp. Eye Res.*, vol. 51, no. 6, pp. 691–9, 1990.

[30] E. Lütjen-Drecoll, M. Rittig, J. Rauterberg, R. Jander, and J. Mollenhauer, "Immunomicroscopical study of type VI collagen in the trabecular meshwork of normal and glaucomatous eyes," *Exp. Eye Res.*, vol. 48, no. 1, pp. 139–47, 1989.

[31] E. Lütjen-Drecoll, "Functional morphology of the trabecular meshwork in primate eyes," *Prog. Retin. Eye Res.*, vol. 18, no. 1, pp. 91–119, 1999.

[32] C. R. Hann, M. J. Springett, X. Wang, and D. H. Johnson, "Ultrastructural localization of collagen IV, fibronectin, and laminin in the trabecular meshwork of normal and glaucomatous eyes," *Ophthalmic Res.*, vol. 33, no. 6, pp. 314–24, 2001.

[33] F. Freddo, "Age-related changes of sulfated proteoglycans in the normal human trabecular meshwork," *Exp. Eye Res.*, vol. 55, no. 5, pp. 691–709, 1992.

[34] E. Lütjen-Drecoll, M. Schenholm, A. Tengblad, and E. Tamm, "Visualization of hyaluronic acid in the anterior segment of rabbit and monkey eyes," *Exp. Eye Res.*, vol. 51, no. 1, pp. 55–63, 1990.

[35] C. Flügel-Koch, A. Ohlmann, R. Fuchshofer, U. Welge-Lüssen, and E. R. Tamm, "Thrombospondin-1 in the trabecular meshwork: localization in normal and glaucomatous eyes, and induction by TGF-beta1 and dexamethasone in vitro," *Exp. Eye Res.*, vol. 79, no. 5, pp. 649–63, 2004.

[36] D. J. Rhee, R. N. Fariss, R. Brekken, E. H. Sage, and P. Russell, "The matricellular protein SPARC is expressed in human trabecular meshwork," *Exp. Eye Res.*, vol. 77, no. 5, pp. 601–7, 2003.

[37] S. I. Tomarev, "Gene expression profile of the human trabecular meshwork: NEIBank sequence tag analysis," *Invest. Ophthalmol. Vis. Sci.*, vol. 44, no. 6, pp. 2588–96, 2003.

[38] J. W. Rohen and E. van der Zypen, "The phagocytic activity of the trabecularmeshwork endothelium. An electron-microscopic study of the vervet (Cercopithecus aethiops)," *Albr. Von Graefes Arch Klin Exp. Ophthalmol.*, vol. 175, no. 2, pp. 143–60, 1968.

[39] T. S. Acott, M. J. Kelley, K. E. Keller, J. A. Vranka, D. W. Abu-Hassan, X. Li, M. Aga, and J. M. Bradley, "Intraocular pressure homeostasis: maintaining balance in a high-pressure environment," *J. Ocul. Pharmacol. Ther.*, vol. 30, no. 2–3, pp. 94–101, 2014.

[40] D. H. Johnson, T. M. Richardson, and D. L. Epstein, "Trabecular meshwork recovery after phagocytic challenge," *Curr. Eye Res.*, vol. 8, no. 11, pp. 1121–30, 1989.

[41] X. Zhang, C. M. Ognibene, A. F. Clark, and T. Yorio, "Dexamethasone inhibition of trabecular meshwork cell phagocytosis and its modulation by glucocorticoid receptor beta," *Exp. Eye Res.*, vol. 84, no. 2, pp. 275–84, 2007.

[42] C. Buller, D. H. Johnson, and R. C. Tschumper, "Human trabecular meshwork phagocytosis. Observations in an organ culture system," *Invest. Ophthalmol. Vis. Sci.*, vol. 31, no. 10, pp. 2156–63, 1990.

[43] T. S. Acott and M. J. Kelley, "Extracellular matrix in the trabecular meshwork," *Exp. Eye Res.*, vol. 86, no. 4, pp. 543–61, 2008.

[44] R. Fuchshofer and E. R. Tamm, "Modulation of extracellular matrix turnover in the trabecular meshwork," *Exp. Eye Res.*, vol. 88, no. 4, pp. 683–8, 2009.

[45] J. M. Bradley, M. J. Kelley, X. Zhu, A. M. Anderssohn, J. P. Alexander, and T. S. Acott, "Effects of mechanical stretching on trabecular matrix metalloproteinases," *Invest. Ophthalmol. Vis. Sci.*, vol. 42, no. 7, pp. 1505–13, 2001.

[46] J. M. Bradley, "Signaling pathways used in trabecular matrix metalloproteinase response to mechanical stretch," *Invest. Ophthalmol. Vis. Sci.*, vol. 44, no. 12, pp. 5174–81, 2003.

[47] J. M. Bradley, J. Vranka, C. M. Colvis, D. M. Conger, J. P. Alexander, A. S. Fisk, J. R. Samples, and T. S. Acott, "Effect of matrix metalloproteinases activity on outflow in perfused human organ culture," *Invest. Ophthalmol. Vis. Sci.*, vol. 39, no. 13, pp. 2649–58, 1998.

[48] V. Vittal, A. Rose, K. E. Gregory, M. J. Kelley, and T. S. Acott, "Changes in gene expression by trabecular meshwork cells in response to mechanical stretching," *Invest. Ophthalmol. Vis. Sci.*, vol. 46, no. 8, pp. 2857–68, 2005.

[49] K. E. Keller, M. J. Kelley, and T. S. Acott, "Extracellular matrix gene alternative splicing by trabecular meshwork cells in response to mechanical stretching," *Invest. Ophthalmol. Vis. Sci.*, vol. 48, no. 3, pp. 1164–72, 2007.

[50] M. T. Coroneo, C. Korbmacher, C. Flügel, B. Stiemer, E. Lütjen-Drecoll, and M. Wiederholt, "Electrical populations and morphological evidence for heterogeneous of cultured bovine trabecular meshwork," *Exp. Cell Res.*, vol. 52, no. 4, pp. 375–88, 1991.

[51] M. Wiederholt, H. Thieme, and F. Stumpff, "The regulation of trabecular meshwork and ciliary muscle contractility," *Prog. Retin. Eye Res.*, vol. 19, no. 3, pp. 271–95, 2000.

[52] M. Wiederholt, S. Bielka, F. Schweig, E. Lütjen-Drecoll, and A. Lepple-Wienhues, "Regulation of outflow rate and resistance in the perfused anterior segment of the bovine eye," *Exp. Eye Res.*, vol. 61, no. 2, pp. 223–34, 1995.

[53] B. Tian, B. Geiger, D. L. Epstein, and P. L. Kaufman, "Cytoskeletal involvement in the regulation of aqueous humor outflow," *Invest. Ophthalmol. Vis. Sci.*, vol. 41, no. 3, pp. 619–23, 2000.

[54] W. M. Grant, "Clinical measurements of aqueous outflow," *A.M.A. Arch. Ophthalmol.*, vol. 46, no. 2, pp. 113–31, 1951.

[55] J. Alvarado, C. Murphy, R. Juster, "Trabecular meshwork cellularity in primary open-angle glaucoma and nonglaucomatous normals," *Ophthalmology*, vol. 91, no. 6, pp. 564–79, 1984.

[56] E. Liitjen-Drecoll, C. A. May, J. R. Polansky, D. H. Johnson, H. Bloemendal, and T. D. Nguyen, "Localization of the stress proteins alpha B-Crystallin and trabecular meshwork inducible glucocorticoid response protein in normal and glaucomatous trabecular meshwork," *Invest. Ophthalmol. Vis. Sci.*, vol. 39, no. 3, pp. 517–25, 1998.

[57] R. Fernández-Durango, A. Fernández-Martínez, J. García-Feijoo, A. Castillo, J. M. de la Casa, B. García-Bueno, B. G. Pérez-Nievas, A. Fernández-Cruz, and J. C. Leza, "Expression of nitrotyrosine and oxidative consequences in the trabecular meshwork of patients with primary open-angle glaucoma," *Invest. Ophthalmol. Vis. Sci.*, vol. 49, no. 6, pp. 2506–11, 2008.

[58] J. Baleriola, J. García-Feijoo, J. M. Martínez-de-la-Casa, A. Fernández-Cruz, J. Enrique, D. Rosa, and R. Fernández-Durango, "Apoptosis in the trabecular meshwork of glaucomatous patients," *Mol. Vis.*, vol. 14, pp. 1513–16, 2008.

[59] A. Izzotti, S. C. Saccà, M. Longobardi, and C. Cartiglia, "Mitochondrial damage in the trabecular meshwork of patients with glaucoma," *Arch. Ophthalmol.*, vol. 128, no. 6, pp. 724–30, 2010.

[60] P. B. Liton, C. Luna, P. Challa, D. L. Epstein, and P. Gonzalez, "Genome-wide expression profile of human trabecular meshwork cultured cells, nonglaucomatous and primary open angle glaucoma tissue," *Mol. Vis.*, vol. 12, pp. 774–790, 2006.

[61] J. W. Rohen, E. Lütjen-Drecoll, C. Flügel, M. Meyer, and I. Grierson, "Ultrastructure of the trabecular meshwork in untreated cases of primary open-angle glaucoma (POAG)," *Exp. Cell Res.*, vol. 56, no. 6, pp. 683–92, 1993.

[62] M. A. Babizhayev and M. W. Brodskaya, "Fibronectin detection in drainage outflow system of human eyes in ageing and progression of open-angle glaucoma," *Mech. Ageing Dev.*, vol. 47, no. 2, pp. 145–57, 1989.

[63] E. Liitjen-Drecoll, R. Futa, and J. W. Rohen, "Ultrahistochemical studies on tangential sections of the trabecular meshwork in normal and glaucomatous eyes," *Invest. Ophthalmol. Vis. Sci.*, vol. 21, no. 4, pp. 563–73, 1981.

[64] P. A. Knepper, W. Goossens, M. Hvizd, and P. F. Palmbergf, "Glycosaminoglycans of the human trabecular meshwork in primary open-angle glaucoma," *Invest. Ophthalmol. Vis. Sci.*, vol. 37, no. 7, pp. 1360-7, 1996.

[65] P. A. Knepper, W. Goossens, and P. F. Palmberg, "Glycosaminoglycan stratification of the juxtacanalicular tissue in normal and primary open-angle glaucoma," *Invest. Ophthalmol. Vis. Sci.*, vol. 37, no. 12, pp. 2414–25, 1996.

[66] J. Gottanka, D. H. Johnson, P. Martus, and E. Lütjen-Drecoll, "Severity of optic nerve damage in eyes with POAG is correlated with changes in the trabecular meshwork," *J. Glaucoma*, vol. 6, no. 2, pp. 123–32, 1997.

[67] J. A. Last, T. Pan, Y. Ding, C. M. Reilly, K. Keller, T. S. Acott, M. P. Fautsch, C. J. Murphy, and P. Russell, "Elastic modulus determination of normal and glaucomatous human trabecular meshwork," *Invest. Ophthalmol. Vis. Sci.*, vol. 52, no. 5, pp. 2147–52, 2011.

[68] W. Xue, R. Wallin, E. A. Olmsted-Davis, and T. Borrás, "Matrix GLA protein function in human trabecular meshwork cells: inhibition of BMP2-induced calcification process," *Invest. Ophthalmol. Vis. Sci.*, vol. 47, no. 3, pp. 997–1007, 2006.

[69] A. F. Clark, S. T. Miggans, K. Wilson, S. Browder, and M. D. McCartney, "Cytoskeletal changes in cultured human glaucoma trabecular meshwork cells," *J. Glaucoma*, vol. 4, no. 3, pp. 183–8, 1995.

[70] H. A. Quigley and E. M. Addicks, "Regional differences in the structure of the lamina cribrosa and their relation to glaucomatous optic nerve damage," *Arch. Ophthalmol.*, vol. 99, no. 1, pp. 137–43, 1981.

[71] R. L. Radius and D. R. Anderson, "Rapid axonal transport in primate optic nerve distribution of pressure-induced interruption," *Arch. Ophthalmol.*, vol. 99, no. 4, pp. 650–4, 1981.

[72] D. R. Buus and D. R. Anderson, "Peripapillary crescents and halos in normal-tension glaucoma and ocular hypertension," *Ophthalmology*, vol. 96, no. 1, pp. 16–9, 1989.

[73] N. Sossi and D. R. Anderson, "Blockage of axonal transport in optic nerve induced by elevation of intraocular pressure effect of arterial hypertension induced by angiotensin I," *Arch. Ophthalmol.*, vol. 101, no. 1, pp. 94–7, 1983.

[74] E. M. Stone, J. H. Fingert, W. L. Alward, T. D. Nguyen, J. R. Polansky, S. L. Sunden, D. Nishimura, A. F. Clark, A. Nystuen, B. E. Nichols, D. A. Mackey, R. Ritch, J. W. Kalenak, E. R. Craven, and V. C. Sheffield, "Identification of a gene that causes primary open angle glaucoma," *Science*, vol. 275, no. 5300, pp. 668–70, 1997.

[75] J. R. Polansky, D. J. Fauss, P. Chen, H. Chen, E. Lütjen-Drecoll, D. Johnson, R. M. Kurtz, Z. D. Ma, E. Bloom, and T. D. Nguyen, "Cellular pharmacology and molecular biology of the trabecular meshwork inducible glucocorticoid response gene product," *Ophthalmologica*, vol. 211, no. 3, pp. 126–39, 1997.

[76] W. L. Alward, J. H. Fingert, M. A. Coote, A. T. Johnson, S. F. Lerner, D. Junqua, F. J. Durcan, P. J. McCartney, D. A. Mackey, V. C. Sheffield, and E. M. Stone, "Clinical features associated with mutations in the chromosome 1 open-angle glaucoma gene (GLC1A)," *N. Engl. J. Med.*, vol. 338, no. 15, pp. 1022–7, 1998.

[77] H. Sakai, X. Shen, T. Koga, B. C. Park, Y. Noskina, M. Tibudan, and B. Y. Yue, "Mitochondrial association of myocilin, product of a glaucoma gene, in human trabecular meshwork cells," *J. Cell Physiol.*, vol. 213, no. 3, pp. 775–84, 2007.

[78] M. Mertts, S. Garfield, K. Tanemoto, and S. I. Tomarev, "Identification of the region in the N-terminal domain responsible for the cytoplasmic localization of Myoc/Tigr and its association with microtubules," *Lab Invest.*, vol. 79, no. 10, pp. 1237–45, 1999.

[79] M. P. Fautsch, A. M. Vrabel, and D. H. Johnson, "The identification of myocilin-associated proteins in the human trabecular meshwork," *Exp. Eye Res.*, vol. 82, no. 6, pp. 1046–52, 2006.

[80] K. M. Hardy, E. A. Hoffman, P. Gonzalez, B. S. McKay, and W. D. Stamer, "Extracellular trafficking of myocilin in human trabecular meshwork cells," *J. Biol. Chem.*, vol. 280, no. 32, pp. 28917–26, 2005.

[81] J. Ueda, K. Wentz-Hunter, and B. Y. Yue, "Distribution of myocilin and extracellular matrix components in the juxtacanalicular tissue of human eyes," *Invest. Ophthalmol. Vis. Sci.*, vol. 43, no. 4, pp. 1068–76, 2002.

[82] J. Ueda and B. Y. Yue, "Distribution of myocilin and extracellular matrix components in the corneoscleral meshwork of human eyes," *Invest. Ophthalmol. Vis. Sci.*, vol. 44, no. 11, pp. 4772–9, 2003.

[83] X. Shen, T. Koga, B. C. Park, N. SundarRaj, and B. Y. Yue, "Rho GTPase and cAMP/protein kinase A signaling mediates myocilin-induced alterations in cultured human trabecular meshwork cells," *J. Biol. Chem.*, vol. 283, no. 1, pp. 603–12, 2008.

[84] M. P. Fautsch, C. K. Bahler, A. M. Vrabel, K. G. Howell, N. Loewen, W. L. Teo, E. M. Poeschla, and D. H. Johnson, "Perfusion of his-tagged eukaryotic myocilin increases outflow resistance in human anterior segments in the presence of aqueous humor," *Invest. Ophthalmol. Vis. Sci.*, vol. 47, no. 1, pp. 213–21, 2006.

[85] M. Caballero, L. L. Rowlette, and T. Borrás, "Altered secretion of a TIGR/MYOC mutant lacking the olfactomedin domain," *Biochim. Biophys. Acta.*, vol. 1502, no. 3, pp. 447–60, 2000.

[86] D. B. Gould, L. Miceli-Libby, O. V. Savinova, M. Torrado, S. I. Tomarev, R. S. Smith, and S. W. John, "Genetically increasing Myoc expression supports a necessary

pathologic role of abnormal proteins in glaucoma," *Mol. Cell Biol.*, vol. 24, no. 20, pp. 9019–25, 2004.

[87] M. Zillig, A. Wurm, F. J. Grehn, P. Russell, and E. R. Tamm, "Overexpression and properties of wild-type and Tyr437His mutated myocilin in the eyes of transgenic mice," *Invest. Ophthalmol. Vis. Sci.*, vol. 46, no. 1, pp. 223–34, 2005.

[88] M. Caballero and T. Borrás, "Inefficient processing of an olfactomedin-deficient myocilin mutant: potential physiological relevance to glaucoma," *Biochem. Biophys. Res. Commun.*, vol. 282, no. 3, pp. 662–70, 2001.

[89] S. Gobeil, M. A. Rodrigue, S. Moisan, T. D. Nguyen, J. R. Polansky, J. Morissette, and V. Raymond, "Intracellular sequestration of hetero-oligomers formed by wild-type and glaucoma-causing myocilin mutants," *Invest. Ophthalmol. Vis. Sci.*, vol. 45, no. 10, pp. 3506–7, 2004.

[90] V. Senatorov, I. Malyukova, R. Fariss, E. F. Wawrousek, S. Swaminathan, S. K. Sharan, and S. Tomarev, "Expression of mutated mouse myocilin induces open-angle glaucoma in transgenic mice," *J. Neurosci.*, vol. 26, no. 46, pp. 11903–14, 2006.

[91] Y. Zhou, O. Grinchuk, and S. I. Tomarev, "Transgenic mice expressing the Tyr437His mutant of human myocilin protein develop glaucoma," *Invest. Ophthalmol. Vis. Sci.*, vol. 49, no. 5, pp. 1932–9, 2008.

[92] G. Zhu, C. J. Wu, Y. Zhao, and J. D. Ashwell, "Optineurin negatively regulates TNFalpha- induced NF-kappaB activation by competing with NEMO for ubiquitinated RIP," *Curr. Biol.*, vol. 17, no. 16, pp. 1438–43, 2007.

[93] S. Morton, L. Hesson, M. Peggie, and P. Cohen, "Enhanced binding of TBK1 by an optineurin mutant that causes a familial form of primary open angle glaucoma," *FEBS Lett.*, vol. 582, no. 6, pp. 997–1002, 2008.

[94] N. De Marco, M. Buono, F. Troise, and G. Diez-Roux, "Optineurin increases cell survival and translocates to the nucleus in a Rab8-dependent manner upon an apoptotic stimulus," *J. Biol. Chem.*, vol. 281, no. 23, pp. 16147–56, 2006.

[95] J. M. Skarie and B. A. Link, "The primary open-angle glaucoma gene WDR36 functions in ribosomal RNA processing and interacts with the p53 stress-response pathway," *Hum. Mol. Genet.*, vol. 17, no. 16, pp. 2474–85, 2008.

[96] M. A. Hauser, R. R. Allingham, K. Linkroum, J. Wang, K. LaRocque-Abramson, D. Figueiredo, C. Santiago-Turla, E. del Bono, J. L. Haines, M. A. Pericak-Vance, and J. L. Wiggs, "Distribution of WDR36 DNA sequence variants in patients with primary open-angle glaucoma," *Invest. Ophthalmol. Vis. Sci.*, vol. 47, no. 6, pp. 2542–6, 2006.

[97] Y. Liu, S. Schmidt, X. Qin, J. Gibson, D. Munro, J. L. Wiggs, M. A. Hauser, and R. R. Allingham, "No association between OPA1 polymorphisms and primary open-angle glaucoma in three different populations," *Mol. Vis.*, vol. 13, pp. 2137–41, 2007.

[98] H. J. Lin, W. C. Chen, F. J. Tsai, and S. W. Tsai, "Distributions of p53 codon 72 polymorphism in primary open angle glaucoma," *Br. J. Ophthalmol.*, vol. 86, no. 7, pp. 767–70, 2002.

[99] H. J. Lin, F. J. Tsai, W. C. Chen, Y. R. Shi, Y. Hsu, and S. W. Tsai, "Association of tumour necrosis factor alpha-308 gene polymorphism with primary open-angle glaucoma in Chinese," *Eye*, vol. 17, no. 1, pp. 31–4, 2003.

[100] A. Bhattacharjee, D. Banerjee, S. Mookherjee, M. Acharya, A. Banerjee, A. Ray, A. Sen, and K. Ray, "Variation consortium, Leu432Val polymorphism in CYP1B1 as a susceptible factor towards predisposition to primary open-angle glaucoma," *Mol. Vis.*, vol. 14, pp. 841–50, 2008.

[101] R. Melki, E. Colomb, N. Lefort, A. P. Brezin, and H. J. Garchon, "CYP1B1 mutations in French patients with early-onset primary open-angle glaucoma," *J. Med. Genet.*, vol. 41, no. 9, pp. 647–51, 2004.

[102] E. Banin, A. Obolensky, M. Idelson, I. Hemo, E. Reinhardtz, E. Pikarsky, T. Ben-Hur, and B. Reubinoff, "Retinal incorporation and differentiation of neural precursors derived from human embryonic stem cells," *Stem Cells*, vol. 24, no. 2, pp. 246–57, 2006.

[103] J. S. Meyer, M. L. Katz, J. A. Maruniak, and M. D. Kirk, "Embryonic stem cell-derived neural progenitors incorporate into degenerating retina and enhance survival of host photoreceptors," *Stem Cells*, vol. 24, no. 2, pp. 274–83, 2006.

[104] M. J. Young, J. Ray, S. J. Whiteley, H. Klassen, and F. H. Gage, "Neuronal differentiation and morphological integration of hippocampal progenitor cells transplanted to the retina of immature and mature dystrophic rats," *Mol. Cell Neurosci.*, vol. 16, no. 3, pp. 197–205, 2000.

[105] Y. Inoue, A. Iriyama, S. Ueno, H. Takahashi, M. Kondo, Y. Tamaki, M. Araie, and Y. Yanagi, "Subretinal transplantation of bone marrow mesenchymal stem cells delays retinal degeneration in the RCS rat model of retinal degeneration," *Exp. Eye Res.*, vol. 85, no. 2, pp. 234–41, 2007.

[106] Y. Kurimoto, H. Shibuki, Y. Kaneko, M. Ichikawa, T. Kurokawa, M. Takahashi, and N. Yoshimura, "Transplantation of adult rat hippocampus-derived neural stem cells into retina injured by transient ischemia," *Neurosci. Lett.*, vol. 306, no. 1–2, pp. 57–60, 2001.

[107] M. Takahashi, T. D. Palmer, J. Takahashi, and F. H. Gage, "Widespread integration and survival of adult-derived neural progenitor cells in the developing optic retina," *Mol. Cell Neurosci.*, vol. 12, pp. 340–8, 1998.

[108] N. D. Bull, G. A. Limb, and K. R. Martin, "Human Müller stem cell (MIO-M1) transplantation in a rat model of glaucoma: survival, differentiation, and integration.," *Invest. Ophthalmol. Vis. Sci.*, vol. 49, no. 8, pp. 3449–56, 2008.

[109] M. L. Ko, D. N. Hu, R. Ritch, S. C. Sharma, and C. F. Chen, "Patterns of retinal ganglion cell survival after brain-derived neurotrophic factor administration in hypertensive eyes of rats," *Neurosci. Lett.*, vol. 305, no. 2, pp. 139–42, 2001.

[110] Q. L. Fu, X. Li, H. K. Yip, Z. Shao, W. Wu, S. Mi, and K. F. So, "Combined effect of brain-derived neurotrophic factor and LINGO-1 fusion protein on long-term survival of retinal ganglion cells in chronic glaucoma," *Neuroscience*, vol. 162, no. 2, pp. 375–82, 2009.

[111] K. R. Martin, H. A. Quigley, D. J. Zack, H. Levkovitch-Verbin, J. Kielczewski, D. Valenta, L. Baumrind, M. E. Pease, R. L. Klein, and W. W. Hauswirth, "Gene therapy with brain-derived neurotrophic factor as a protection: retinal ganglion cells in a rat glaucoma model," *Invest. Ophthalmol. Vis. Sci.*, vol. 44, no. 10, pp. 4357–65, 2003.

[112] M. E. Pease, D. J. Zack, C. Berlinicke, K. Bloom, F. Cone, Y. Wang, R. L. Klein, W. W. Hauswirth, and H. A. Quigley, "Effect of CNTF on retinal ganglion cell survival in experimental glaucoma," *Invest. Ophthalmol. Vis. Sci.*, vol. 50, no. 5, pp. 2194–200, 2009.

[113] G. Raviola, "Schwalbe line's cells: a new cell type in the trabecular meshwork of Macaca mulatta," *Invest. Ophthalmol. Vis. Sci.*, vol. 22, no. 1, pp. 45–56, 1982.

[114] S. L. McGowan, H. F. Edelhauser, R. R. Pfister, and D. R. Whikehart, "Stem cell markers in the human posterior limbus and corneal endothelium of unwounded and wounded corneas," *Mol. Vis.*, vol. 13, pp. 1984–2000, 2007.

[115] T. S. Acott, J. R. Samples, J. M. Bradley, D. R. Bacon, S. S. Bylsma, and E. M. Van Buskirk, "Trabecular repopulation by anterior trabecular meshwork cells after laser trabeculoplasty," *Am. J. Ophthalmol.*, vol. 107, no. 1, pp. 1–6, 1989.

[116] P. Gonzalez, D. L. Epstein, C. Luna, and P. B. Liton, "Characterization of free-floating spheres from human trabecular meshwork (HTM) cell culture in vitro," *Exp. Eye Res.*, vol. 82, no. 6, pp. 959–67, 2006.

[117] W. D. Stamer, R. E. Seftor, R. W. Snyder, and J. W. Regan, "Cultured human trabecular meshwork cells express aquaporin-1 water channels," *Curr. Eye Res.*, vol. 14, no. 12, pp. 1095–100, 1995.

[118] I. L. Chang, G. Elner, Y. J. Yue, A. Cornicelli, J. E. Kawa, and V. M. Elner, "Expression of modified low-density lipoprotein receptors by trabecular meshwork cells," *Curr. Eye Res.*, vol. 10, no. 12, pp. 1101–12, 1991.

[119] P. B. Liton, X. Liu, W. D. Stamer, P. Challa, D. L. Epstein, and P. Gonzalez, "Specific targeting of gene expression to a subset of human trabecular meshwork cells using the chitinase 3-like 1 promoter," *Invest. Ophthalmol. Vis. Sci.*, vol. 46, no. 1, pp. 183–90, 2005.

[120] P. Gonzalez, M. Caballero, P. B. Liton, W. D. Stamer, and D. L. Epstein, "Expression analysis of the matrix GLA protein and VE-cadherin gene promoters in the outflow pathway," *Invest. Ophthalmol. Vis. Sci.*, vol. 45, no. 5, pp. 1389–95, 2004.

[121] J. Z. Gasiorowski and P. Russell, "Biological properties of trabecular meshwork cells," *Exp. Eye Res.*, vol. 88, no. 4, pp. 671–5, 2009.

[122] J. R. Polansky, R. M. Kurtz, J. A. Alvarado, R. N. Weinreb, and M. D. Mitchell, "Eicosanoid production and glucocorticoid regulatory mechanisms in cultured human trabecular meshwork cells," *Prog. Clin. Biol. Res.*, vol. 312, pp. 113–38, 1989.

[123] J. Ortego, J. Escribano, and M. Coca-Prados, "Cloning and characterization of subtracted cDNAs from a human ciliary body library encoding TIGR, a protein involved in juvenile open angle glaucoma with homology to myosin and olfactomedin," *FEBS Lett.*, vol. 413, no. 2, pp. 349–53, 1997.

[124] Challa et al., "ARVO E-Abstract 3164," *Invest. Ophthlmol. Vis. Sci.*, vol. 44, 2003.

[125] U. Stromberg, "Ocular hypertension. Frequency, course and relation to other disorders occuring in glaucoma, as seen from mass survey of all inhabitants over forty years of age in a Swedish town," *Acta Ophthalmol. Suppl.*, vol. Suppl 69, pp. 1–75, 1962.

[126] J. W. Rohen and E. Lütjen-Drecoll, "Age changes of the trabecular meshwork in human and monkey eyes," in *Aging and Development. Eds. Bredt, H. and Rohen, J. W. F. K. Schattauer Verlag-Stuttgart, New York*, pp. 1–36, 1971.

[127] B. Becker, "The decline in aqueous secretion and outflow facility with age," *Am. J. Ophthalmol.*, vol. 46, no. 5 Part 1, pp. 731–6, 1958.

[128] J. Alvarado, C. Murphy, and R. Juster, "Trabecular meshwork cellularity in primary open-angle glaucoma and nonglaucomatous normals," *Ophthalmology*, vol. 91, no. 6, pp. 564–79, 1984.

[129] J. Alvarado, C. Murphy, J. Polansky, and R. Juster, "Age-related changes in trabecular meshwork cellularity," *Invest. Ophthalmol. Vis. Sci.*, vol. 21, no. 5, pp. 714–27, 1981.

[130] I. Grierson and R. C. Howes, "Age-related depletion of the cell population in the human trabecular meshwork," *Eye*, vol. 1, no. 2, pp. 204–10, 1987.

[131] L. M. Franks, "Cellular aspects of ageing," *Exp. Gerontol.*, vol. 5, no. 4, pp. 281–9, 1970.

[132] H. Tauchi, T. Yoshioka, and H. Kobayashi, "Age change of skeletal muscles of rats," *Gerontologia.*, vol. 17, no. 4, pp. 219–27, 1971.

[133] H. Brody, "An examination of cerebral cortex and brain stem in aging," in *Aging: Neurobiology of aging, Terry R. D. and Gershon S., Editors. Raven Press, New York*, pp. 177–82, 1976.

[134] I. Grierson and P. Hogg, "The proliferative and migratory activities of trabecular meshwork cells," *Prog. Retin. Eye Res.*, vol. 15, no. 1, pp. 33–67, 1995.

[135] I. Grierson, "What is open angle glaucoma?," *Eye*, vol. 1, no. 1, pp. 15–28, 1987.

[136] Y. Du, H. Yun, E. Yang, and J. S. Schuman, "Stem cells from trabecular meshwork home to TM tissue in vivo," *Invest. Ophthalmol. Vis. Sci.*, vol. 54, no. 2, pp. 1450–9, 2013.

[137] B. J. Tripathi, and R. C. Tripathi, "H u m a n trabecular endothelium, corneal endothelium, keratocytes, and scleral fibroblasts in primary cell culture. A comparative study of growth characteristics, morphology, and phagocytic activity by light and scanning electron microscopy," *Exp. Eye Res.*, vol. 35, no. 6, pp. 611–24, 1982.

[138] A. J. Friedenstein, U. F. Deriglasova, N. N. Kulagina, A. F. Panasuk, S. F. Rudakowa, E. A. Luriá, and I. A. Ruadkow, "Precursors for fibroblasts in different populations of hematopoietic cells as detected by the in vitro colony," *Exp. Hematol.*, vol. 2, no. 2, pp. 83–92, 1974.

[139] A. Muraglia, A. Corsi, M. Riminucci, M. Mastrogiacomo, R. Cancedda, P. Bianco, and R. Quarto, "Formation of a chondro-osseous rudiment in micromass cultures of human bone-marrow stromal cells," *J. Cell Sci.*, vol. 116, no. 14, pp. 2949–55, 2003.

[140] B. Johnstone, T. M. Hering, A. I. Caplan, V. M. Goldberg, and J. U. Yoo, "In Vitro chondrogenesis of bone marrow-derived mesenchymal progenitor cells," *Exp. Cell Res.*, vol. 272, no. 238, pp. 265–72, 1998.

[141] X. Wang and B. Seed, "A PCR primer bank for quantitative gene expression analysis," *Nucleic Acids Res.*, vol. 31, no. 24, p. 154e, 2003.

[142] O. J. Marshall, "PerlPrimer: cross-platform, graphical primer design for standard, bisulphite and real-time PCR," *Bioinformatics*, vol. 20, no. 15, pp. 2471–2, 2004.

[143] T. Koressaar and M. Remm, "Enhancements and modifications of primer design program Primer3," *Bioinformatics*, vol. 23, no. 10, pp. 1289–91, 2007.

[144] A. Untergasser, I. Cutcutache, T. Koressaar, J. Ye, B. C. Faircloth, M. Remm, and S. G. Rozen, "Primer3 - new capabilities and interfaces," *Nucleic Acids Res.*, vol. 40, no. 15, p. e115, 2012.

[145] D. W. Huang, B. T. Sherman, and R. A. Lempicki, "Bioinformatics enrichment tools: paths toward the comprehensive functional analysis of large gene lists," *Nucleic Acids Res.*, vol. 37, no. 1, pp. 1–13, 2009.

[146] D. W. Huang, B. T. Sherman, and R. A. Lempicki, "Systematic and integrative analysis of large gene lists using DAVID bioinformatics resources," *Nat. Protoc.*, vol. 4, no. 1, pp. 44–57, 2009.

[147] M. Huaiyu, A. Muruganujan, J. T. Casagrande, and D. Paul, "Large-scale gene function analysis with the PANTHER classification system," *Nat. Protoc.*, vol. 8, no. 8, pp. 1551–66, 2013.

[148] B. A. Reynolds, W. Tetzlaff, and S. Weiss, "A multipotent EGF-responsive striatal embryonic progenitor cell produces neurons and astrocytes," *J. Neurosci.*, vol. 12, no. 11, pp. 4565–74, 1992.

[149] E. A. Milward, C. G. Lundberg, B. Ge, D. Lipsitz, M. Zhao, and I. D. Duncan, "Isolation and transplantation of multipotential populations of epidermal growth factor-responsive, neural progenitor cells from the canine brain," *J. Neurosci. Res.*, vol. 50, no. 5, pp. 862–71, 1997.

[150] S. Yoshida, S. Shimmura, J. Shimazaki, N. Shinozaki, and K. Tsubota, "Serum-free spheroid culture of mouse corneal keratocytes," *Invest. Ophthalmol. Vis. Sci.*, vol. 46, no. 5, pp. 1653–8, 2005.

[151] H. Yu, D. Fang, S. M. Kumar, L. Li, T. K. Nguyen, G. Acs, M. Herlyn, and X. Xu, "Isolation of a novel population of multipotent adult stem cells from human hair follicles," *Am. J. Pathol.*, vol. 168, no. 6, pp. 1879–88, 2006.

[152] B. Junglas, A. H. Yu, U. Welge-Lüssen, E. R. Tamm, and R. Fuchshofer, "Connective tissue growth factor induces extracellular matrix deposition in human trabecular meshwork cells," *Exp. Eye Res.*, vol. 88, no. 6, pp. 1065–75, 2009.

[153] M. D. McCartney, D. Cantu-Crouch, and A. F. Clark, "Freeze-fracture examination of cultured human trabecular meshwork cells: effect of dexamethasone," *Exp. Eye Res.*, vol. 82, no. 6, pp. 994–1001, 2006.

[154] D. S. Yoon, Y. H. Kim, H. S. Jung, S. Paik, and J. W. Lee, "Importance of Sox2 in maintenance of cell proliferation and multipotency of mesenchymal stem cells in low-density culture," *Cell Prolif.*, vol. 44, no. 5, pp. 428–40, 2011.

[155] M. Dominici, K. Le Blanc, I. Mueller, I. Slaper-Cortenbach, F. Marini, D. Krause, R. Deans, A. Keating, Dj. Prockop, and E. Horwitz, "Minimal criteria for defining multipotent mesenchymal stromal cells. The International Society for Cellular Therapy position statement," *Cytotherapy*, vol. 8, no. 4, pp. 315–7, 2006.

[156] E. J. Caterson, L. J. Nesti, K. G. Danielson, and R. S. Tuan, "Human marrow-derived mesenchymal progenitor cells: isolation, culture expansion, and analysis of differentiation," *Mol. Biotechnol.*, vol. 20, no. 3, pp. 245–56, 2002.

[157] M. Owen, and A. J. Friedenstein, "Stromal stem cells: marrow-derived osteogenic precursors," *Ciba Found. Symp.*, vol. 136, pp. 42–60, 1988.

[158] D. T. Harris, M. Badowski, N. Ahmad, and M. A. Gaballa, "The potential of cord blood stem cells for use in regenerative medicine," *Expert Opin. Biol. Ther.*, vol. 7, no. 9, pp. 1311–22, 2007.

[159] M. J. Haller, H. L. Viener, C. Wasserfall, T. Brusko, M. A. Atkinson, and D. A. Schatz, "Autologous umbilical cord blood infusion for type 1 diabetes," *Exp. Hematol.*, vol. 36, no. 6, pp. 710–5, 2008.

[160] D. Lu, P. R. Sanberg, A. Mahmood, Y. Li, L. Wang, J. Sanchez-Ramos, and M. Chopp, "Intravenous administration of human umbilical cord blood reduces neurological deficit in the rat after traumatic brain injury," *Cell Transplant.*, vol. 11, no. 3, pp. 275–81, 2002.

[161] C. Meier, J. Middelanis, B. Wasielewski, S. Neuhoff, A. Roth-Haerer, M. Gantert, H. R. Dinse, R. Dermietzel, and A. Jensen, "Spastic paresis after perinatal brain damage in rats is reduced by human cord blood mononuclear cells," *Pediatr. Res.*, vol. 59, no. 2, pp. 244–9, 2006.

[162] R. C. Tripathi, "Proceedings: Comparative aspects of the outflow of aqueous humour," *Exp. Eye Res.*, vol. 20, no. 2, pp. 173–4, 1975.

[163] R. C. Tripathi, "The functional morphology of the outflow systems of ocular and cerebrospinal fluids," *Exp. Eye Res.*, vol. 25, no. Suppl, pp. 65–116, 1977.

[164] C. Y. Tay, P. Sathiyanathan, S. W. L. Chu, L. W. Stanton, and T. T. Wong, "Identification and characterization of mesenchymal stem cells derived from the trabecular meshwork of the human eye," *Stem Cells Dev.*, vol. 21, no. 9, pp. 1381–90, 2012.

[165] Y. Du, D. S. Roh, M. M. Mann, M. L. Funderburgh, J. L. Funderburgh, and J. S. Schuman, "Multipotent stem cells from trabecular meshwork become phagocytic TM cells," *Invest. Ophthalmol. Vis. Sci.*, vol. 53, no. 3, pp. 1566–75, 2012.

[166] S. Nadri, S. Yazdani, E. Arefian, Z. Gohari, M. B. Eslaminejad, B. Kazemi, and M. Soleimani, "Mesenchymal stem cells from trabecular meshwork become photoreceptor-like cells on amniotic membrane," *Neurosci. Lett.*, vol. 541, pp. 43–8, 2013.

[167] D. A. Rider, C. Dombrowski, A. A. Sawyer, G. H. Ng, D. Leong, D. Hutmacher, V. Nurcombe, and S. M. Cool, "Autocrine fibroblast growth factor 2 increases the multipotency of human adipose-derived mesenchymal stem cells," *Stem Cells*, vol. 26, pp. 1598–608, 2008.

[168] A. J. Friedenstein, J. F. Gorskaja, and N. N. Kulagina, "Fibroblast precursors in normal and irradiated mouse hematopoietic organs," *Exp. Hematol.*, vol. 4, no. 5, pp. 267–74, 1976.

[169] A. Alhadlaq and J. J. Mao, "Mesenchymal stem cells: isolation and therapeutics," *Stem Cells Dev.*, vol. 13, no. 4, pp. 436–48, 2004.

[170] K. LeBlanc and M. F. Pittenger, "Mesenchymal stem cells: progress toward promise," *Cytotherapy*, vol. 7, no. 1, pp. 36–45, 2005.

[171] M. J. Hoogduijn, M. J. Crop, A. M. Peeters, G. J. Van Osch, A. H. Balk, J. N. Ijzermans, W. Weimar, and C. C. Baan, "Human heart, spleen, and perirenal fat-derived mesenchymal stem cells have immunomodulatory capacities," *Stem Cells Dev.*, vol. 16, no. 4, pp. 597–604, 2007.

[172] C. S. Sondergaard, C. J. Hodonsky, L. Khait, J. Shaw, B. Sarkar, R. Birla, E. Bove, J. Nolta, and M. S. Si, "Human thymus mesenchymal stromal cells augment force production in self-organized cardiac tissue," *Ann. Thorac. Surg.*, vol. 90, no. 3, pp. 796–803, 2010.

[173] W. E. Fibbe, A. J. Nauta, and H. Roelofs, "Modulation of immune responses by mesenchymal stem cells," *Ann. N. Y. Acad. Sci.*, vol. 1106, pp. 272–78, 2007.

[174] Z. Selmani, A. Naji, I. Zidi, B. Favier, E. Gaiffe, L. Obert, C. Borg, P. Saas, P. Tiberghien, N. Rouas-Freiss, and E. D. Carosella, "Human leukocyte antigen-G5 secretion by human mesenchymal stem cells is required to suppress T lymphocyte and natural killer function and to induce CD4+ CD25 high FOXP3+ regulatory T cells," *Stem Cells*, vol. 26, no. 1, pp. 212–22, 2008.

[175] M. B. Oliveira, J. P. Vasconcellos, V. P. Costa, and M. B. Melo, "Inflammatory cytokines in aqueous humor and plasma are associated with primary open angle glaucoma in a Brazilian population," *Invest. Ophthalmol. Vis. Sci.*, Meetings, p. 5711, 2014.

[176] J. Gao, J. E. Dennis, R. F. Muzic, M. Lundberg, and A. I. Caplan, "The dynamic in vivo distribution of bone marrow-derived mesenchymal stem cells after infusion," *Cells Tissues Organs*, vol. 169, no. 1, pp. 12–20, 2001.

[177] M. B. Herrera, B. Bussolati, S. Bruno, V. Fonsato, V. F. Romanazzi, and G. Camussi, "Mesenchymal stem cells contribute to the renal repair of acute tubular epithelial injury," *Int. J. Mol. Med.*, vol. 14, no. 6, pp. 1035–41, 2004.

[178] G. J. Block, S. Ohkouchi, F. Fung, J. Frenkel, C. Gregory, R. Pochampally, G. DiMattia, D. E. Sullivan, and D. J. Prockop, "Multipotent stromal cells are activated to reduce apoptosis in part by upregulation and secretion of stanniocalcin-1," *Stem Cells*, vol. 27, no. 3, pp. 670–81, 2009.

[179] L. Chen, E. E. Tredget, P. Y. Wu, and Y. Wu, "Paracrine factors of mesenchymal stem cells recruit macrophages and endothelial lineage cells and enhance wound healing," *PLoS One*, vol. 3, no. 4, p. e1886, 2008.

[180] S. Wang, X. Qu, and R. C. Zhao, "Clinical applications of mesenchymal stem cells," *J. Hematol. Oncol.*, vol. 5, p. 19, 2012.

[181] R. Manuguerra-Gagné, P. R. Boulos, A. Ammar, F. A. Leblond, G. Krosl, V. Pichette, M. R. Lesk, and D. C. Roy, "Transplantation of mesenchymal stem cells promotes tissue regeneration in a glaucoma model through laser-induced paracrine factor secretion and progenitor cell recruitment," *Stem Cells*, vol. 31, no. 6, pp. 1136–48, 2013.

[182] D. W. Abu-Hassan, X. Li, E. I. Ryan, T. S. Acott, and M. J. Kelley, "Induced pluripotent stem cells restore function in a human cell loss model of open-angle glaucoma," *Stem Cells*, vol. 33, no. 3, pp. 751–61, 2015.

[183] W. Y. Yu, C. Sheridan, I. Grierson, S. Mason, V. Kearns, A. C. Lo, and D. Wong, "Progenitors for the corneal endothelium and trabecular meshwork: A potential source for personalized stem cell therapy in corneal endothelial diseases and glaucoma," *J. Biomed. Biotechnol.*, vol. 2011, p. 412743, 2011.

[184] B. Schimmelpfennig, "Direct and indirect determination of nonuniform cell density distribution in human corneal endothelium," *Invest. Ophthalmol. Vis. Sci.*, vol. 25, no. 2, pp. 223–29, 1984.

[185] J. Amann, G. P. Holley, S. B. Lee, and H. F. Edelhauser, "Increased endothelial cell density in the paracentral and peripheral regions of the human cornea," *Am. J. Ophthalmol.*, vol. 135, no. 5, pp. 584–90, 2003.

[186] J. Schwartzkopff, L. Bredow, S. Mahlenbrey, D. Boehringer, and T. Reinhard, "Regeneration of corneal endothelium following complete endothelial cell loss in rat keratoplasty," *Mol. Vis.*, vol. 16, pp. 2368–75, 2010.

[187] W. Y. Yu, I. Grierson, C. Sheridan, A. C. Lo, and D. S. Wong, "Bovine posterior limbus: An evaluation of an alternative source for corneal endothelial and trabecular meshwork stem/ progenitor cells," *Stem Cells Dev.*, vol. 24, no. 5, pp. 624–39, 2015.

[188] Y. Liu, D. Munro, D. Layfield, A. Dellinger, J. Walter, K. Peterson, C. B. Rickman, R. R. Allingham, and M. A. Hauser, "Serial analysis of gene expression (SAGE) in normal human trabecular meshwork," *Mol. Vis.*, vol. 17, pp. 885–93, 2011.

[189] M. P. Fautsch and D. H. Johnson, "Characterization of myocilin-myocilin interactions," *Invest. Ophthalmol. Vis. Sci.*, vol. 42, no. 10, pp. 2324–31, 2001.

[190] A. Karali, P. Russell, F. H. Stefani, and E. R. Tamm, "Localization of myocilin/trabecular meshwork--inducible glucocorticoid response protein in the human eye," *Invest. Ophthalmol. Vis. Sci.*, vol. 41, no. 3, pp. 729–40, 2000.

[191] P. V. Rao, R. R. Allingham, and D. L. Epstein, "TIGR/myocilin in human aqueous humor," *Exp. Eye Res.*, vol. 71, no. 6, pp. 637–41, 2000.

[192] P. Russell, E. R. Tamm, F. J. Grehn, G. Picht, and M. Johnson, "The presence and properties of myocilin in the aqueous humor," *Invest. Ophthalmol. Vis. Sci.*, vol. 42, no. 5, pp. 983–6, 2001.

[193] D. Niki, K. Katsu, and Y. Yokouchi, "Ontogeny of angiopoietin-like protein 1, 2, 3, 4, 5, and 7 genes during chick embryonic development," *Dev. Growth Differ.*, vol. 51, no. 9, pp. 821–32, 2009.

[194] P. Gonzalez, D. L. Epstein, and T. Borrás, "Characterization of gene expression in human trabecular meshwork using single-pass sequencing of 1060 clones," *Invest. Ophthalmol. Vis. Sci.*, vol. 41, no. 12, pp. 3678–93, 2000.

[195] P. Gonzalez, J. S. J. Zigler, D. L. Epstein, and T. Borrás, "Identification and isolation of differentially expressed genes from very small tissue samples," *Biotechniques*, vol. 26, no. 5, pp. 884–6, 888–92, 1999.

[196] R. J. Wordinger, W. Lambert, R. Agarwal, M. Talati, and A. F. Clark, "Human trabecular meshwork cells secrete neurotrophins and express neurotrophin receptors (Trk)," *Invest. Ophthalmol. Vis. Sci.*, vol. 41, no. 12, pp. 3833–41, 2000.

[197] A. Nowak, J. P. Szaflik, M. Gacek, K. Przybylowska-Sygut, A. Kamińska, J. Szaflik, and I. Majsterek, "BDNF and HSP gene polymorphisms and their influence on the progression of primary open-angle glaucoma in a Polish population," *Arch. Med. Sci.*, vol. 10, no. 6, pp. 1206–13, 2014.

[198] Q. J. Ding, W. Zhu, A. C. Cook, K. R. Anfinson, B. A. Tucker, and H. Markus, "Induction of trabecular meshwork cells from induced pluripotent stem cells," *Invest. Ophthalmol. Vis. Sci.*, vol. 55, no. 11, pp. 7065–72, 2014.

[199] C. R. Hann, M. J. Springett, X. Wang, and D. H. Johnson, "Ultrastructural localization of collagen IV, fibronectin, and laminin in the trabecular meshwork of normal and glaucomatous eyes," *Ophthalmic Res.*, vol. 33, no. 6, pp. 314–24, 2001.

[200] E. Lütjen-Drecoll and J. W. Rohen, "Functional morphology of the trabecular meshwork," *JB Lippencott Co., Philadelphia, PA*, 2001.

[201] S. Kleff, E. D. Andrulis, C. W. Anderson, and R. Sternglanz, "Identification of a gene encoding a yeast histone H4 acetyltransferase," *J. Biol. Chem.*, vol. 270, no. 42, pp. 24674–7, 1995.

[202] S. Barua and K. Rege, "The influence of mediators of intracellular trafficking on transgene expression efficacy of polymer-plasmid DNA complexes," *Biomaterials*, vol. 31, no. 22, pp. 5894–902, 2010.

[203] H. F. Duncan, A. J. Smith, G. J. Fleming, and P. R. Cooper, "HDACi: cellular effects, opportunities for restorative dentistry," *J. Dent. Res.*, vol. 90, no. 12, pp. 1377–88, 2011.

[204] X. J. Yang and E. Seto, "HATs and HDACs: from structure, function and regulation to novel strategies for therapy and prevention," *Oncogene*, vol. 26, no. 37, pp. 5310–8, 2007.

[205] J. E. Bolden, M. J. Peart, and R. W. Johnstone, "Anticancer activities of histone deacetylase inhibitors," *Nat. Rev. Drug Discov.*, vol. 5, no. 9, pp. 769–84, 2006.

[206] S. Balasubramanian, E. Verner, and J. J. Buggy, "Isoform-specific histone deacetylase inhibitors: the next step?," *Cancer Lett.*, vol. 280, no. 2, pp. 211–21, 2009.

[207] M. Hosseinkhani, K. Hasegawa, K. Ono, T. Kawamura, T. Takaya, T. Morimoto, H. Wada, A. Shimatsu, S. G. Prat, H. Suemori, N. Nakatsuji, and T. Kita, "Trichostatin A induces myocardial differentiation of monkey ES cells," *Biochem. Biophys. Res. Commun.*, vol. 356, no. 2, pp. 386–91, 2007.

[208] S. Snykers, T. Vanhaecke, A. De Becker, P. Papeleu, M. Vinken, I. Van Riet, and V. Rogiers, "Chromatin remodeling agent trichostatin A: a key-factor in the hepatic differentiation of human mesenchymal stem cells derived of adult bone marrow," *BMC Dev. Biol.*, vol. 7, p. 24, 2007.

[209] H. F. Duncan, A. J. Smith, G. J. Fleming, and P. R. Cooper, "Histone deacetylase inhibitors induced differentiation and accelerated mineralization of pulp-derived cells," *J. Endod.*, vol. 38, no. 3, pp. 339–45, 2012.

[210] M. Marin-Husstege, M. Muggironi, A. Liu, and P. Casaccia-Bonnefil, "Histone deacetylase activity is necessary for oligodendrocyte lineage progression," *J. Neurosci.*, vol. 22, no. 23, pp. 10333–45, 2002.

[211] E. S. Ng, R. P. Davis, L. Azzola, E. G. Stanley, and A. G. Elefanty, "Forced aggregation of defined numbers of human embryonic stem cells into embryoid bodies fosters robust, reproducible hematopoietic differentiation," *Blood*, vol. 106, no. 5, pp. 1601–3, 2005.

[212] P. W. Burridge, D. Anderson, H. Priddle, M. D. Barbadillo Muñoz, S. Chamberlain, C. Allegrucci, L. E. Young, and C. Denning, "Improved human embryonic stem cell embryoid body homogeneity and cardiomyocyte differentiation from a novel V-96 plate aggregation system highlights interline variability," *Stem Cells*, vol. 25, no. 4, pp. 929–38, 2007.

[213] K. Matsumoto, H. Mizumoto, K. Nakazawa, H. Ijima, K. Funatsu, and T. Kajiwara, "Hepatic differentiation of mouse embryonic stem cells in a bioreactor using polyurethane/spheroid culture," *Transplant. Proc.*, vol. 40, no. 2, pp. 614–6, 2008.

[214] G. D'Ippolito, P. C. Schiller, C. Ricordi, B. A. Roos, and G. A. Howard, "Age-related osteogenic potential of mesenchymal stromal stem cells from human vertebral bone marrow," *J. Bone Miner. Res.*, vol. 14, no. 7, pp. 1115–22, 1999.

[215] J. M. Zahn, R. Sonu, H. Vogel, E. Crane, K. Mazan-Mamczarz, R. Rabkin, R. W. Davis, K. G. Becker, A. B. Owen, and S. K. Kim, "Transcriptional profiling of aging in human muscle reveals a common aging signature," *PLoS Genet.*, vol. 2, no. 7, pp. 1058–69, 2006.

[216] P. Hogg, M. Calthorpe, M. Batterbury, and I. Grierson, "Aqueous humor stimulates the migration of human trabecular meshwork cells in vitro," *Invest. Ophthalmol. Vis. Sci.*, vol. 41, no. 5, pp. 1091–8, 2000.

[217] J. Xie, J. D. Mendez, V. Mendez-Valenzuela, and M. M. Aguilar-Hernandez, "Cellular signalling of the receptor for advanced glycation end products (RAGE)," *Cell Signal*, vol. 25, no. 11, pp. 2185–97, 2013.

[218] G. Maubach, M. C. Lim, J. Chen, H. Yang, and L. Zhuo, "miRNA studies in in vitro and in vivo activated hepatic stellate cells," *World J. Gastroenterol.*, vol. 17, no. 22, pp. 2748–73, 2011.

[219] W. Li, L. B. Kong, J. T. Li, Z. Y. Guo, Q. Xue, T. Yang, Y. L. Meng, B. Q. Jin, W. H. Wen, and A. G. Yang, "MiR-568 inhibits the activation and function of $CD4^+$ T cells and Treg cells by targeting NFAT5," *Int. Immunol.*, vol. 26, no. 5, pp. 269–81, 2014.

8. Appendix

Supplementary Table 1

List of Antibodies used in the study

Antibody	Protein	Company (Catalogue No)	Dilution used
Primary	AQP1	Santa Cruz (sc-32737)	1:100
Primary	ANK3	Santa Cruz (sc-12719)	1:250
Primary	BDNF	Abcam (ab104769)	1:250
Primary	CD73	Abcam (ab81720)	1:50
Primary	CD90	BD Pharmingen (555593)	1:100
Primary	CD105	R&D Systems (AF1097)	1:25
Primary	CD146	Miltenyi-Biotec (130-092-850)	1:100
Primary	CDH23	Abcam (ab131135)	1:500
Primary	F5	Santa Cruz (sc-66041)	1:250
Primary	FGF9	Abcam (ab71395)	1:750
Primary	HEY1	Abcam (ab22614)	1:750
Primary	HMFG1	Thermo Scientific (#MS-512-P1)	1:100
Primary	KCNAB1	Abcam (ab156700)	1:250
Primary	SPP1	Abcam (ab8448)	1:750
Secondary	Goat anti-Mouse Alexa Fluor 594	Invitrogen (A-11005)	1:1000
Secondary	Donkey anti-Goat Alexa Fluor 488	Invitrogen (A-11055)	1:1000
Secondary	Donkey anti-Mouse Alexa Fluor 594	Invitrogen (A-11058)	1:1000

Conjugated	PE Mouse Anti-Human CD11b	BD Pharmingen (555388)	1µl/ 10^5cells
Conjugated	PE-Cy 5 Mouse Anti-Human CD34	BD Pharmingen (555823)	1µl/10^5cells
Conjugated	PE-Cy 5 Mouse Anti-Human CD45	BD Pharmingen (555484)	1µl/10^5cells
Conjugated	PE Mouse Anti-Human CD73	BD Pharmingen (550257)	1µl/10^5cells
Conjugated	APC Mouse Anti-Human CD79a	BD Pharmingen (551134)	1µl/10^5cells
Conjugated	APC Mouse Anti-Human CD90	BD Pharmingen (559869)	1µl/10^5cells
Conjugated	FITC Mouse Anti-Human CD105	Abcam (ab11415)	1µl/10^5cells
Conjugated	PerCP-Cy 5.5 Mouse Anti-Human HLA-DR	BD Pharmingen (560652)	1µl/10^5cells

Supplementary Table 2

List of primers used in the study

Gene	Forward (5' → 3')	Reverse (5'→ 3')
ACTB	CAC CAC ACC TTC TAC AAT GAG C	TCG TAG ATG GGC ACA GTG TGG G
ANK3	GAC CAT GAC CAC AAC TAC TG	CAT CTT CAC CTT CTT CAA CAT CTG
LDLR	CAT CTA CTG GAC CGA CTC TG	TAC ATG AAG CCA TGA ACA GGA
CHI3L1	GTC TCA AAC AGG CTT TGT GG	TAG ATG ATG TGG GTA CAG AGG
HMFG1	GTT TAT GCG AGG AGA TTT CCC	CTC GAC ACA TTT CGT CTC AC
MMP1	GGA CTT AGT CCA GAA ATA CCT	CTT TCA GCC CAA AGA ATT CC
AQP1	TGC CAT CGG CCT CTC TGT A	CAG GGT TAA TCC CAC AGC CA
ABCG2	TGC AAC AGG AAA CAA TCC TTG T	AGA TCGATG CCC TGC TTT ACC
KRT3	TGG AGG ACC TGG TGG AAG ACT TCA	GAG ATA GCT CAG CGT CGT AGA GGG
KRT12	TGC GAG ACT AGC TGC TGA GGA	TGG AGC TCA TCC TCG TGG TTC T
ITGA9	ACG ACA ACA CGC GCT GGG TC	CCC GGC AGG TCT TTC CGC AG
vWF	CTG TGC TCT GGA TTT GTT AGG	AAA TTC TGC CCA TCA AAG GT
VE-Cad	CAG CCC AAA GTG TGT GAG AA	TGT GAT GTT GGC CGT GTT AT
CD11b	ACT TGC AGT GAG AAC ACG TAT G	AGA GCC ATC AAT CAA GAA GGC
CD19	AAC GTC TCT CAA CAG ATG GGG	TTT GGC CCA CAC ATA CAG CTT
CD31	CCC AGC CCA GGA TTT CTT AT	ACC GCA GGA TCA TTT GAG TT
CD34	CAA ACA TCA CAG AAA CGA CAG	GAA ACA TTT CCA GGT GAC AG
CD45	AAT GCT ATC TCA GAT GTC CCA G	CAG AGT GGT TGT TTC AGA GG
CD73	TCA ATC ATG CCG CTT TAG AG	TAA TTG TGC CAT TGT TGC GT
CD90	CCA GCA AAT ACA ACA TGA AGG	TTG ACC AGT TTG TCT CTG AG
CD105	GCC AGC ATT GTC TCA CTT CA	GGC ACA CTT TGT CTG GAT CA
HLADRα	GAC CAA TCA GGC GAG TTT ATG T	TGA GCA CAG TTA CCT CTG GAG
P75	GCC TTC AAG AGG TGG AAC AG	AGC CGT TGA GAA GCT TCT CC
PPARG	ATG TCT CAT AAT GCC ATC AGG T	GTG ATT TGT CTG TTG TCT TTC C
FABP4	AAA GTC AAG AGC ACC ATA ACC	CAC CAC CAG TTT ATC ATC CT

LPL	CCC TAC AAA GTC TTC CAT TAC C	AGT TCT CCA ATA TCT ACC TCT G
RUNX2	CAT TTC AGA TGA TGA CAC TGC C	GTG TAA GTA AAG GTG GCT GG
Osteocalcin	AAA GGT GCA GCC TTT GTG TC	CTG AAA GCC GAT GTG GTC AG
MYC	GCG TCC TGG GAA GGG AGA TCC GGA GC	TTG AGG GGC ATC GTC GCG GGA GGC TG
NANOG	CAG CCC TGA TTC TTC CAC CAG TCC C	CGG AAG ATT CCC ACT CGG GTT CAC C
OCT4	GAC AAC AAT GAA AAT CTT CAG GAG A	TTC TGG CGC CGG TTA CAG AAC CA
SOX2	GGG AAA TGG GAG GGG TGC AAA AGA GG	TTG CGT GAG TGT GGA TGG GAT TGG TG
KLF4	ACG ATC GTG GCC CCG GAA AAG GAC C	TGA TTG TAG TGC TTT CTG GCT GGG CTC C
REX1	CAG ATC CTA AAC AGC TCG CAG AAT	GCG TAC GCA AAT TAA AGT CCA GA
NESTIN	ATC TCC AGA AAC TCA AGC AC	ATT CCT GAT TCT CCT CTT CCA

9. Author's Publications

1. **HMGA2 exhibits dRP/AP site cleavage activity and protects cancer cells from DNA-damage-induced cytotoxicity during chemotherapy.**
   Summer H, Li O, Bao Q, Zhan L, Peter S, Sathiyanathan P, Henderson D, Klonisch T, Goodman SD, Dröge P.
   Nucleic Acids Res. 2009 Jul;37(13):4371-84.

2. **Chaperoning HMGA2 protein protects stalled replication forks in stem and cancer cells.**
   Yu H, Lim HH, Tjokro NO, Sathiyanathan P, Natarajan S, Chew TW, Klonisch T, Goodman SD, Surana U, Dröge P.
   Cell Rep. 2014 Feb 27;6(4):684-97.

3. **Identification and characterization of mesenchymal stem cells derived from the trabecular meshwork of the human eye.**
   Tay CY, Sathiyanathan P, Chu SW, Stanton LW, Wong TT.
   Stem Cells Dev. 2012 Jun 10;21(9):1381-90.
   * Co-first author

4. **Establishing criteria for human mesenchymal stem cell potency**
   Rebekah M. Samsonraj , Bina Rai, Padmapriya Sathiyanathan, Kia Joo Puan, Olaf Rötzschke, James H. Hui, Michael Raghunath, Lawrence W. Stanton, Victor Nurcombe, and Simon M. Cool.
   Stem Cells. 2015 Jun;33(6):1878-91.

10. Posters

Isolation and Characterization of Human Trabecular Meshwork Progenitors.

Padmapriya Sathiyanathan, Cheryl Y. Tay, Stephanie W.L. Chu, Tina T. Wong, Lawrence W. Stanton.

International Society for Stem Cells Research (ISSCR) Regional Conference 2013.
Florence, Italy.

Abstract

Development of primary open-angle glaucoma (POAG) is associated with increased resistance to aqueous humour outflow through the dysfunctional trabecular meshwork (TM). The positive correlation of POAG manifestation with age and significant decrease in the TM cell population in glaucomatous TM, raises the possibility that it may be a stem cell-related disease. Putative stem cells are believed to exist in the TM. The purpose of the study is to isolate and propagate progenitors of the TM which could have the capacity to differentiate into functional TM cells to treat POAG. The TM-derived cells (TM-DC) express TM markers, and certain stem cell markers. Morphologically, they resemble mesenchymal stem cell (MSC). Gene expression and FACS analyses show that TM-DC express the positive MSC marker and lack the negative MSC markers. The capacity of TM-DC to differentiate into mesenchymal lineages of adipocytes, chondroblasts and osteoblasts, is indicative of their multipotency, another defining characteristic of MSC. Genomic characterization showed the TM-DC to have gene expression patterns similar to MSC derived from other tissues. These cells may have the potential to help replace lost or dysfunctional cells in the TM tissue associated with POAG.

Identification of Human Trabecular Meshwork Specific Differentiation Markers.

Padmapriya Sathiyanathan, Lawrence W. Stanton.

International Society for Stem Cells Research (ISSCR) Conference 2014.
Vancouver, Canada.

Abstract

Glaucoma as the second leading cause of blindness is a world health problem. The common subtype, primary open-angle glaucoma (POAG) is associated with increased resistance to aqueous humor outflow in the trabecular meshwork (TM). Decline in TM cells and malfunctioning existing ones are believed to contribute to the resistance. Regenerative medicine to restore functionality to the diseased tissue is widely being investigated.
Previously we reported the isolation and characterization of progenitors from the TM as TM-derived mesenchymal stem cells (TM-MSC). The potential for TM-MSC to replace lost/ dysfunctional TM cells is being investigated. The lack of TM-specific markers, however, has challenged such efforts of regenerative medicine for POAG. The purpose of this study is to identify markers specific to the TM that can also be used to track TM lineage differentiation. To this end, gene expression profiling by microarray was performed on the TM tissue and TM-MSC to find TM differentiation markers. An additional comparison with the expression profiles of the corneal and scleral tissues identified markers enriched in the TM. 13 genes were found to be TM-specific with respect to cornea and sclera. Immunofluorescence of the markers shows their specificity to the TM in the anterior segment of the eye. These genes also have differential expression between the TM cells and TM-MSC as analyzed by qRT-PCR. Preliminary differentiation results also indicate their relevance as TM differentiation markers.

This study reports the identification of a panel of genes that (i) ascertains TM cell type and also (ii) applicable as TM differentiation markers. They have the possibility to advance the search for a cell-based therapy for POAG.